

DYNAMIC PERFORMANCE OF LONG COMMERCIAL VEHICLE



UNIVERSITI TEKNIKAL MALAYSIA MELAKA

DYNAMIC PERFORMANCE OF LONG COMMERCIAL VEHICLE

MUHAMMAD ZARUL BIN KHAIRUL AZMAN



UNIVERSITI TEKNIKAL MALAYSIA MELAKA

2019

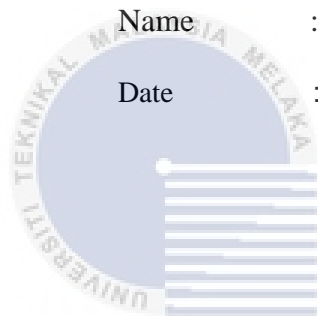
DECLARATION

I declare that this project report entitled “Dynamic Performance Of Long Commercial Vehicle”
is the result of my own work except as cited in the references

Signature :

Name :

Date :





اونيورسيتي تيكنيكل مليسيا ملاك

UNIVERSITI TEKNIKAL MALAYSIA MELAKA

APPROVAL

I hereby declare that I have read this project report and in my opinion this report is sufficient in terms of scope and quality for the award of the degree of Bachelor of Mechanical Engineering.

	Signature	:
	Name of Supervisor :	:
	Date	:



اونيورسيتي تېكنيكل مليسيا ملاك

UNIVERSITI TEKNIKAL MALAYSIA MELAKA

DEDICATION

To my beloved mother, Maimun Binti Abdullah and my supportive father, Khairul Azman Bin Hosnan.



ABSTRACT

Dynamic performance of a vehicle is the important aspect in designing a vehicle. As for commercial vehicle which is related in delivering passengers and goods, comfort and safety are the crucial characteristics that must be taken into consideration. Three type of test simulation which cover ride, handling and stability criteria were carried out to determine the behavior of the vehicle in real world driving condition. Every test was carried out with different test parameters at different vehicle's speeds and masses. In the ride criteria, the bounce sine sweep test was carried out to represent the motion of vehicle when travelling on uneven road surface. Then, the handling criteria used double lane change test to represent the motion of vehicle during overtaking on the highway. For the stability criteria, J-turn type test was carried out to represent motion of vehicle when a sharp steering input was applied to the vehicle in an event of avoiding obstacle during emergency situation. All of the results from the tests are analyzed based on different test parameters to determine the difference in dynamic behavior of the vehicle. Higher values of vehicle's speed and produce higher value of test output results.

ABSTRAK

Prestasi dinamik sesebuah kenderaan ialah suatu aspek yang amat penting dalam fasa rekaan kenderaan. Bagi kenderaan komersial yang amat berkait dalam kerja penghantaran penumpang dan barang-barangan, keselesaan dan keselamatan adalah ciri penting yang perlu diambil kira dalam fasa rekaan kenderaan. Oleh itu, tiga jenis ujian simulasi yang merangkumi ciri penunggangan, pengendalian dan kestabilan telah dijalankan untuk menilai kelakuan kenderaan dalam situasi pemanduan sebenar. Setiap ujian dijalankan dengan menggunakan parameter ujian yang berbeza iaitu kelajuan berbeza dan berat berbeza. Dalam ciri penunggangan, ujian “Bounce sine sweep” telah dijalankan untuk mewakili pergerakan kenderaan ketika melalui permukaan jalan yang tidak rata. Selepas itu, ciri pengendalian menggunakan ujian “Double lane change” untuk mewakili pergerakan kenderaan kereta ketika memotong di jalan raya. Untuk ciri kestabilan, ujian “J-turn type” telah dijalankan untuk menunjukkan pergerakan kenderaan ketika stereng diputarkan dengan keadaan yang tergesa-gesa untuk mengelak daripada halangan ketika situasi kecemasan. Semua keputusan ujian yang telah dijalankan akan dianalisa berdasarkan perbezaan parameter ujian untuk menentukan keadaan kenderaan. Kelajuan dan berat kenderaan yang tinggi akan menghasilkan keputusan ujian yang tinggi.

ACKNOWLEDGEMENT

I would like to thank my supportive supervisor, PM. Dr. Mohd Azman Bin Abdullah, for guiding me throughout this project. He already gave me many ideas regarding this project and helped me to understand this research better. I could not have imagined having a better supervisor for my final year project.

I also want to express my sincere thanks to my seminar panels, Mr. Amrik Singh A/L Phuman Singh and Mr. Adzni Bin Md. Saad for giving me a lot of comments and inputs during the seminar. I acknowledged all the comments and inputs for improving my research.

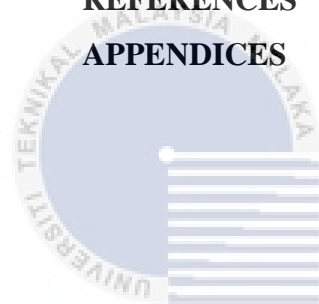
Last but not least, I would to thank my family for giving me support to finish this project.

TABLE OF CONTENT

CHAPTER	CONTENT	PAGE
	DECLARATION	ii
	APPROVAL	iii
	DEDICATION	iv
	ABSTRACT	v
	<i>ABSTRAK</i>	vi
	ACKNOWLEDGEMENT	vii
	TABLE OF CONTENT	viii
	LIST OF TABLES	xi
	LIST OF FIGURES	xiv
	LIST OF ABBREVIATIONS	xx
	LIST OF SYMBOLS	xxi
	LIST OF APPENDICES	xxiii
CHAPTER 1	INTRODUCTION	
	1.1 Background	1
	1.2 Problem Statement	3
	1.3 Objective	3
	1.4 Scope of Project	4
	1.5 Thesis Outline	4
CHAPTER 2	LITERATURE REVIEW	
	2.1 Introduction	6
	2.2 Comfort aspect	6
	2.3 Safety aspect	8
	2.4 Vehicle axis system	8
	2.5 Vehicle suspension system	9
	2.6 Tire	11
	2.7 Vehicle dynamic analysis	14
	2.7.1 Ride	14

2.7.2 Handling	17
2.7.3 Stability	19
2.8 Vehicle test	21
2.8.1 Bounce sine sweep test	21
2.8.2 Double lane change	21
2.8.3 J turn test	23
2.8.4 Test output results	24
CHAPTER 3 METHODOLOGY	
3.1 Introduction	25
3.2 Literature review	25
3.3 Vehicle specification	26
3.4 Test simulation	30
3.4.1 Bounce sine sweep test	30
3.4.2 Double lane change	34
3.4.3 J turn type test	38
3.5 Data collection and analysis	42
CHAPTER 4 RESULT AND DISCUSSION	
4.1 Bounce sine sweep test (Ride)	46
4.1.1 Pitch angle of sprung mass	46
4.1.2 Maximum pitch moment calculation	49
4.1.3 Vertical acceleration of sprung masses	52
4.1.4 Comparison between tire forces of R1	56
4.1.5 Vertical tire force, R1	56
4.2 Double lane change (Handling)	59
4.2.1 Trajectory Y vs X	59
4.2.2 Lateral acceleration of CG	63
4.2.3 Yaw angle of sprung masses	68
4.2.4 Comparison between tire forces for tire R1	71
4.2.5 Lateral tire force	72
4.2.6 Vertical tire force, R1	75
4.3 J-turn type test (Stability)	79

4.3.1 Trajectory Y vs X	79
4.3.2 Lateral Acceleration of CG	82
4.3.3 Roll moment calculation	86
4.3.4 Roll angle of sprung mass	91
4.3.5 Comparison between tire forces R1	94
4.3.6 Lateral tire force, R1	95
4.3.7 Vertical tire force, R1	98
4.3.8 Rollover index	101
CHAPTER 5 CONCLUSION AND RECOMMENDATIONS	
5.1 Conclusion	106
5.2 Recommendations	107
REFERENCES	108
APPENDICES	111



اونيورسيتي تيكنيكل مليسيا ملاك

UNIVERSITI TEKNIKAL MALAYSIA MELAKA

LIST OF TABLES

TABLE	TITLE	PAGE
2.1	ISO 2631-1 comfort guidelines	7
3.1	General specification 1	27
3.2	General specification 2	28
4.1	Maximum pitch angle comparison for different speeds	50
4.2	Maximum pitch angle comparison for different masses	51
4.3	Maximum pitch moment value at different speeds	53
4.4	Maximum roll moment when unladen and fully laden vehicle	53
4.5	Comparison of maximum vertical acceleration at different speeds	55
4.6	Comparison of maximum vertical acceleration when fully laden and unladen vehicle	57
4.7	Comparison of vertical tire force at different speeds	59
4.8	Comparison of vertical tire force when fully laden and unladen vehicle	60

4.9	Comparison of maximum Y displacement at region C at different speeds	63
4.10	Comparison of maximum Y displacement at region C when fully laden and unladen vehicle	65
4.11	Comparison of maximum lateral acceleration at different speeds	67
4.12	Comparison of maximum lateral acceleration when fully laden and unladen vehicle	69
4.13	Comparison of maximum yaw angle at different speeds	71
4.14	Comparison of maximum yaw angle when fully laden and unladen vehicle	73
4.15	Comparison of lateral tire forces at different speeds	76
4.16	Comparison of lateral tire forces when fully laden and unladen vehicle	77
4.17	Comparison of vertical tire force at different speeds	80
4.18	Comparison of vertical tire force when fully laden and unladen vehicle	81
4.19	Vehicle trajectory comparison at different speeds	83
4.20	Comparison of vehicle trajectory when fully laden and unladen vehicle	84

4.21	Comparison of maximum lateral acceleration at different speeds	87
4.22	Comparison of maximum lateral acceleration when fully laden and unladen vehicle	88
4.23	Maximum roll moment value at different speeds	90
4.24	Maximum roll moment when unladen and fully laden vehicle	91
4.25	Comparison of maximum yaw angle at different speeds	93
4.26	Comparison of maximum yaw angle when fully laden and unladen vehicle	94
4.27	Comparison of roll angle at different speeds	96
4.28	Comparison of roll angle when fully laden and unladen vehicle	97
4.29	Comparison of lateral tire forces at different speeds	100
4.30	Comparison of lateral tire forces of R1 when fully laden and unladen vehicle	101
4.31	Comparison of vertical tire force of R1 at different speeds	103
4.32	Comparison of vertical tire force when fully laden and unladen vehicle	104
4.33	Maximum rollover index for different speeds	106
4.34	Maximum rollover index when fully laden and unladen vehicle	108

LIST OF FIGURES

2.1	Vehicle axis system [6]	9
2.2	Air suspension system [9]	11
2.3	Tire axis system	12
2.4	Behaviour of tire when subjected to side force	12
2.5	Friction ellipse concept	13
2.6	Tire slip condition [22]	14
2.7	Vertical and longitudinal vibration response gain [11]	16
2.8	Curvature response of the vehicle	18
2.9	Steering amplitude for Fishhook manoeuvre test [17]	20
2.10	Sine manoeuvre test path [17]	20
2.11	Bounce sine sweep test procedure	21
2.12	Double lane change test procedure	22
2.13	The trail of J turn test [20]	23

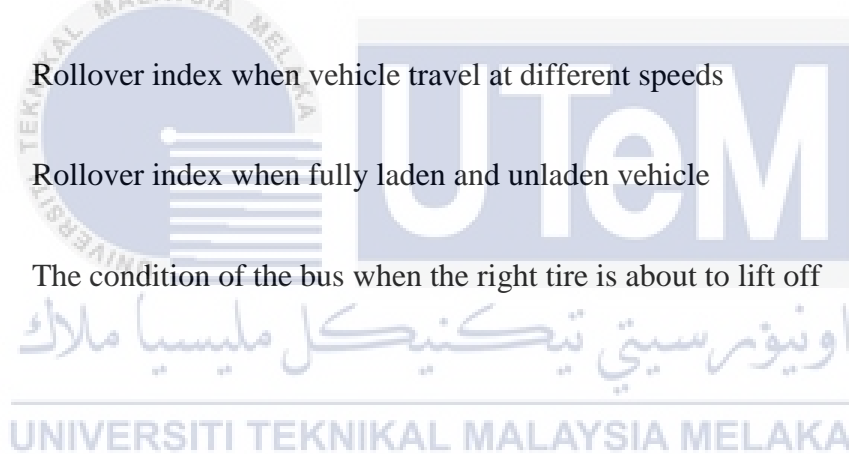
3.1	Vehicle type for simulation	26
3.2	The power flow of the bus (RWD)	29
3.3	Selection of test procedure	32
3.4	Setup the vehicle's target speed	32
3.5	Setup the vehicle's mass	33
3.6	Ground elevation of tire R1 for standard speed	33
3.7	Graph plot and 3D vehicle animation	34
3.8	Selection of test procedure	35
3.9	Setup the vehicle's target speed	36
3.10	Setup the vehicle's mass	36
3.11	Test procedure in form of vehicle trajectory	37
3.12	Graph plot and 3D vehicle animation	38
3.13	Selection of test procedure	39
3.14	Setup the vehicle's target speed	40
3.15	Setup the vehicle's mass	40
3.16	Test procedure in form of vehicle trajectory	41
3.17	Graph plot and 3D vehicle animation	42

3.18	All graphical data based on test parameters	43
3.19	Detailed view of the graph	43
3.20	Data from graph plotted	44
3.21	Example for comparison graph between three different speeds	45
4.1	Pitching motion of the bus	47
4.2	Pitch angle of sprung mass for standard speed	47
4.3	Pitch angle of sprung masses with different speed	48
4.4	Pitch angle of sprung masses with different when fully laden and unladen vehicle	49
4.5	Diagram of pitch moment acting on the bus	50
4.6	Vertical acceleration of sprung masses with standard speed	53
4.7	Vertical acceleration of sprung masses with different speed	54
4.8	Vertical acceleration of sprung masses when fully laden and unladen vehicle	55
4.9	Comparison between tire forces of R1	56
4.10	Vertical tire force of R1 at standard speed	57
4.11	Vertical tire force of R1 at different speeds	58

4.12	Vertical tire force of R1 when fully laden and unladen vehicle	59
4.13	Vehicle trajectory for standard speed	60
4.14	Vehicle trajectory at different speeds	61
4.15	Vehicle trajectory when fully laden and unladen vehicle	63
4.16	Lateral acceleration of vehicle's center of gravity at standard speed	64
4.17	Lateral acceleration of CG at different speeds	65
4.18	Lateral acceleration of CG when fully laden and unladen vehicle	67
4.19	Yaw angle of sprung masses at standard speed	68
4.20	Yaw angle of sprung masses at different speeds	69
4.21	Yaw angle of sprung masses when fully laden and unladen vehicle	70
4.22	Comparison between three tire forces	71
4.23	Lateral tire forces of R1 at standard speed	72
4.24	Lateral tire force of R1 at different speeds	73
4.25	Lateral tire force of R1 when fully laden and unladen vehicle	75
4.26	Vertical tire force of R1 at standard speed	76

4.27	Vertical tire force of R1 at different speeds	77
4.28	Vertical tire force of R1 when fully laden and unladen vehicle	78
4.29	Vehicle trajectory at standard speed	80
4.30	Vehicle trajectory at different speeds	81
4.31	Vehicle trajectory for fully laden and unladen vehicle	82
4.32	Lateral acceleration at standard speed	83
4.33	Lateral acceleration at different speeds	84
4.34	Lateral acceleration when fully laden and unladen vehicle	85
4.35	Diagram of roll moment acting on the bus	86
4.36	Yaw angle of sprung mass at standard speed	89
4.37	Yaw angle of sprung mass at different speeds	90
4.38	Yaw angle of sprung mass when fully laden and unladen vehicle	91
4.39	Representation of roll moment of vehicle	92
4.40	Roll angle of sprung mass at standard speed	92
4.41	Roll angle of sprung mass at different speeds	93
4.42	Roll angle of sprung mass when fully laden and unladen vehicle	94

4.43	Comparison of tire force of R1	95
4.44	Lateral tire force of R1 at standard speed	96
4.45	Lateral tire forces of R1 at different speeds	97
4.46	Lateral tire force of R1 when fully laden and unladen vehicle	98
4.47	Vertical tire force of R1 at standard speed	99
4.48	Vertical tire force of R1 at standard speed	100
4.49	Vertical tire force of R1 when fully laden and unladen vehicle	101
4.50	Rollover index when vehicle travel at different speeds	103
4.51	Rollover index when fully laden and unladen vehicle	104
4.52	The condition of the bus when the right tire is about to lift off	104



LIST OF ABBREVIATIONS

MIROS	Malaysian Institute of Road Safety Research
3D	3 Dimensional
ISO	International Organization for Standardization
CG	Center of Gravity
SAE	Society of Automotive Engineers
ESC	Electronic Stability Control
WSS	Wheel Speed Sensor
SAS	Steering Angle Sensor
RWD	Rear Wheel Drive
R1	Front right tire
RMS	Root Mean Square
NHTSA	National Highway Traffic Safety Administration

LIST OF SYMBOLS

a_v	=	RMS acceleration
a_x	=	Longitudinal acceleration
a_y	=	Lateral acceleration
a_z	=	Vertical acceleration
p	=	Roll
q	=	Pitch
r	=	Yaw
F_x	=	Tractive force/Longitudinal force
F_{xmax}	=	Maximum longitudinal force
F_y	=	Lateral force
F_{ymax}	=	Maximum lateral force
F_z	=	Vertical force
F_s	=	Side force
α	=	Side slip angle
δ	=	Steering angle
ψ	=	Drift angle
K_s	=	Understeer coefficient
α_f	=	Front tire slip angle
α_r	=	Rear tire slip angle
θ	=	Pitch angle

ϕ	=	Roll angle
γ	=	Yaw angle
M_y	=	Pitch moment
M_{ymax}	=	Maximum pitch moment
m_b	=	Sprung mas of the bus
h	=	Height of CG to the ground
F_{zr}	=	Vertical tire force for right side of vehicle
F_{zl}	=	Vertical tire force for left side of vehicle
R	=	Rollover index



LIST OF APPENDICES

APPENDIX	TITLE	PAGE
A	Gantt chart for PSM 1	112
B	Gantt chart for PSM 2	113



CHAPTER 1

INTRODUCTION

1.1 Background

Vehicle dynamic is a major aspect that need to be considered in designing a vehicle for commercial use or personal use [1]. The commercial vehicle is intended for business purpose such as bus, truck and train. This project is mainly focused on the dynamic performance of bus. The main goal of designing the vehicle dynamic of the bus are safety and comfort for the driver and the passenger.

Based on the research done by Malaysian Institute of Road Safety Research (MIROS) regarding on the crash investigation on bus accidents in Malaysia, the accident that have been investigated with rollover collision recorded 11 % cases from all type of collision [2]. This data shows that rollover collision contribute a quite significant amount of cases to the overall bus accidents in Malaysia. This rollover collision happened when the vehicle exceed the dynamic performance limits during cornering or changing lane at high speed. When the driver and passenger of the bus encounter this situation, it could cause severe injury to them.

The comfort of the passenger is the important aspect in this commercial vehicle type as it affect the business operation of the company. There is a theoretical way to determine the level of comfort of the vehicle [1]. The level of comfort when the vehicle undergo these three type of

tests can be determined by the limits suggested from the international standard ISO 2631-1 which originally developed for public transports. The level of comfort take account the vibration that is transmitted to the body of passenger. There are two sources of vibration that influence the ride comfort of the vehicle which are internal and external sources. This project only analyze the vibration form external source which is the road surface.

The specification of the vehicle such as weight, dimension and type of suspension plays a vital role in determining the vehicle dynamic performance. The vehicle dynamic performance can be divided into three aspects which are ride, handling and stability. The parameters that are being analyzed for the vehicle dynamic performance are lateral acceleration, vertical acceleration, vehicle trajectory, ground elevation of the tire, pitch angle, yaw angle and roll angle.

Three type of tests are done as the representation of real world driving situation. The first test is bounce sine sweep test that require the vehicle to go through bumpy roads and this test is done to analyze the ride performance of the vehicle. This test is the representation to the uneven road surface and the ride performance of the vehicle can be evaluated. The second test is double lane change test as the representation of the vehicle during changing lane situation at the highway. The vehicle handling performance is evaluated during this test. The third test is J-turn stability test to evaluate the stability of the vehicle during emergency such as avoiding obstacle. All of the test will use two different parameters which are different speeds and different masses to determine the behavior of the vehicle when the test parameters are changed.

1.2 Problem Statement

The dynamic performance of long commercial vehicle is different with passenger vehicle as the center of gravity is higher than on the passenger vehicle. The size and weight of the long commercial vehicle is significantly higher than on the passenger car and resulting in the different behavior of the vehicle in certain driving situation. The long commercial vehicle has a long wheelbase and causing understeer problem during cornering. The dynamic performance of the bus will be different when travelling with passengers on board and when the bus is travelling with no passengers on board as the weight of the bus will be different. When doing this research, I found that there is lack of dynamic performance data published by the vehicle manufacturer.

1.3 Objective

The objective of this project are to determine the behavior of long commercial vehicle when tested with real driving situation by using simulator, to perform analysis of the vehicle dynamic at different speed from the tests conducted and to differentiate the dynamic performance of the vehicle with full laden and unladen condition.

1.4 Scope of Project

The scope of this project are the test simulation is only done by using TruckSim for this project without the real world driving condition experiment and this project only use Tour Bus as the vehicle of interest for long commercial vehicle.

1.5 Thesis Outline

This report consist of five chapters which are Chapter 1: Introduction, Chapter 2: Literature Review, Chapter 3: Methodology, Chapter 4: Results and Discussions and Chapter 5: Conclusion and Recommendations. In Chapter 1, there are description for background of the project, problem statement regarding this project, objective that need to achieve and scope of this project. As for Chapter 2, the literature reviews of this project are explained in details. A number of journals, websites and books are reviewed for further understanding of vehicle dynamic performance. The factor that affecting the vehicle dynamic performance, vehicle comfort and vehicle safety also being studied through the literature review. In order to determine the dynamic performance of the vehicle, the tests that are related to three aspects which are ride, handling and stability are being reviewed for determining the purpose of the tests and the application at the real world driving conditions. For Chapter 3, the methodology to perform the test simulation and analysis are explained. All of the test simulation is done by using TruckSim simulation. The test simulation is viewed in 3D animation and graphical plot. In Chapter 4, all of the results from the test simulation are compared based on the test parameters in graphical form. All of the graph are analyzed to determine the behavior of the vehicle during the test

simulation. The last part in this report is Chapter 5 where the results obtained are concluded according to the objectives and some recommendations in the future research.



CHAPTER 2

LITERATURE REVIEW

2.1 Introduction

The main goal in designing the vehicle in dynamic performance approach is by achieving both comfort aspect and safety aspect. There are many factors that influence the dynamic performance of long commercial vehicle such as the vehicle suspension system and the tires. In order to analyse the dynamic performance of large commercial vehicle, three parameter are being analysed which are ride, handling and stability of the vehicle. As for determining the performance of the vehicle based on the parameters aforementioned, the tests that are related to the parameters are carried out which are Bounce Sine Sweep Test for ride, Double Lane Change Test for handling and J-Turn Type Test for stability.

2.2 Comfort aspect

The comfort of the passenger is the important aspect in vehicle dynamics analysis. There is a guide to determine the level of comfort of the vehicle based on a standard [1]. The level of comfort when the vehicle is manoeuvring can be determined by the limits suggested from the international standard ISO 2631-1 which originally developed for public transports as in **Table 2.1**. The magnitude that is being compared to the limits is the magnitude of vibration which can be calculated with **Eq. (1.1)**. a_v is the RMS acceleration while a_x , a_y and a_z is the vehicle acceleration at CG for x-axis, y-axis and z-axis.

$$a_v = (a_x^2 + a_y^2 + a_z^2)^{1/2} \quad (1.1)$$

Table 2.1: ISO 2631-1 comfort guidelines

RMS Acceleration (g)	Comfort level
≤ 0.032	Not uncomfortable
0.032 to 0.064	A little uncomfortable
0.051 to 0.102	Fairly uncomfortable
0.082 to 0.163	Uncomfortable
0.115 to 0.255	Very uncomfortable
≥ 0.204	Extremely uncomfortable

There are two sources of vibration that influence the ride comfort of the vehicle which are internal and external sources [4]. Internal sources are the vibration from engine, transmission and driveline while external sources are from the road surface input, noise from other vehicles and wind noise. In this analysis, only external source is taken into account which is from the uneven road surface. The driver's work intensity and psychology are affected by the ride comfort of the occupant when travelling. Ride comfort is also influenced by the speed of the vehicle. The higher the speed of the vehicle travels, the lower the ride comfort of the respective vehicle [3].

2.3 Safety aspect

Safety aspect is one of the main concern for bus industry as any accident that will occur will involve driver, a lot of passengers and other road users. Based on the research done on the crash investigation on bus accidents in Malaysia done by MIROS, statistic shown that rollover accident recorded 11% cases out of all type of collision and categorized as the most severe event and recorded the most fatalities in term of second impact event [2]. This type of accident will cause severe injury to both driver and passengers on board. The factor that cause rollover accident is mainly by the vehicle dynamic behaviour during cornering or turning as the dynamic performance of the vehicle is at its limit during this situation.

In term of safety, the most important information of centre of gravity, CG position is its height because it influencing the roll stability of that particular vehicle to avoid rollover accident [5]. Vehicle with lower position of CG might have advantage over the vehicle with higher position of CG because it has higher roll stability. As for the long commercial vehicle, the position of CG is higher compared to the passenger cars and it will resulting in difference dynamic performance between both vehicle.

2.4 Vehicle axis system

In order to perform the dynamic analysis of the vehicle, the dynamic parameters that need to be analysed must be based on a standard. The vehicle axis system used for this entire analysis is based on SAE convention [6]. Based on **Figure 2.1**, the vehicle is represented as a mass concentrated at its Centre of Gravity (CG). X-axis is the longitudinal direction of the car

and roll velocity, \mathbf{p} . Y-axis is the lateral direction of the car and pitch velocity, \mathbf{q} . Z-axis is the downward vertical direction of the car and contains yaw velocity, \mathbf{r} .

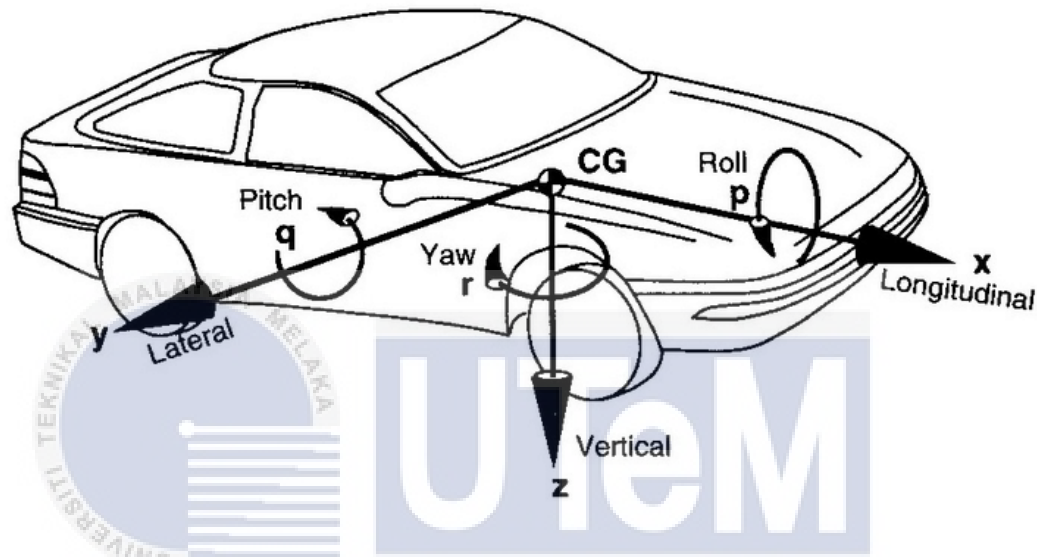


Figure 2.1: Vehicle axis system [6]

2.5 Vehicle suspension system

The main goal of suspension system for every vehicle is limiting the transmissibility of vibration from the road to the sprung mass for the comfort of the driver and the passengers [7]. The handling behaviour of the vehicle also being influenced by the suspension system so, we need to consider both comfort and handling criteria in choosing the best suspension system. In active suspension design criteria, there are seven criteria listed which are ride, suspension working space, energy consumption, infrastructure damage, rollover stability, braking and traction. Based on the criteria listed, the focus of this analysis are solely for ride and rollover stability when the vehicle travel at different speeds.

The suspension system is an important system in determining the dynamic performance of a vehicle. Springs and dampers are the main components of the suspension system. As an example, when the vehicle is passing through a bump on the road, the vehicle springs and dampers are compressed to compensate the movement of the tire due to increasing elevation on the surface of the road and the energy will be stored in the spring. The springs tend to oscillate for releasing the energy and dampers resist the oscillation by converting the kinetic energy to heat that is dissipated through a hydraulic fluid. In vehicle modelling process, the damping ratio of the damper influence the ride comfort, roll and pitch behaviour of the planar motion of the vehicle [8].

This analysis is done for the bus that is equipped with air suspension. The advantages of air suspension compared to conventional leaf-type spring are the vehicle is more comfort and less vibration transmitted from the tire when the vehicle is driven through uneven road surface at different speeds [5]. In addition, the air suspension can withstand higher axle load limits and enables the vehicle to transport more load in a single trip which is important for the bus that if it travels with more loads in cargo area. A disadvantage of any type of leaf-type similar springs is the dynamic behaviour which has non-constant eigen frequency, while the air spring has constant eigen frequency that can be controlled for tuning purpose according to the needs.

Air suspension consist of three main components which are air compressor, air bags and suspension computer [9]. The mechanism of the air suspension system initiated by air compressor that inflate the air bag that is located between the axle and chassis. The air bag act as the spring and shock to absorb the shock from road vibrations. The suspension computer control the timing and quantity of the air that is needed to be pumped into the air bag. **Figure 2.2** shows the schematic diagram for the air suspension system at every axle of the vehicle.

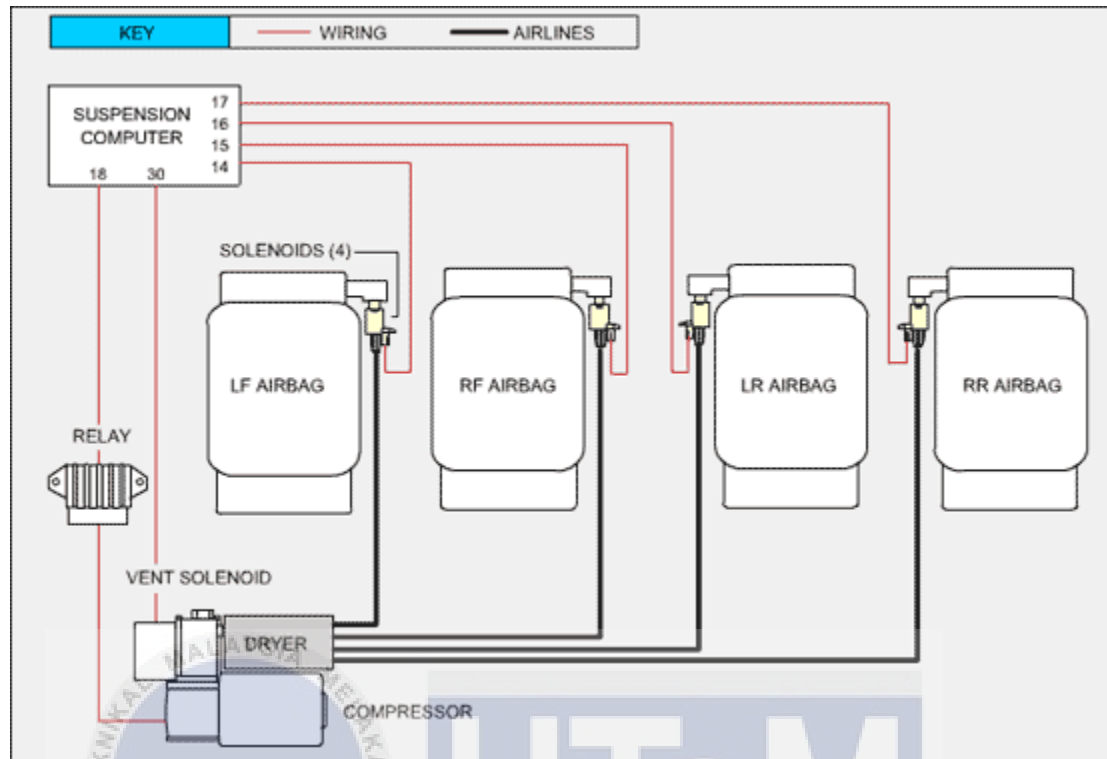


Figure 2.2: Air suspension system [9]

1.5 Tire

When a vehicle is moving, the only component that in contact with the ground is tire. Tire functions as the component that support the weight of vehicle, dampen the reaction of vehicle due to travel on uneven surface , provide the sufficient traction for longitudinal motion and provide adequate steering control and directional stability [23]. The axis system for the tire is based on **Figure 2.3**.

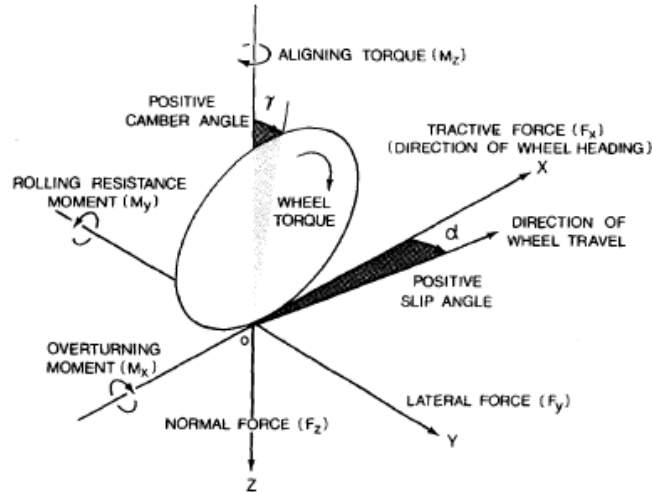


Figure 2.3: Tire axis system [23]

Tractive force, F_x on tire is present when the vehicle start to accelerate and brake which is in longitudinal motion. The force is the integration of longitudinal shear stress on the entire contact patch. Lateral force, F_y located at the position where tire and ground is in contact and is a function of slip angle and camber angle. Side slip angle, α for every tire is resulting from side force when the vehicle is negotiating a turn. The behavior of the tire when subjected to side force, F_s is represented as in **Figure 2.4**.

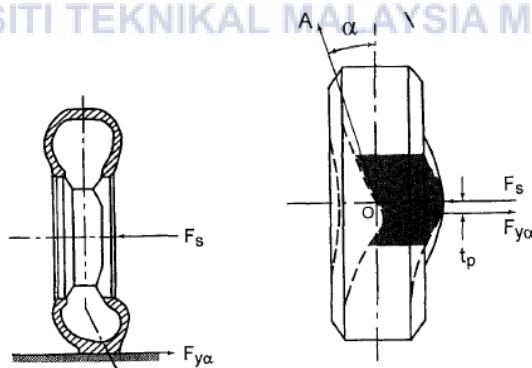


Figure 2.4: Behavior of tire when subjected to side force [23]

As for the bus, it follows the most used tires by heavy vehicle which used natural rubber as the base polymer for the tread. It is different with passenger cars which used synthetic rubber

compound. The properties for natural rubber compound are higher abrasion resistance, lower hysteresis losses and lower value of coefficient of road adhesion during wet condition.

In order to determine the tire sliding condition on the ground in any direction, friction ellipse concept can be used by comparing the resultant of longitudinal tire force and lateral tire force with the maximum value of road adhesion coefficient and normal load on tire. As shown in **Figure 2.5**, F_{xmax} and F_{ymax} can be calculated from measured tire data and develop the major and minor axis of the friction ellipse.

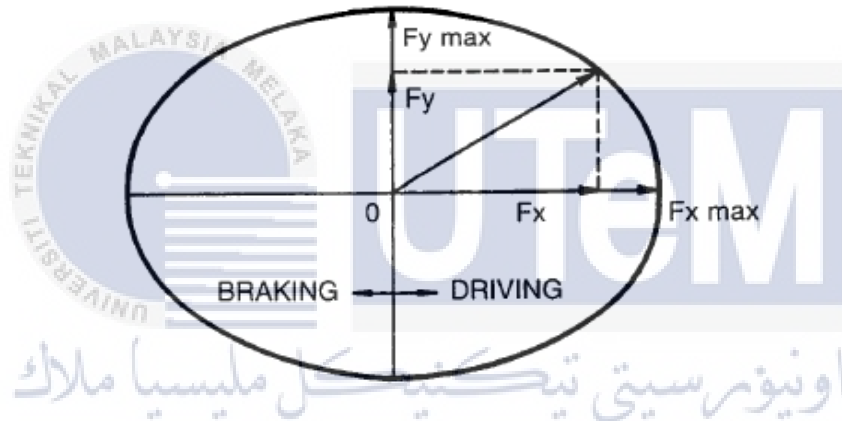


Figure 2.5: Friction ellipse concept [23]

Tire is an important component for the vehicle when an event of changing directions by applying force to tire. During this condition, tire slip will occur due to the physical process when tire is in contact with the road surface [10]. The contact area of tire, contact patch, will experience stress as the rubber mechanism in contact with a frictional surface and causes them to deform or flex resulting partially slide of the tire surface. The illustration of tire slip condition when the driver turns the vehicle can be represented by **Figure 2.6**. Lateral force vector forces the front of the vehicle away from the initial vehicle vector velocity according to the new direction of front wheels during turning. The turning of the wheels will form a steering angle, δ

and a drift angle, ψ will build up that resulting from the deformation of the contact patch [22]. This condition will affect the dynamic performance of the vehicle during cornering.

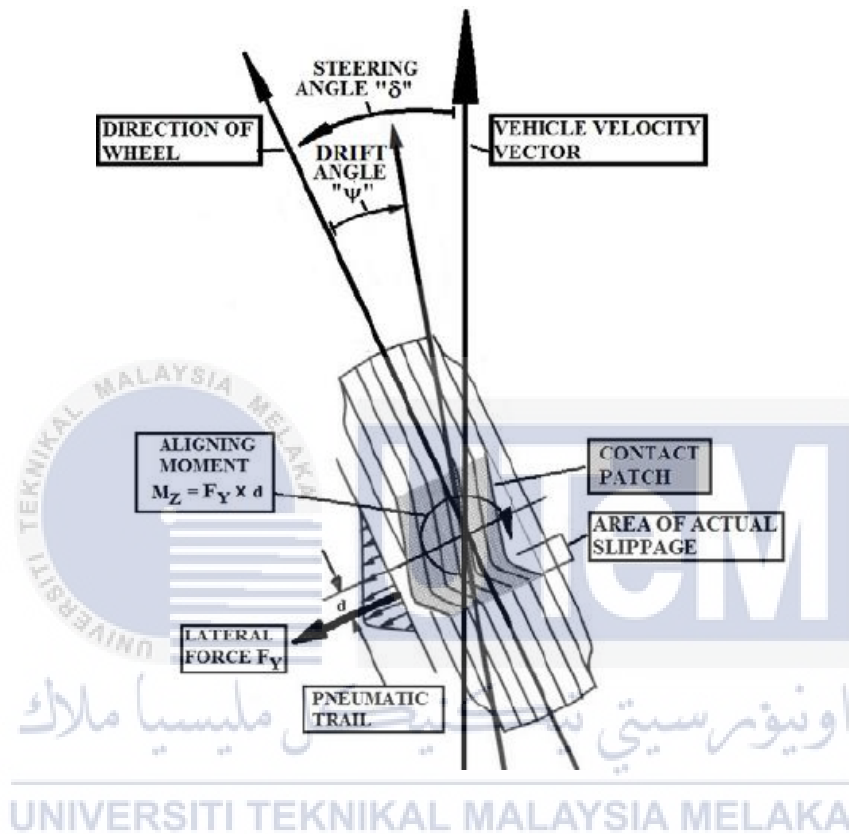


Figure 2.6: Tire slip condition [22]

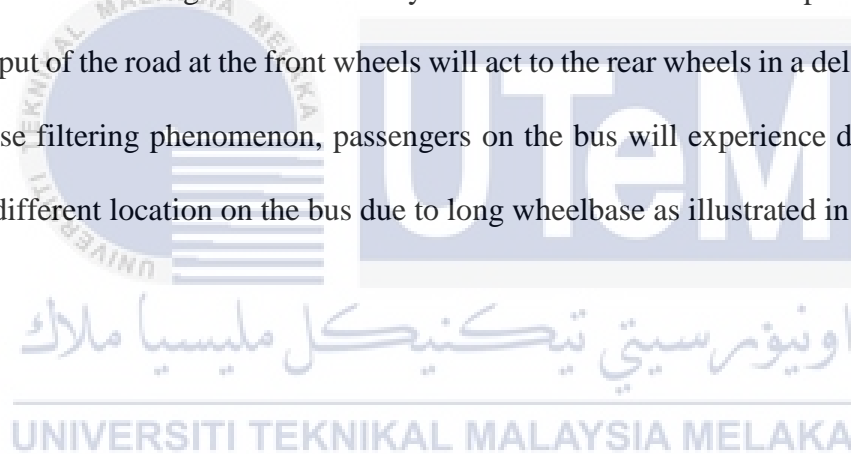
2.7 Vehicle dynamic analysis

2.7.1 Ride

Ride quality of a vehicle can be evaluated by the comfort of the driver and passenger when the vehicle is travelling through an uneven road surface. The ride comfort can be maximized by minimizing the vehicle body acceleration as the vibration from the uneven road surface is transmitted to the body of driver and passenger through the vehicle body acceleration

[21]. As from this criteria, vertical acceleration of vehicle's sprung mass can be analysed to determine the ride comfort of the vehicle.

In order to analyse the ride quality of a vehicle, we must understand three main criteria which are ride excitation sources, basic mechanics of vehicle vibration response and human perception and tolerance of the vibrations [11]. The ride excitation sources from the road roughness, tire or wheel, driveline and engine. The basics mechanics of vehicle vibration response influence the magnitude and direction of vibrations transmitted to the passenger. Human perception and tolerance of vibrations is important to determine the ride quality of the vehicle. Wheelbase filtering is the time delay acts to filter the bounce and pitch motion as the roughness input of the road at the front wheels will act to the rear wheels in a delayed time. With this wheelbase filtering phenomenon, passengers on the bus will experience different vertical vibration at different location on the bus due to long wheelbase as illustrated in **Figure 2.7**.



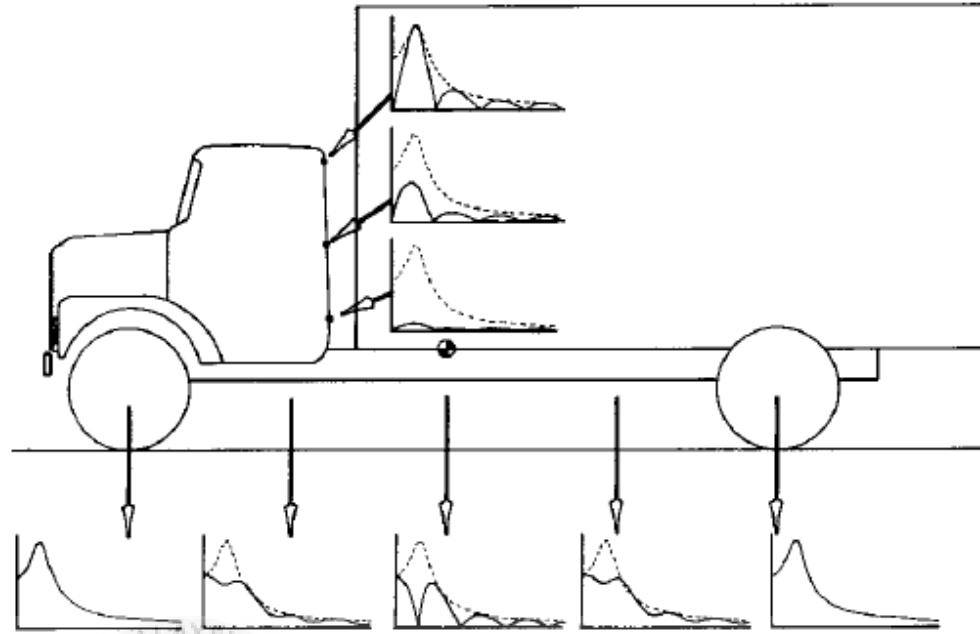


Figure 2.7: Vertical and longitudinal vibration response gain [11]

The value of the vehicle pitch affect the ride comfort of the vehicle. It can be determined by analysing the value of overshoot pitch when the vehicle hit the bump on the road [12]. The lower the value of overshoot pitch, the more comfort the vehicle. When the amplitude of overshoot increase, the vehicle will get a great amount of vibration that resulting in low level of comfort and damage to the vehicle due to a lot amount of wear and tear in the system.

For further understanding of the pitch motion of the vehicle, a simple simulation of braking is performed, the negative pitch angle and negative heave displacement, which is the equal vertical motion of the front and rear of the car, represent the motion of vehicle that is pitching forward and CG is moving upward with respect to ground [13]. From this simulation, it can shows that the vehicle response will change at different speed and also at different road geometries.

2.7.2 Handling

Handling of the vehicle is related with the cornering behaviour of the vehicle [11]. It is the responsiveness of the vehicle to driver input for controlling the car as the test for determining the handling requires the steering input from the driver during lane changing. The handling behaviour of the car during cornering or turning will be tested at low and high speed because it will shows different behaviour at different speeds. Vehicle response to specific steering input can be measured by understeer gradient. Handling performance of a vehicle is directly related to the understeer gradient [5]. A larger positive value for understeer gradient corresponds to a stabilizing effect at the cost of less responsiveness of the vehicle whereas a negative understeer gradient, which also defined as oversteer, results in loss of yaw stability at a certain critical speed and will cause the car to drift away from the actual path. The quality of handling is related to the vehicle response to driver's commands and the ability to stabilize motion from external disturbances [23].

An experiment were carried out by using a test car to determine the vehicle dynamics behaviour during lane changing in different speeds, it resulting in a large peak amplitude of yaw angle produced for the car that is travelling with higher speed compared to the lower speed. This different value is due to a bigger inertia value that is carried out by higher speed car that will produce a larger value of yaw angle [14]. From this experiment, it can be conclude that the higher the speed of vehicle, the bigger the yaw angle that will be produced.

Vehicle lateral acceleration is a significant influence to the safety aspect of the vehicle but there is still no standards available regarding the performance of vehicle lateral acceleration [22]. As for the limit of the vehicle lateral acceleration, it can be generalized that the higher the maximum lateral acceleration limit of a vehicle, the safer the vehicle in the event of cornering or turning.

There are three conditions that will occur during cornering which are neutral steer, understeer and oversteer [23]. Neutral steer occurs when understeer coefficient is equal to zero ($K_s = 0$) in the condition of the front and rear tires slip angle are equal. As for understeer condition, the value of understeer coefficient is greater than zero ($K_s > 0$) in the condition of front tire slip angle is higher than rear tire slip angle ($\alpha_f > \alpha_r$). In order to negotiate a given curve, the steer angle must be increased with the lateral acceleration. Oversteer condition occurs when the front tire slip angle is lower than rear tire slip angle ($\alpha_f < \alpha_r$) and the understeer gradient is lower than zero ($K_s < 0$). When negotiating a given curve, the steer angle must decrease when the lateral acceleration increase. These three conditions during cornering are represented as in **Figure 2.8**.

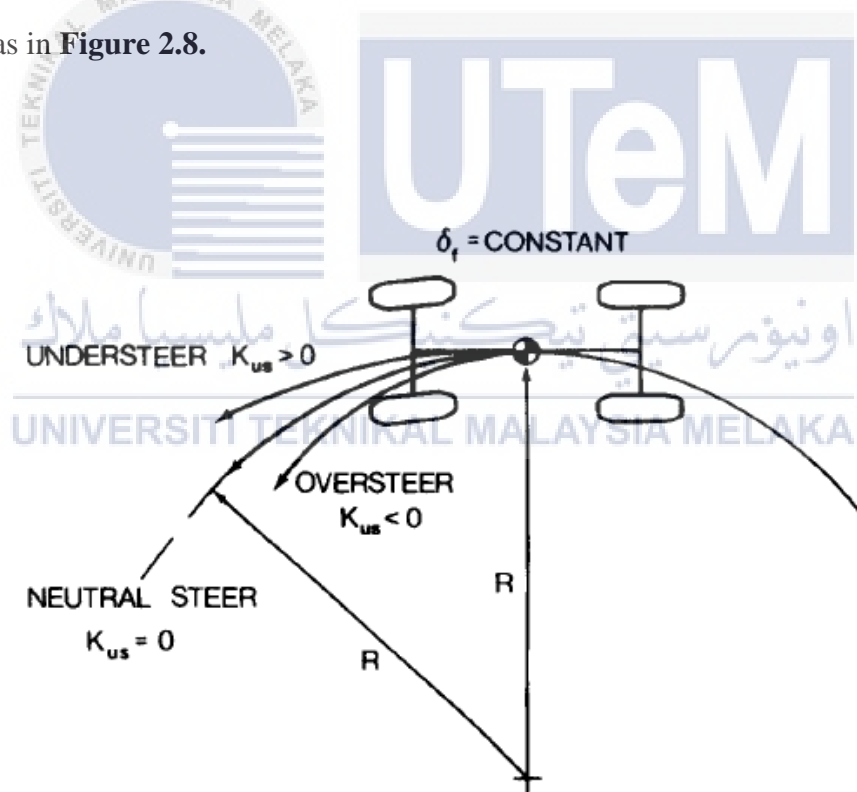


Figure 2.8: Curvature response of the vehicle [23]

2.7.3 Stability

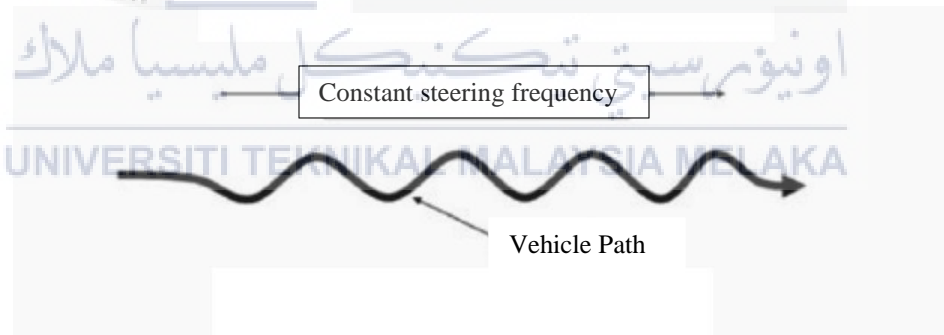
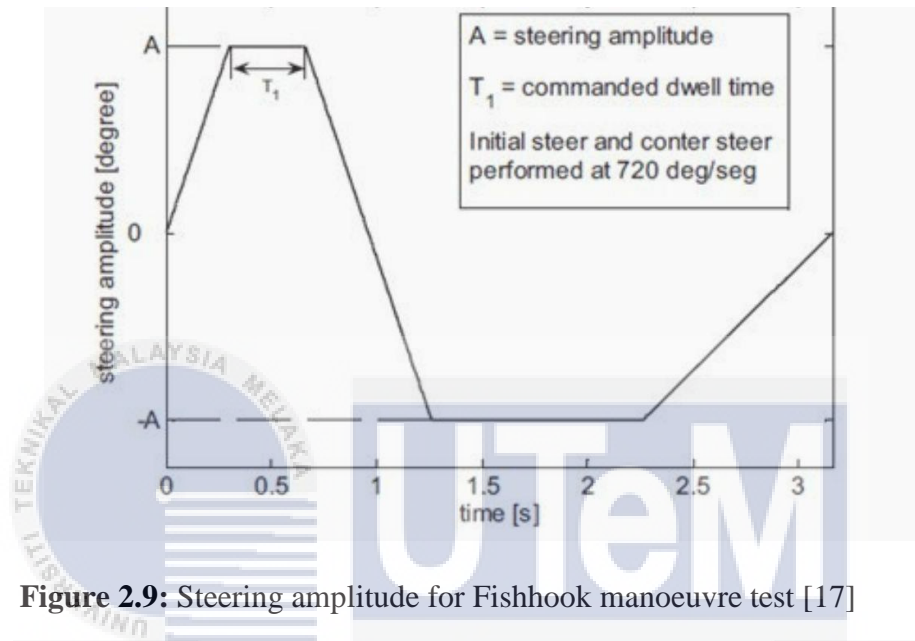
The stability of the vehicle is mainly affected by the vehicle roll behaviour. Vehicle roll behaviour is defined by the roll centre of axle or bogie. The chassis rolls around the roll centre respective to the axle or bogie. It is located in between the link of sprung mass and un-sprung mass and the lateral forces is transmitted to this point. Lateral acceleration is not the only the influence for risk of vehicle rollover, but a function of roll angle and roll angle rate also influence the risk. The risk for rollover can be considered low as long as the roll angle rate is zero and not causing any wheel lift yet or in the opposite direction even at high lateral acceleration [5].

Based on study done on the effect of the track width ratio, wheel base and centre of gravity height to the vehicle stability [15], a lower track width ratio can increase the tendency of vehicle to rollover and wheel base ratio can affect the vehicle directional stability during manoeuvre.

Lateral acceleration influenced the large vehicle safety [16]. The centre of gravity for large vehicle is higher compared to passenger cars. As for large vehicle, rollover occurs typically at 4 ms^{-2} lateral acceleration while passenger cars experience rollover at lateral acceleration of 10 ms^{-2} which clearly indicates that passenger cars have higher roll stability. Centre of gravity for large vehicle located far behind mid-point between axles compared to passenger cars that have the centre of gravity approximately symmetrical between front and rear axle.

Based on study done to investigate untipped rollover of light vehicles, there are two simulation tests that have been carried out to test the stability of the vehicle which are modified fishhook and the sine manoeuvre test [17]. The description of tests that have been done are as **Figure 2.9 and Figure 2.10**. Based on simulation results, it clearly indicate that fishhook manoeuvre evaluates the vehicle's roll instability and sine manoeuvre tests the vehicle's yaw instability. Rollover resistance capability in fishhook manoeuvre test can be improved by

increasing the suspension stiffness and the trade-off of this improvement affect the performance of the vehicle in the sine manoeuvre test which resulting in rollover due to increased yaw instability.



2.8 Vehicle test

2.8.1 Bounce sine sweep test

Bounce sine sweep test is done to represent the road roughness as the test track contain deviation in elevation [11]. The uneven surface of the road is the vertical displacement input to the wheels and resulting in ride vibrations. The ride vibration also can be measured in the form of velocity and acceleration input at the wheels for further understanding in dynamics of ride. The vertical input to the wheels can excite bounce and pitch motion to the vehicle when undergo the test. The test is carried out by driving through the bus across the sine form surface of test track as shown in **Figure 2.11**.



Figure 2.11: Bounce sine sweep test procedure

As the road surface of the bounce sine sweep test contain irregularities, it can be the source of vibration to the vehicle in order to determine the vehicle dynamic behaviour [21]. Vibration from the road surface irregularities will resulting in the vehicle body pitch, roll and tire elevation.

2.8.2 Double lane change

The purpose of double lane change test carried out is to determine and analyse the road holding capability and handling characteristics of the vehicle [18]. The procedure for this test

the vehicle must be driven from its initial lane to another parallel lane and changing it back to the initial lane in sequential form as in **Figure 2.12**. During the event of changing the lane, the vehicle must not exceed the lane boundaries. Oversteer can occur and resulting in the skidding of the vehicle right after the second lane change and it representing the handling behaviour of the vehicle. All the data obtained from the test can be used the setup of vehicle steering and chassis.



Figure 2.12: Double lane change test procedure

Based on study done on lane changing at different speed, the higher the speed of the vehicle during lane changing will resulting in high yaw angle and the abrupt change in steer angle can cause the tire to experience slipping and it is more difficult to control the car from drifting away [14]. So, it is recommended to changing lane at lower speed as the yaw produced is lower and the larger base of steer angle that will provide more grip during changing lane.

A study done shows that the different chassis models of various complexity resulting in minor difference in the value of roll and pitch when performing double lane change manoeuvre [19]. This results shows that the usage of low order models is acceptable when designing on board optimization-based safety systems in order to improve the safety of the vehicle when performing double lane change.

2.8.3 J-turn test

The tendency for the vehicle to experience rollover can be evaluated by using J-turn test [20]. The test represent the ability of the vehicle to avoid obstacle in emergency, chasing trail and detecting roll stability limit of the vehicle. The test can be classified as one of the worst driving conditions in order for the vehicle to be capable of maintaining its stability in real world driving condition. **Figure 2.13** shows the trail of J-turn type test.

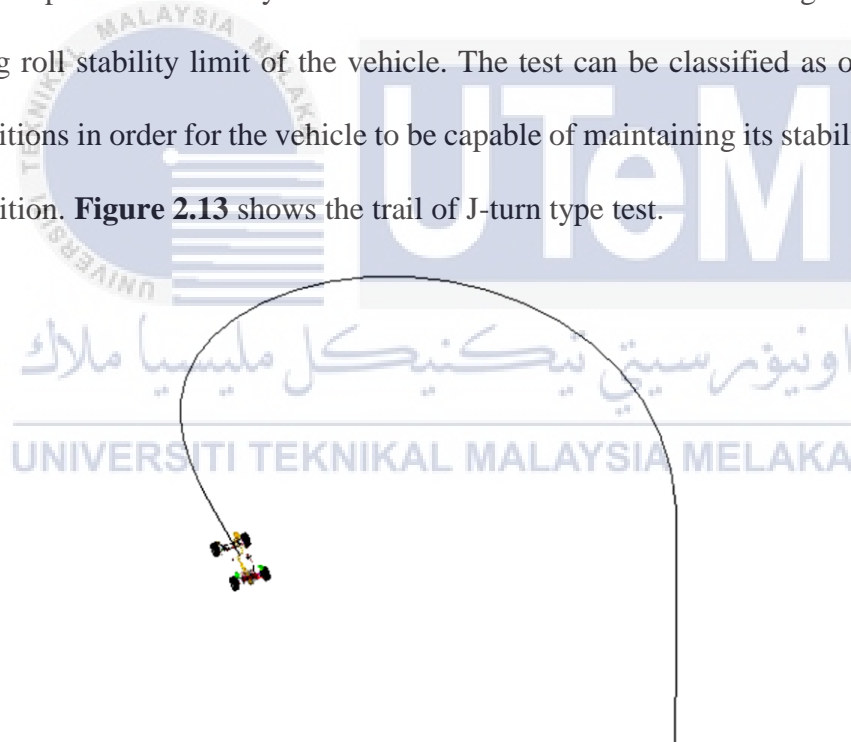


Figure 2.13: The trail of J-turn type test [20]

2.8.4 Test output results

The test output results for every test are chosen based on the importance of the data that influence the behaviour of the vehicle during test manoeuvre. One of the example to follow as a guide to choose the data that influence the behaviour of the vehicle is by referring the input data for ESC system. ESC system will triggered when the certain limit for a particular data is reached which means that the vehicle is exceeding the limit when manoeuvring and the system will give feedback to the vehicle for correcting the error [25]. This simulation test will be further analysed on the maximum value of every output that the vehicle produced during manoeuvre.

The components that are available in ESC system are a controller that uses algorithm, four individual wheel speed sensors (WSS), a steering angle sensor (SAS), yaw rate sensors, longitudinal sensors and accelerometers. WSS detect the vehicle's wheel speed and give input to the ESC module. The wheel speed is related to the vehicle target speed when changing the test parameters for different speeds. The accelerometers function to detect a variation in direction of the vehicle movement in all axis. It will give output which is related to the vehicle's CG trajectory, vertical acceleration and roll angle during manoeuvring. Yaw rate sensor will identify the rate of rotation for the vehicle and measure how much the vehicle deviate from the axis that resulting in rolling or tilting when taking a turn. So, the vehicle's yaw angle must be taken into account for the analysis. Next, lateral acceleration sensor detects the rate of change in Y axis direction movement to calculate vehicle's actual position during a turn. During handling and stability test, the vehicle will move in Y axis direction and the lateral acceleration data is important for the analysis. All of the data are related to each other to determine the behaviour of vehicle during the tests.

CHAPTER 3

METHODOLOGY

3.1 Introduction

This chapter will cover about the methodology that being used in order to complete this project. As a reference to start the analysis on dynamic performance of large commercial vehicle, literature review is done to collect information regarding this subject and further understanding on the vehicle dynamic system. Next, the test simulation for the dynamic performance is done by using TruckSim simulator and the data is collected and analyzed by using Microsoft Excel. The gantt chart for this project are based on **Appendix A and B**.

3.2 Literature review

Literature review is done for gathering information and further understanding in vehicle dynamic performance studies. As a reference for this literature review, a number of books, journals and websites that are related to this project being reviewed thoroughly. From all of these reviews, the test parameters that need to be analyzed for dynamic performance are identified.

3.3 Vehicle specification

The vehicle specification is set before starting the simulation. The specification are based on bus specification that is already available in the market. TruckSim simulator is used to set

the specification of the bus and Tour Bus 5.5T/10T is chosen as the vehicle type for this entire simulation as in **Figure 3.1**.



Figure 3.1: Vehicle type for simulation

Specification of the bus consist of four main criteria which are Powertrain, Vehicle Dimension, Tire and Suspension. The general specification of the bus are shown in **Table 3.1** and **3.2**.

Table 3.1: General specification 1

Powertrain		
	Type	
Configuration	4X2, RWD	
Engine	Diesel, 6 Cylinder	
Power	175kW @ 3000RPM	
Transmission	Manual, 7 speed	
Clutch	Maximum 900 Nm (Linear)	
Differential	Open differential, Gear Ratio – 5.0	
Steer torque	1/25	
Vehicle dimension		
Length	4490 mm	
Height	2920 mm	
Width	2348 mm	
Wheelbase	4490 mm	
Track width	2030 mm (Front), 1863 (Rear)	
Height of CG	1200 mm	
Sprung mass (Fully laden)	6360 kg	
Sprung mass (unladen)	4500 kg	
Tire		
	Front Axle	Rear Axle
Configuration	Single Tire	Dual Tires
Spacing	-	310mm
Width	265 mm	265 mm
Rating	3000kg	3000kg
Rolling radius	510mm	510mm

Table 3.2: General Specification 2

Suspension System		
	Front Axle	Rear Axle
Kinematics	5.5t steer, single wheel	10t drive, dual wheels
Type	6t air suspension, +150mm, - 60mm travel	6t air suspension, +150mm, - 60mm travel
Spring rate	250N/mm	250N/mm
Brake Torque	7.5kNm	10kNm
Steering gear ratio	25	-
Steering System		
Steering gear ratio	25	
Steer torque	1/25	
Brake System		
	Front	Rear
Type	Air	Air
Brake Torque	7.5 kNm	10 kNm

As for the Powertrain, the vehicle configuration that is chosen for this bus is 4X2 and rear wheel drive (RWD). All the power from the 6 cylinder diesel engine is transferred to the rear axle. **Figure 3.2** shows the power flow from the engine to the rear axle of the bus. The engine produced 175 kW of power at the engine speed of 3000 RPM. Transmission that is selected for this bus is 7 speed manual transmission which is commonly used in Malaysia. Maximum torque for the clutch model used is 900 Nm in linear configuration. The differential

at the rear axle is open differential type with a gear ratio of 5.0. A typical steer torque is used at 1/25 ratio of steering-wheel torque and total kingpin moment.

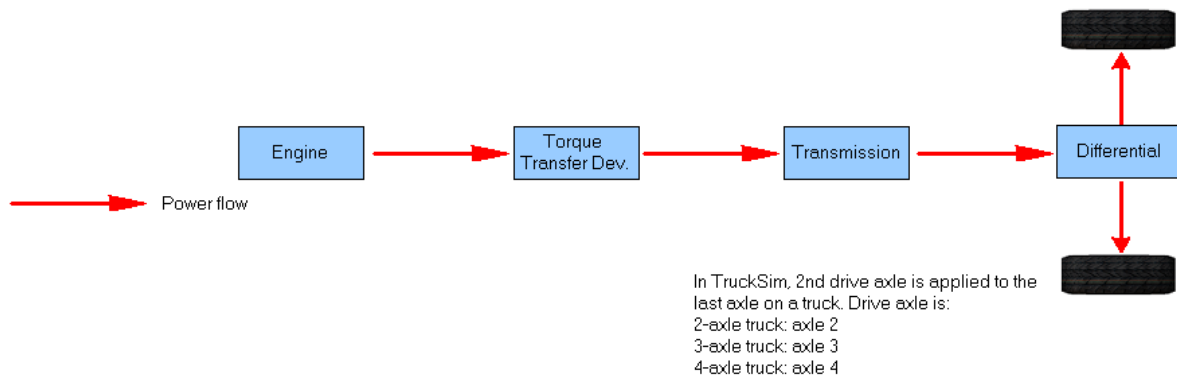


Figure 3.2: The power flow of the bus (RWD)

The vehicle dimension is 4490 mm in length, 2920 mm in height and 2348 mm in width. Wheelbase for this bus is 4490 mm. The track width for the front axle is 2030 mm and 1863 mm for rear axle. Height of the centre of gravity is rated at 1200 mm. The sprung mass is set at 6360 kg.

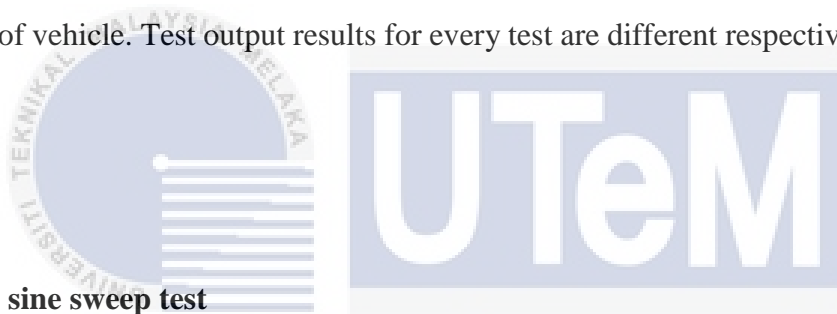
This bus consist of two axle, front and rear, with single tire configuration at the front axle and dual tire configuration at the rear axle. Same type of tires are used for both front and rear axle. The tire width is 265 mm. The spacing of the dual tire configuration is 310 mm. Type of tire used is 3000 kg load rated with effective rolling radius of 510 mm. The spring rate for the tire is 980 N/mm and the maximum allowed force for the tire is 1000000 N.

Suspension system for this bus is same for both front and rear axle which use 6 tonne air suspension. The stroke for this suspension is +150 mm and -60 mm in vertical direction. Damper for this suspension system is rated at 10 kNs/m which is the ratio of shock force over shock

compression rate. The spring rate used for this suspension system is 250 N/mm. For front axle, the suspension kinematics is 5.5 tonne steer axle with the unsprung mass of 570 kg. Roll and yaw inertia for front axle is 335 kgm². As for the rear axle, the bus use 10 tonne drive suspension kinematics with the unsprung mass of 760 kg. Roll and yaw inertia for rear axle is 295 kgm².

3.4 Test simulation

Test simulation is done to determine the dynamic performance of the vehicle when travelling at different speed and different mass. Three type of test are simulated to the same specification of vehicle. Test output results for every test are different respective to the point of interest.



3.4.1 Bounce sine sweep test

Bounce sine sweep test is simulated to test the ride quality of the vehicle. The vehicle is simulated to be driven through a test track that has sine form surface to represent the uneven road surface in real world driving condition. Before starting the simulation, test procedure, test parameters and test output results must be set. The procedure for the test is set to Bounce Sine Sweep Test that is located under ride test as in **Figure 3.3**. The first test parameter that need to be tested is vehicle's target speed which is set to three different speed for each simulation run as in **Figure 3.4** under Driver Controls which is based on Malaysia speed limit at residential area standard, 35 km/h. The speed is reduced to 25 km/h and added up to 45 km/h based on the standard speed for determining the effect of different speed on vehicle behaviour. The next test parameter is the vehicle's mass in fully laden and unladen condition. The vehicle is initially set

to fully laden condition which follow the standard speed of 35 km/h and being compared to the unladen vehicle condition at the same standard speed. There are 30 seats that are available in the bus and the mass for one passenger is set based on standard mass of 62 kg. Unladen vehicle condition means that there is only a driver on board while fully laden vehicle condition is when 30 passengers on board. The vehicle mass is set to 4500 kg for unladen condition and 6360 kg for fully laden condition based on **Figure 3.5**. Test output results are set to 4 types; Ground Elevation, Vertical Acceleration of Sprung Mass CG's, Pitch Angle of Sprung Mass and Tire Forces at 3 axis which will be presented in form of graph plot and 3D vehicle animation. Next, the math model for this test is run by the simulator's Built-In Solvers.

The test track surface is represented by the ground elevation of tire as in **Figure 3.6** which is in sine form. The graph shows the ground elevation for front right tire labelled as R1. The ground elevation is the measurement of the distance of the tire in Z-axis from the initial position to the elevated position of tire when going through the uneven surface of the road. The displacement of the tire decreasing as the vehicle is driven through the surface because the suspension system dampen the vibration from the road surface and decrease the length of suspension travel.

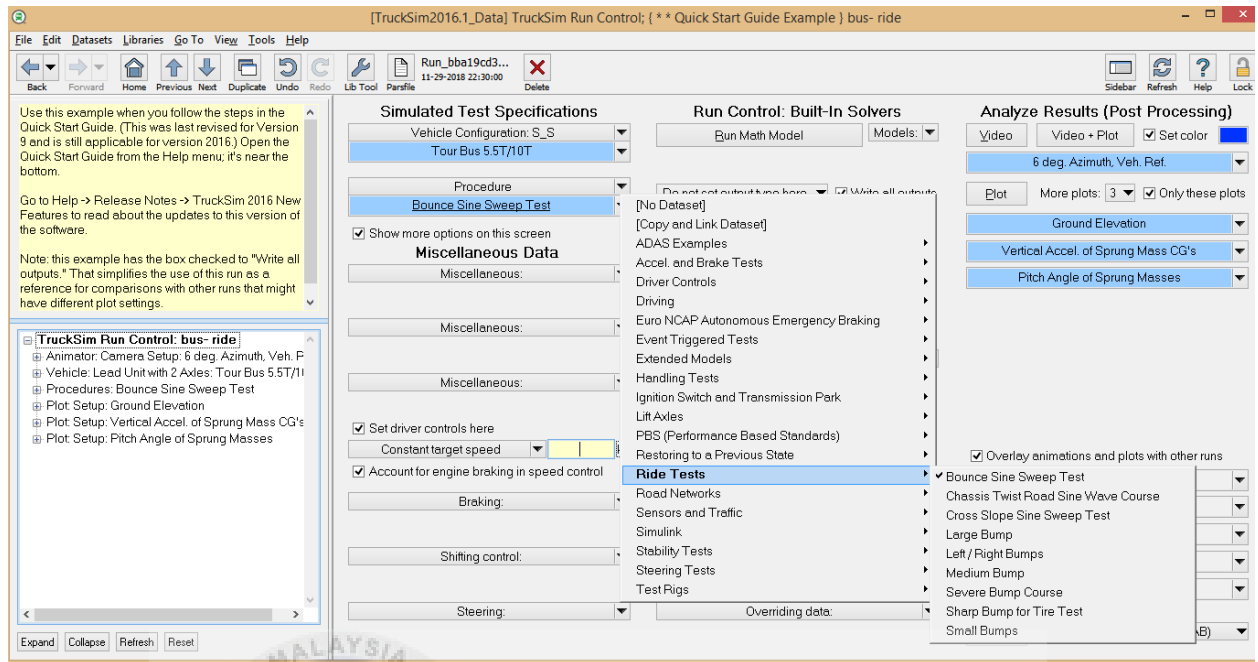


Figure 3.3: Selection of test procedure

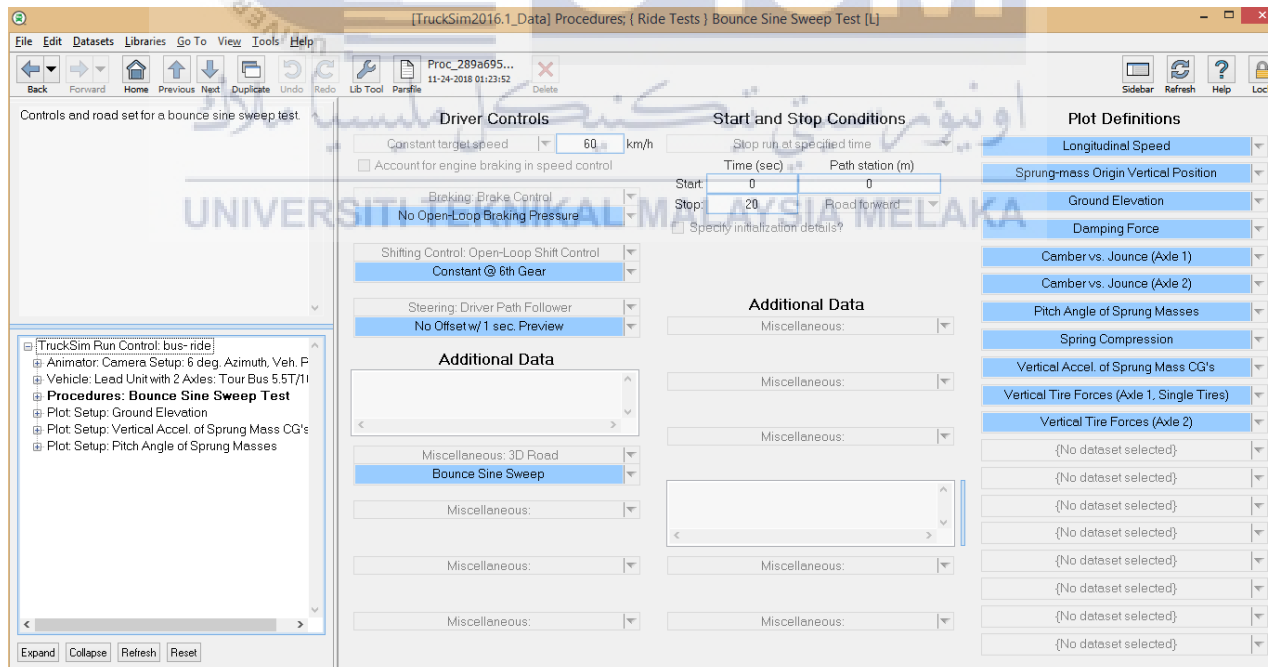


Figure 3.4: Setup the vehicle's target speed

Height (for animator):

Length (for animator):

Width (for animator):

Lateral coordinate of mass center:

Mass center of unladen sprung mass:

Origin of sprung mass coordinate system

All dimensions and coordinates are in millimeters

☐ Frame Torsional Flexibility and Suspended Cab

Check this box to use optional, more detailed math models. The optional models include the effects of torsional flexibility of the chassis (frame) of the lead unit and all trailers, and a further option to define a suspended cab.

The extended models require a separate license feature.

The inertial properties are for the sprung mass in the design configuration, with no additional loading

☒ Edit radii of gyration
 Sprung mass: kg
 Roll inertia (Ixx): kg-m²
 Pitch inertia (Iyy): kg-m²
 Yaw inertia (Izz): kg-m²
 Product (Ixy): kg-m²
 Product (Ixz): kg-m²
 Product (Iyz): kg-m²

Radii of gyration:
 Rxc: m
 Ry: m
 Rz: m

Inertia and radius of gyration are related by the equation: $I = M \cdot R^2$

Radii must be specified with numbers; formulas are not supported

Miscellaneous:

Figure 3.5: Setup the vehicle's mass

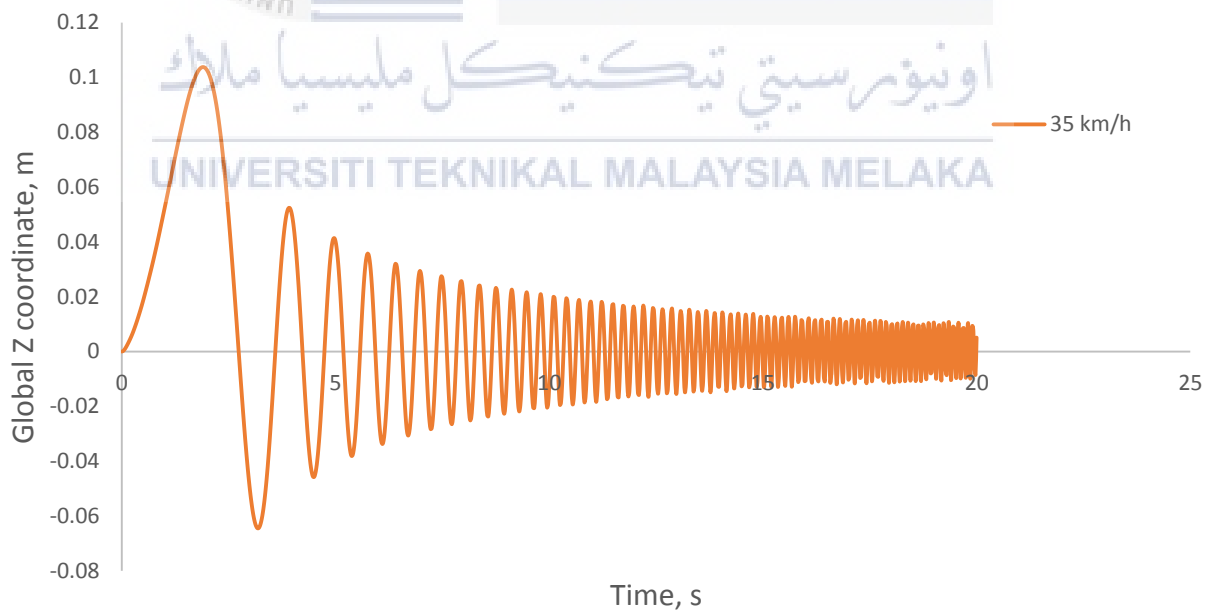


Figure 3.6: Ground elevation of tire R1 for standard speed

The test simulation is run and presented by using VS visualizer in form of graph plot based on test parameters and 3D vehicle animation as in **Figure 3.7**. Three simulation run are done by using the same steps as before but with different vehicle's target speed.

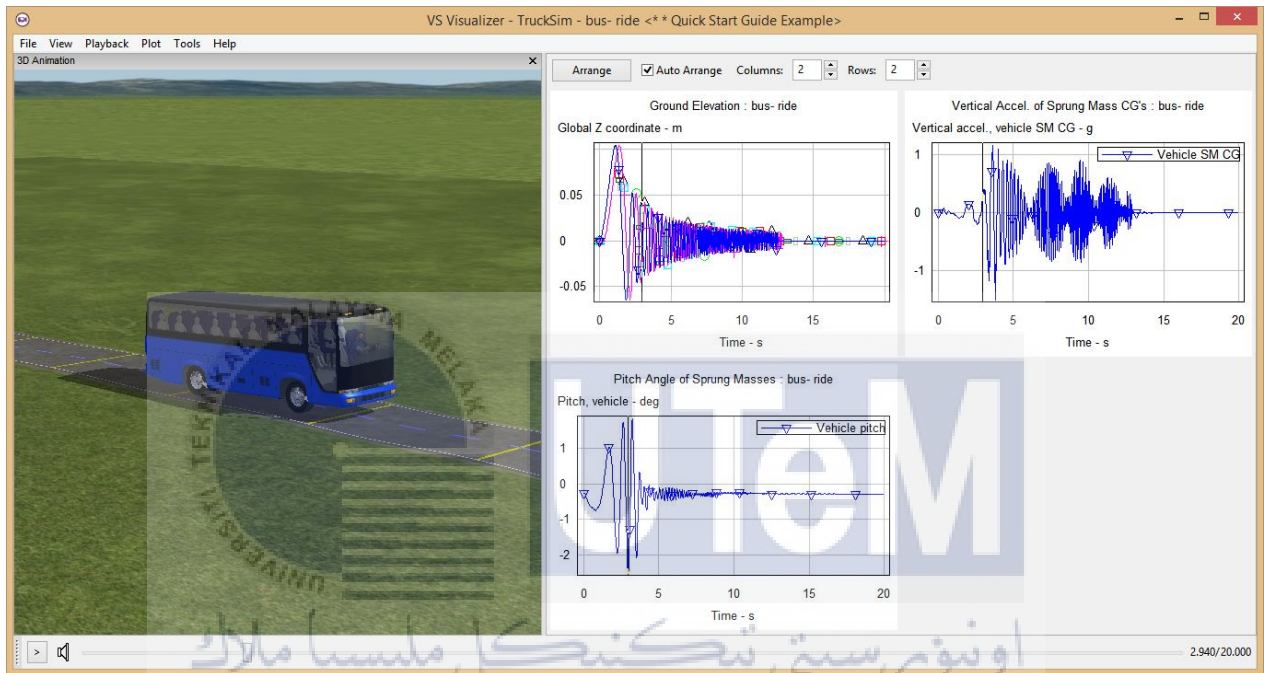


Figure 3.7: Graph plot and 3D vehicle animation

3.4.2 Double lane change

Double lane change test is simulated to test the handling of the vehicle when steering angle is changed abruptly. The vehicle is simulated to change lane just like overtaking a vehicle in real world driving situation. Before starting the simulation, test procedure, vehicle's target speed and the test parameters must be set. The procedure for the test is set to Double Lane Change that is located under Handling Test as in **Figure 3.8**. Vehicle's target speed is set to three different speed for each simulation run which is based on National speed limit for heavy

vehicle, 90 km/h as in **Figure 3.9** under Driver Controls. The speeds are reduced to 70 km/h and increased to 110 km/h based on the standard speed for determining the behavior of the vehicle at different speeds. The next test parameter is the vehicle's mass in fully laden and unladen condition. The vehicle is initially set to fully laden condition which follow the standard speed of 90 km/h and being compared to the unladen vehicle condition at the same standard speed. There are 30 seats that are available in the bus and the mass for one passenger is set based on standard mass of 62 kg. Unladen vehicle condition means that there is only a driver on board while fully laden vehicle condition is when 30 passengers on board. The vehicle mass is set to 4500 kg for unladen condition and 6360 kg for fully laden condition based on **Figure 3.10**. Test parameters are set to 4 types; Y vs X-Trajectory, Lateral Acceleration of CG's, Yaw Angle of Sprung Mass and Tire Forces at 3 axis which will be presented in form of graph plot and 3D vehicle animation. Next, the math model for this test is run by the simulator's Built-In Solvers.

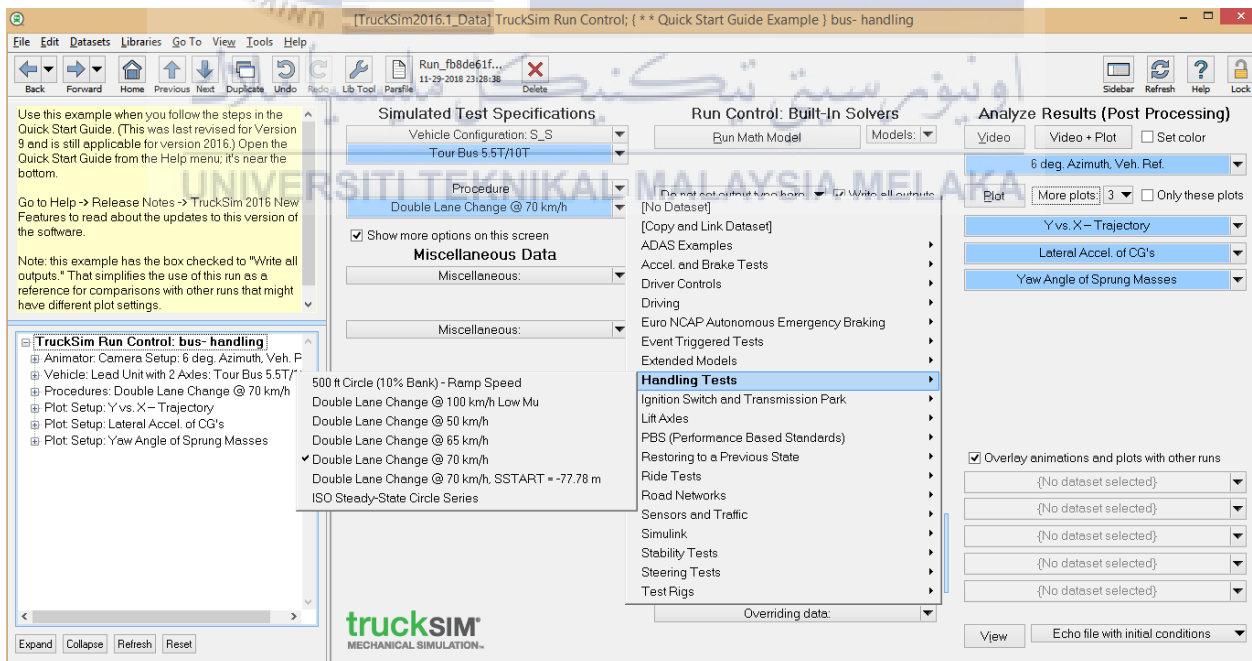


Figure 3.8: Selection of test procedure

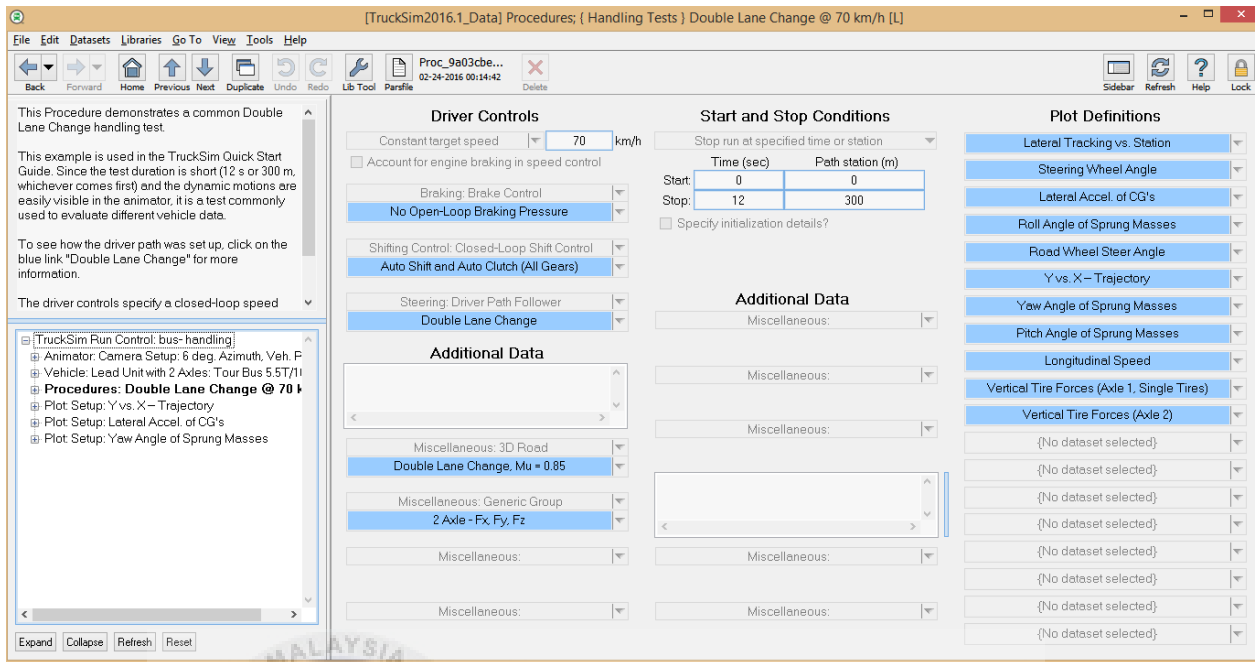


Figure 3.9: Setup the vehicle's target speed

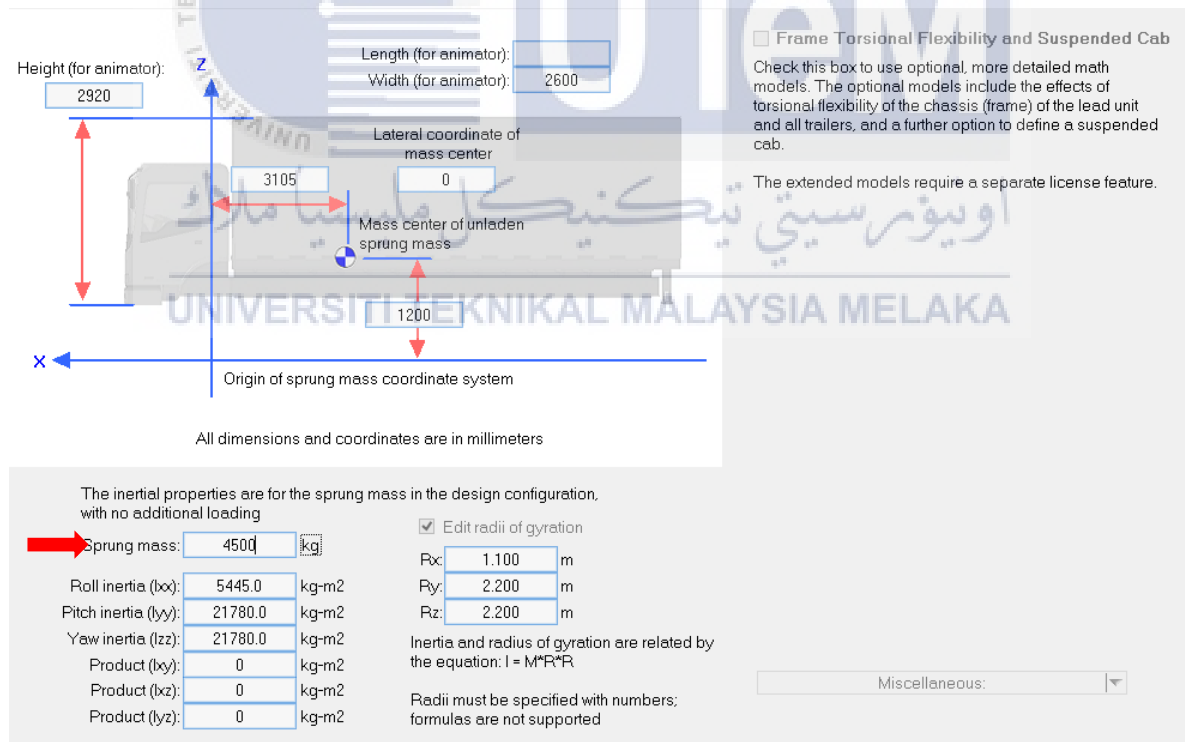


Figure 3.10: Setup the vehicle's mass

The test procedure that the vehicle need to follow is represented as in **Figure 3.11**. It shows the targeted trajectory of vehicle that must be followed by the vehicle during the test. At region A, the vehicle is the phase of vehicle changing into another lane and the trajectory is increasing until region B where the vehicle is at the left-end of the lane which can be considered as the highest displacement of the car from the original lane. Region C is where the vehicle is in the phase of changing into the original lane. The simulation run result will be compared with the targeted trajectory for the analysis.

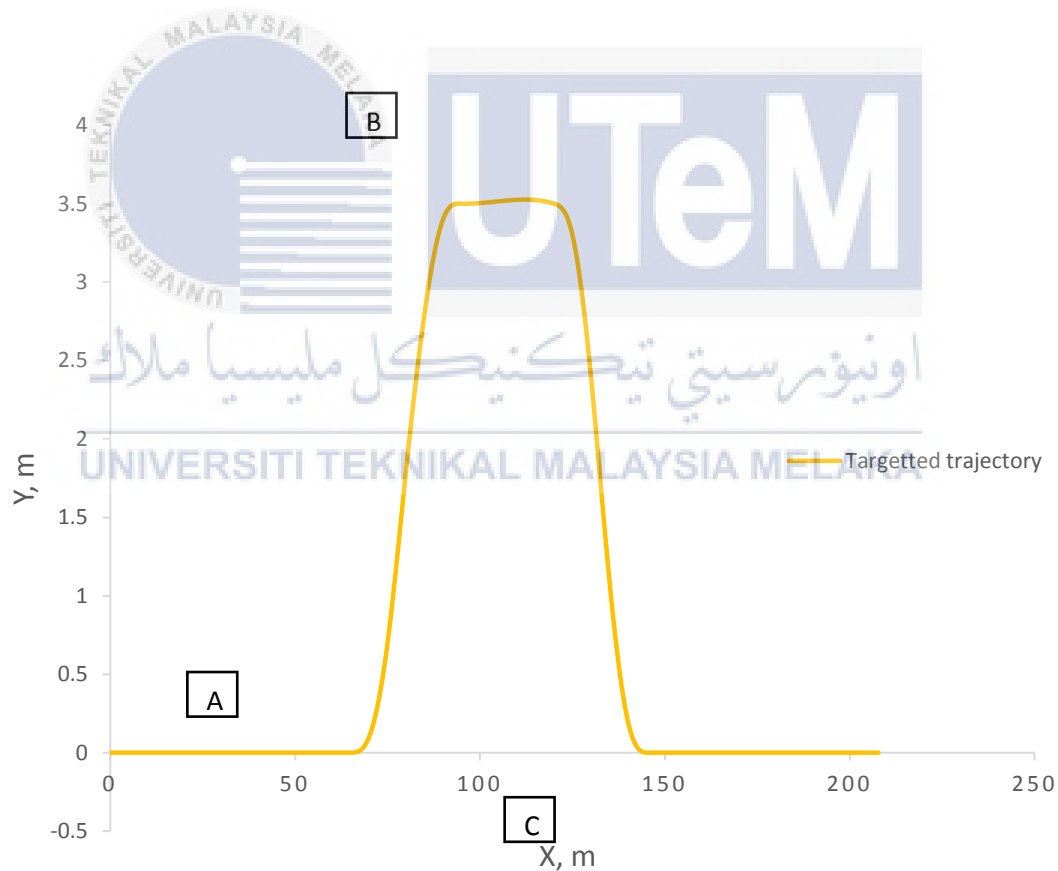


Figure 3.11: Test procedure in form of vehicle trajectory.

The test simulation is run and presented by using VS visualizer in form of graph plot based on test parameters and vehicle animation as in **Figure 3.12**. Three simulation run is done by using the same steps as before but with different vehicle's target speed.

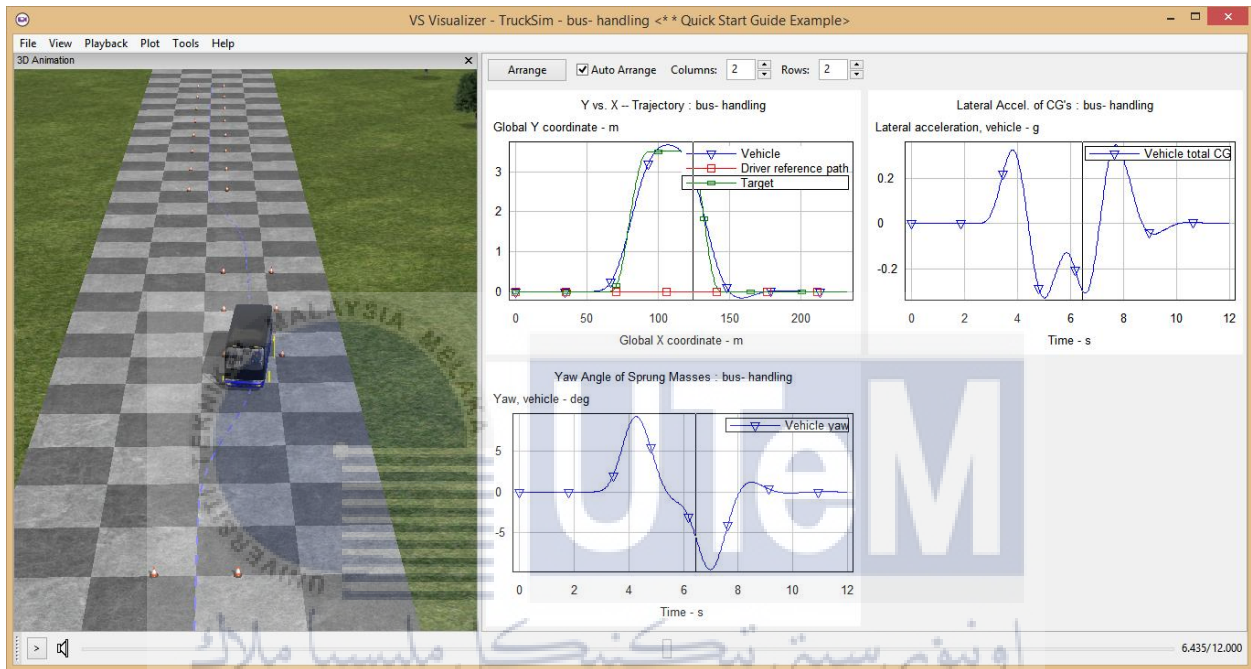


Figure 3.12: Graph plot and 3D vehicle animation

3.4.3 J-turn type test

J-turn type test is simulated to test the stability of the vehicle during cornering. The vehicle is simulated to represent the ability of vehicle to avoid obstacle in emergency situation.. Before starting the simulation, test procedure, vehicle's target speed and the test parameters must be set. The procedure for the test is set to J-Turn type Stability Testing that is located under Stability Test as in **Figure 3.13**. Vehicle's target speed is set to three different speed which is based on J-turn test criteria of NTHSA, 45 km/h as in **Figure 3.14** under Driver Controls [24].

The speeds are reduced to 35 km/h and 25 km/h based on the standard speed because the test criteria stated that the vehicle must not exceed 45 km/h after entering the starting gate of the test. The next test parameter is the vehicle's mass in fully laden and unladen condition. The vehicle is initially set to fully laden condition which follow the standard speed of 45 km/h and being compared to the unladen vehicle condition at the same standard speed. There are 30 seats that are available in the bus and the mass for one passenger is set based on standard mass of 62 kg. Unladen vehicle condition means that there is only a driver on board while fully laden vehicle condition is when 30 passengers on board. The vehicle mass is set to 4500 kg for unladen condition and 6360 kg for fully laden condition based on **Figure 3.15**. Test parameters are set to three type; Y vs X-Trajectory, Lateral Acceleration of CG's, Yaw Angle of Sprung Mass, Roll Angle of Sprung Mass and Tire Forces at 3 axis which will be presented in form of graph plot and 3D vehicle animation. Next, the math model for this test is run by the simulator's Built-In Solvers.

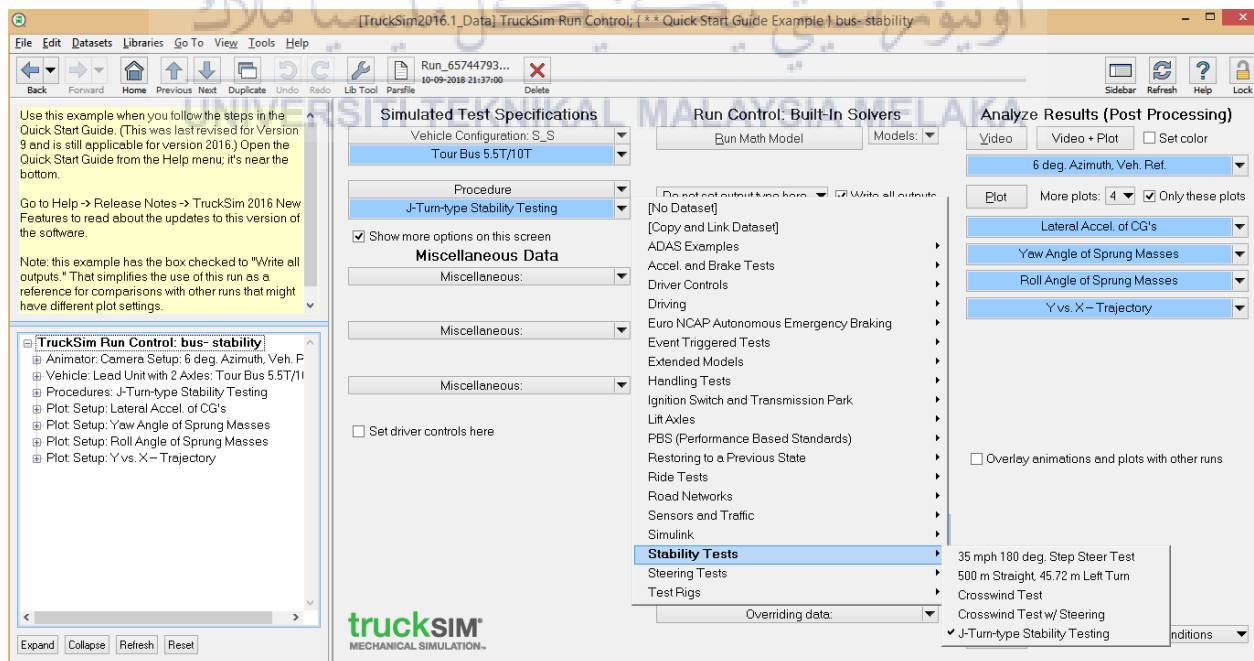


Figure 3.13: Selection of test procedure

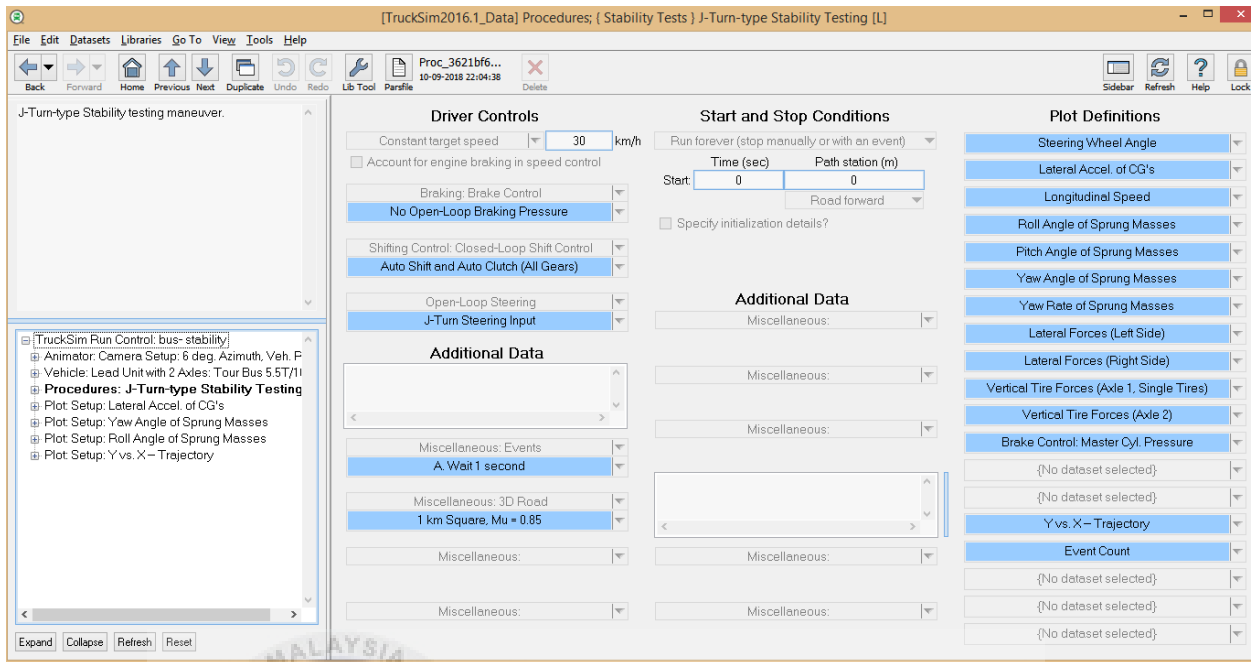


Figure 3.14: Setup the vehicle's target speed

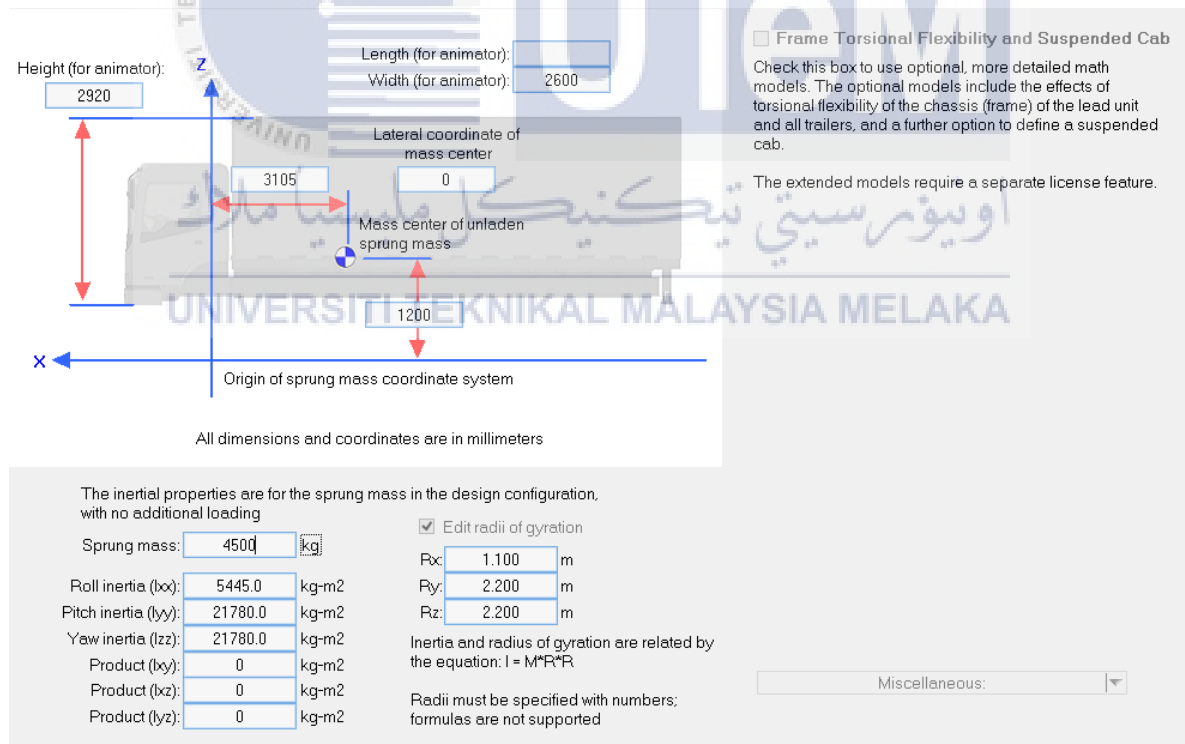


Figure 3.15: Setup the vehicle's mass

The test procedure that the vehicle need to follow is based on **Figure 3.16**. The trajectory is based on coordinate of X-Y plane. Positive Y coordinate indicates that the vehicle is moving to the left while negative Y coordinate indicates that the vehicle is moving to the right. The Y coordinate starting to increase when the vehicle receive steering input to the left until the maximum Y coordinate and the counter steering input the right is applied which resulting in decreasing value of Y coordinate. The steering input applied are based on the J-turn type test. The vehicle trajectory with different parameters will be compared to the trajectory of vehicle at standard speed of 45 km/h.

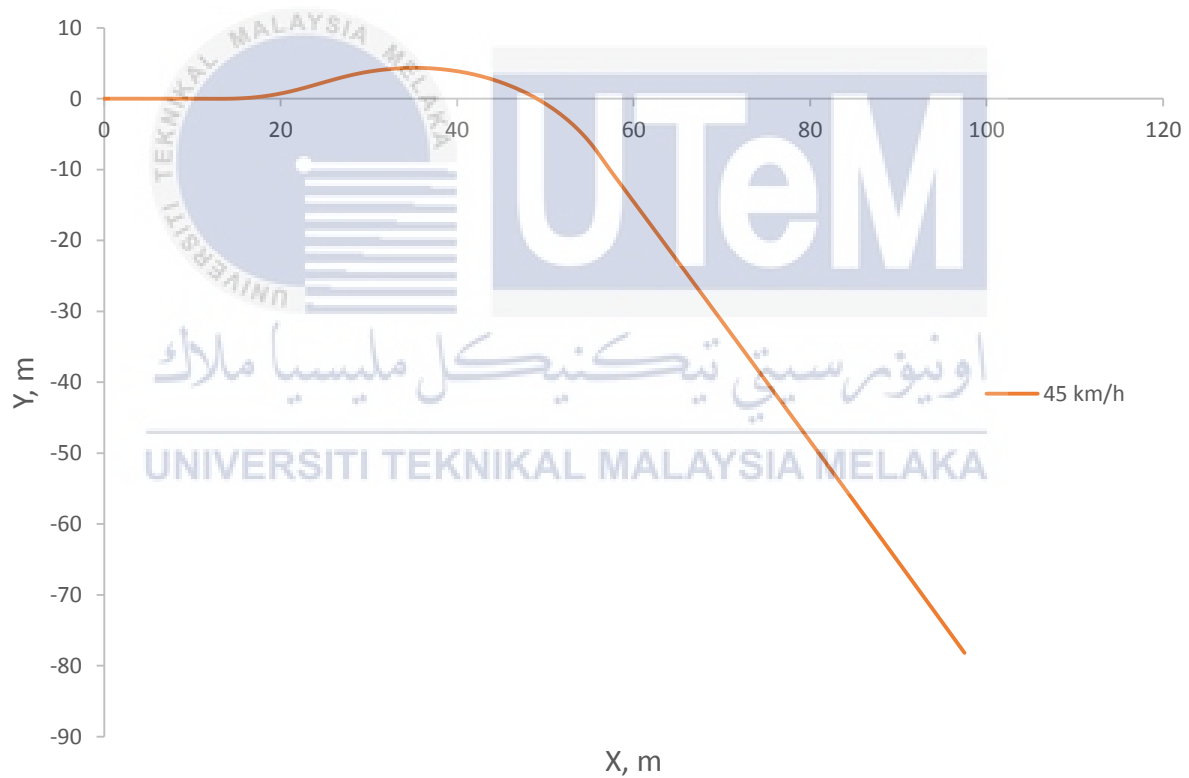


Figure 3.16: Test procedure in form of vehicle trajectory

The test simulation is run and presented by using VS visualizer in form of graph plot based on test parameters and vehicle animation as in **Figure 3.17**. Three simulation run is done by using the same steps as before but with different vehicle's target speed.

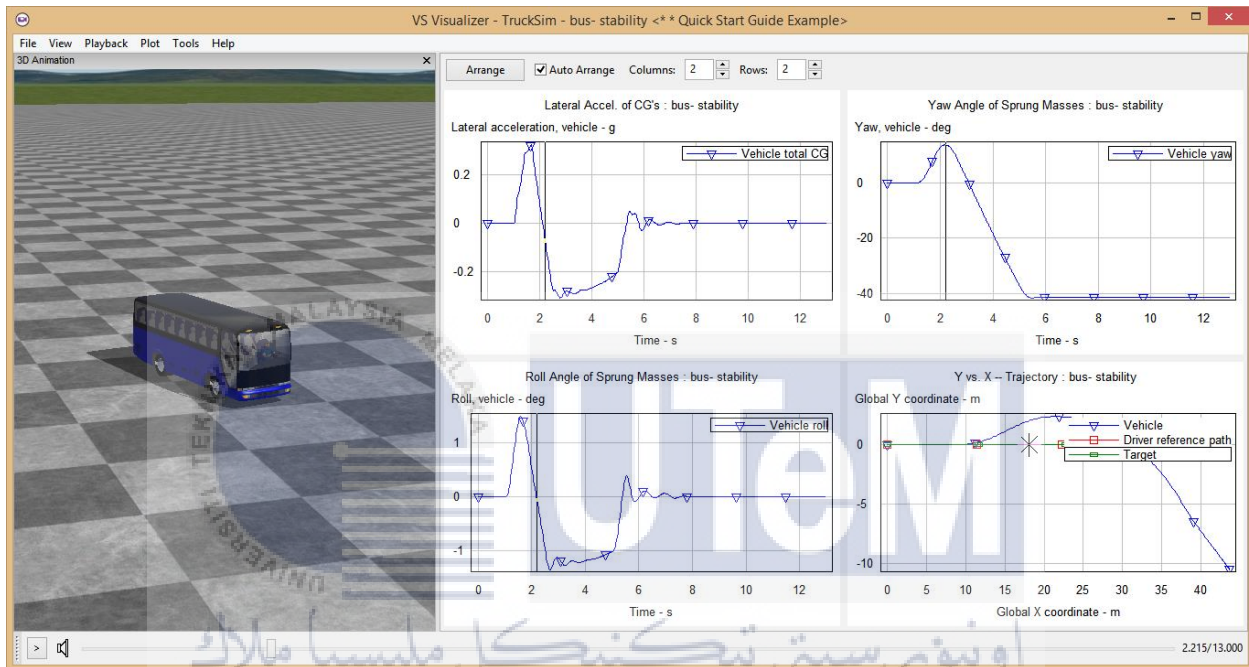


Figure 3.17: Graph plot and 3D vehicle animation

3.5 Data collection and analysis

After completing the test simulation, the graphical data is viewed by using WinEP as in **Figure 3.18**. The interface for this window consist of all plotted graph that have been selected in the test simulation based in the point of inerest of the respective test. In order to view a more detailed graph, select one graph and click the maximize button. **Figure 3.19** shows the more detailed version of the graph for vertical acceleration of sprung masses and the data for the graph must be saved for further analysis by clicking Save Plot Data button.

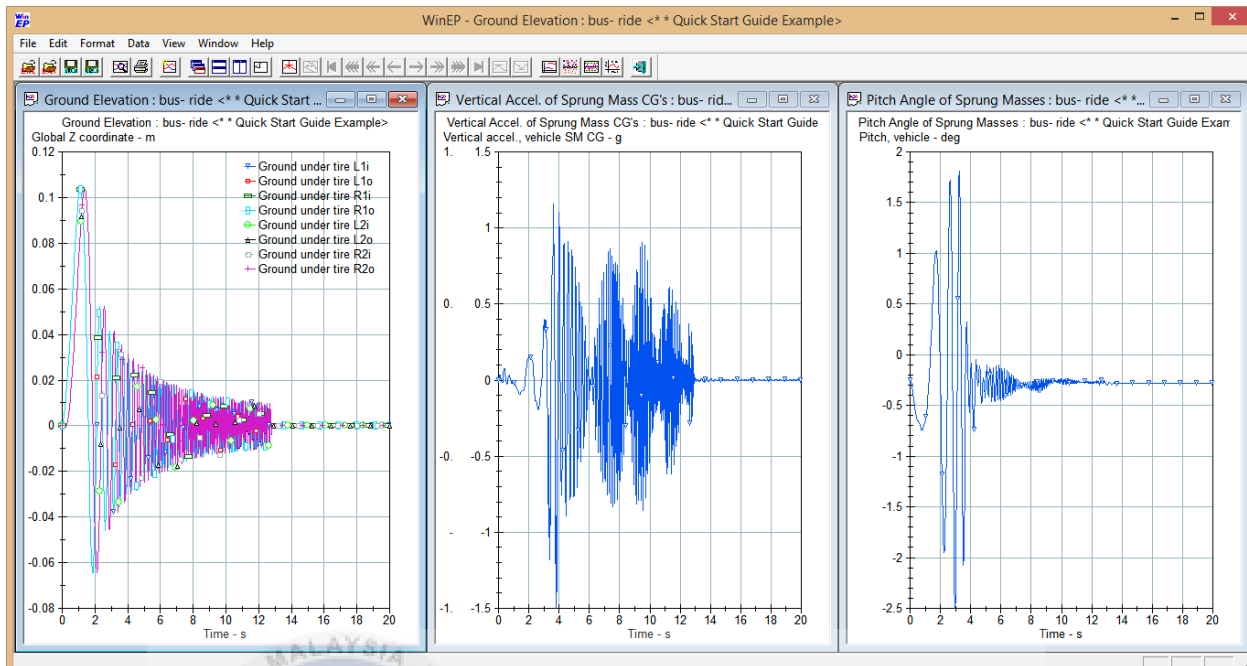


Figure 3.18: All graphical data based on test parameters

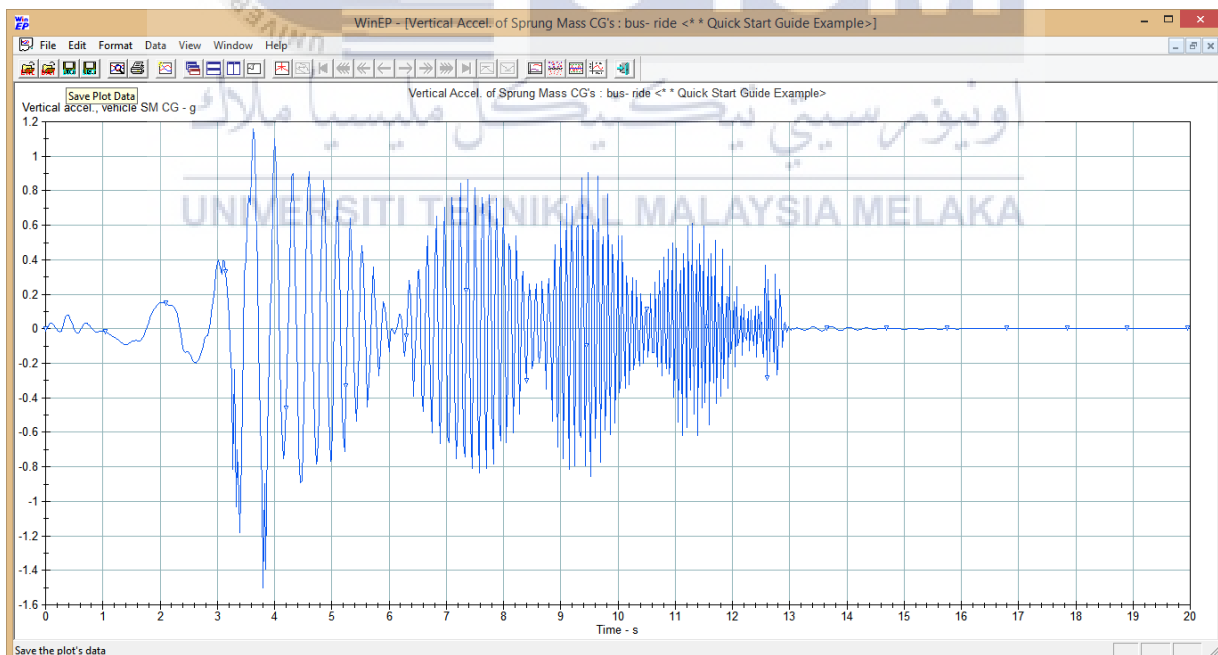
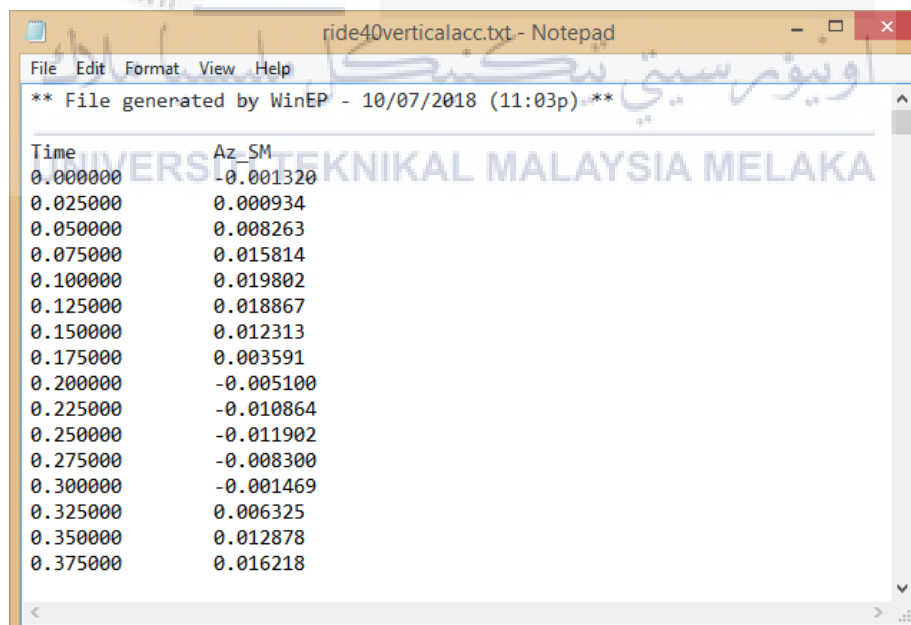


Figure 3.19: Detailed view of the graph

The data for the graph plotted is saved in the form of text file in Notepad as shown in **Figure 3.20**. Data is arranged in form of X axis (Time) and Y axis (Vertical acceleration) of the graph. Data for other speed of this test also need to be saved in the form of text for data analysis phase. All of the data for every speed are transferred to Microsoft Excel to be analyzed. Arrange the data according to the type of graph and different speed of the vehicle; 25 km/h, 35 km/h and 45 km/h. Plot the graph with the respective test parameters and analyze the maximum and minimum data for the respective graph. The graph is plotted with three different speed to determine the behavior of the vehicle when travelling at different speed as shown in **Figure 3.21**. Three different colors and line styles are chosen to distinguish the different speed of the vehicle; blue with small dotted line for 25 km/h, orange with standard line for 35 km/h and grey with large dotted line for 45 km/h.



Time	Az_SM
0.000000	-0.001320
0.025000	0.000934
0.050000	0.008263
0.075000	0.015814
0.100000	0.019802
0.125000	0.018867
0.150000	0.012313
0.175000	0.003591
0.200000	-0.005100
0.225000	-0.010864
0.250000	-0.011902
0.275000	-0.008300
0.300000	-0.001469
0.325000	0.006325
0.350000	0.012878
0.375000	0.016218

Figure 3.20: Data from graph plotted

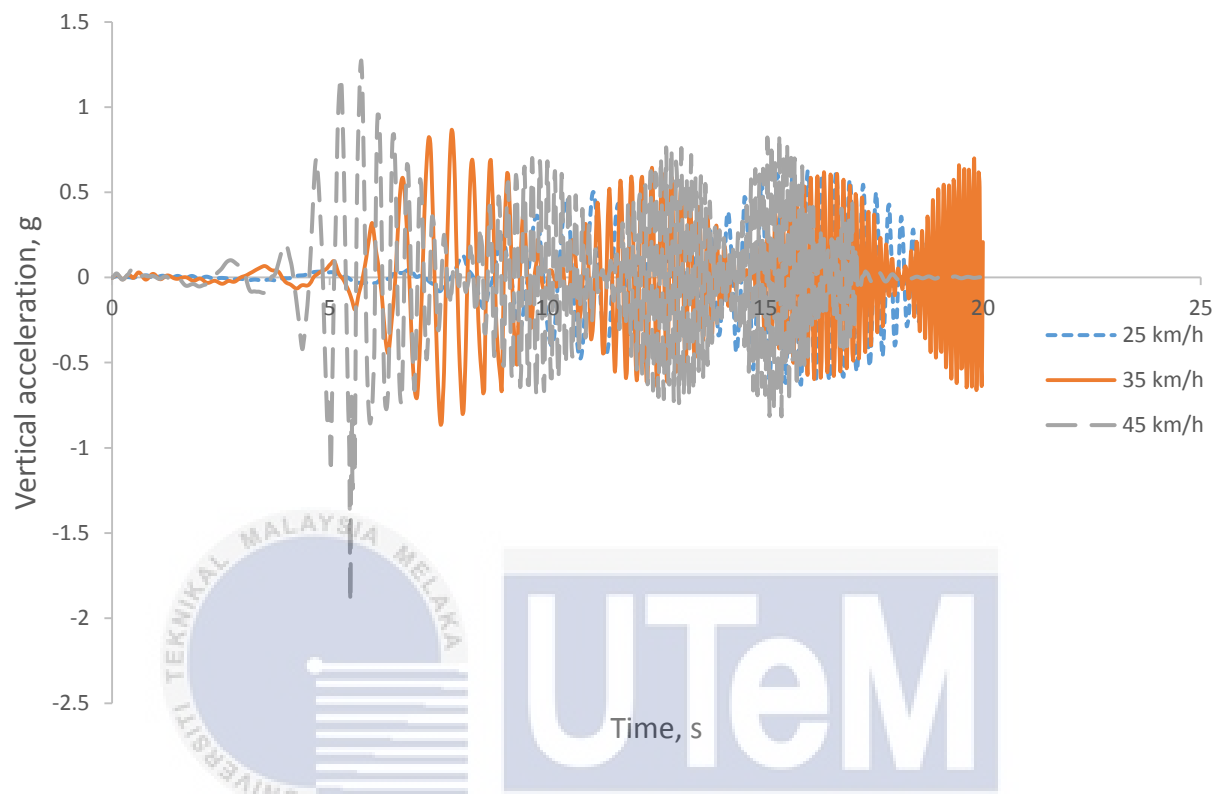


Figure 3.21: Example for comparison graph between three different speeds

اونيورسيتي تېكنيكل مليسيا ملاك
UNIVERSITI TEKNIKAL MALAYSIA MELAKA

CHAPTER 4

RESULT AND DISCUSSION

4.1 Bounce sine sweep test (Ride)

4.1.1 Pitch angle of sprung mass

Pitch is the motion of the vehicle about Y-axis which can be identified when the front and rear part of the vehicle is moving upward and downward during manoeuvre as shown in **Figure 4.1**. **Figure 4.2** shows the graph of pitch angle of sprung mass for standard speed of 35 km/h. The bus experience the first pitch just right after passing through the first bump on the test track. The amount of pitch angle is decreasing as the bus passing through the bumps because the suspension dampen the motion of body and reduce the motion of the front and rear part of the bus.

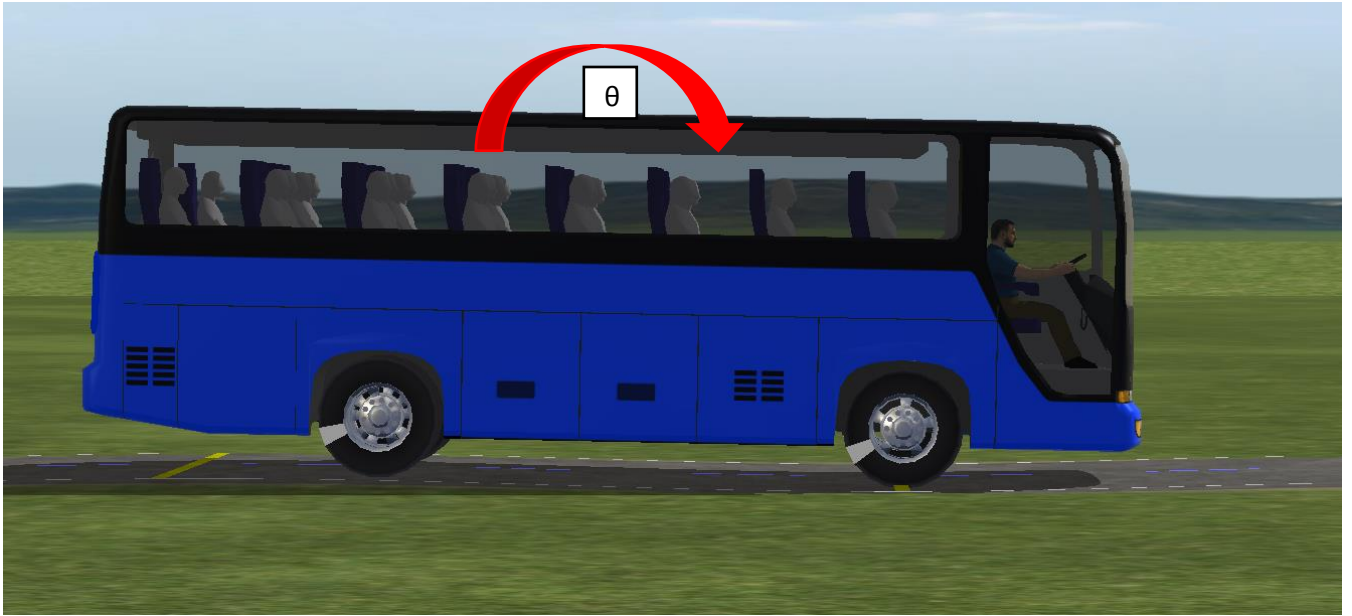


Figure 4.1: Pitching motion of the bus

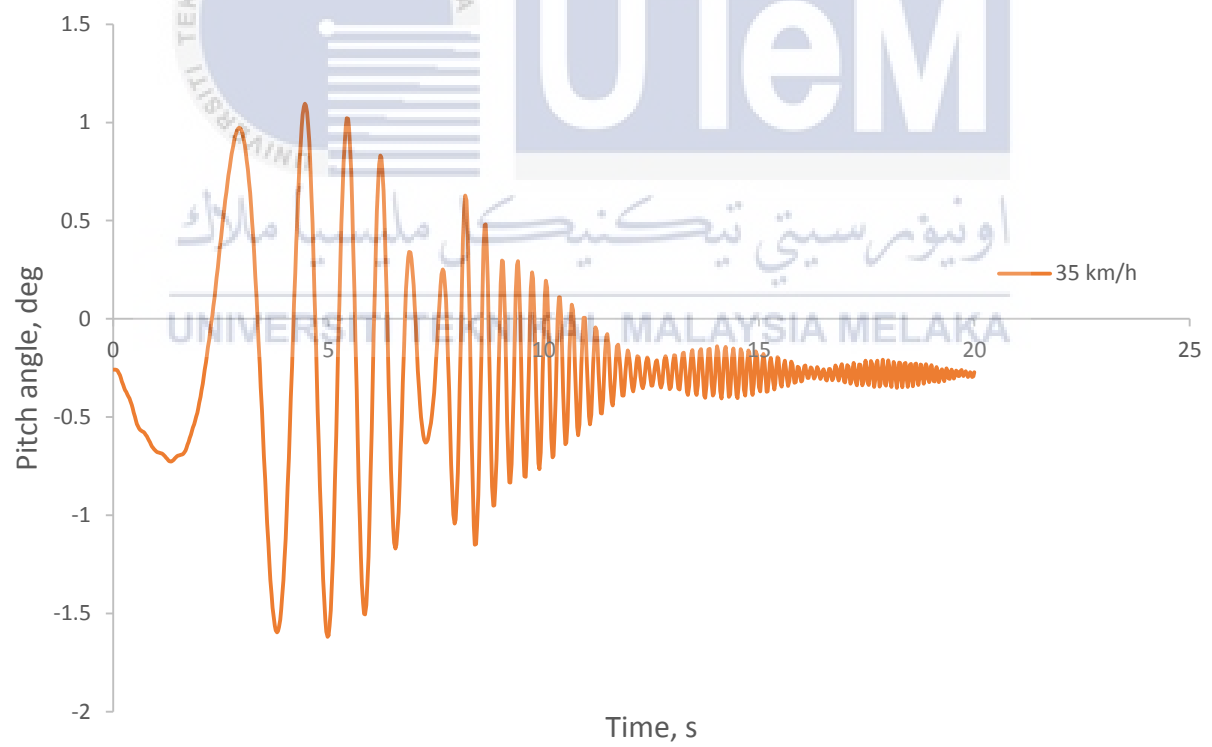


Figure 4.2: Pitch angle of sprung mass for standard speed

Figure 4.3 shows the graph of pitch angle of sprung mass with different speed which the standard speed of 35 km/h is compared to 25 km/h and 45 km/h. The bus that encounter the first pitch in the shortest time is the bus with speed of 45 km/h due to its higher speed compared to the other two. The higher the speed of the bus, the shorter the time taken for the bus to encounter the first pitch. Based on **Table 4.1**, the highest value of maximum pitch angle that is recorded is -1.927 degree at 3.90 seconds when the bus is travelling at the speed of 45 km/h. Based on the graph, it can be considered that the higher the speed of the bus across the bump, the higher the value of the pitch angle experienced by the bus.

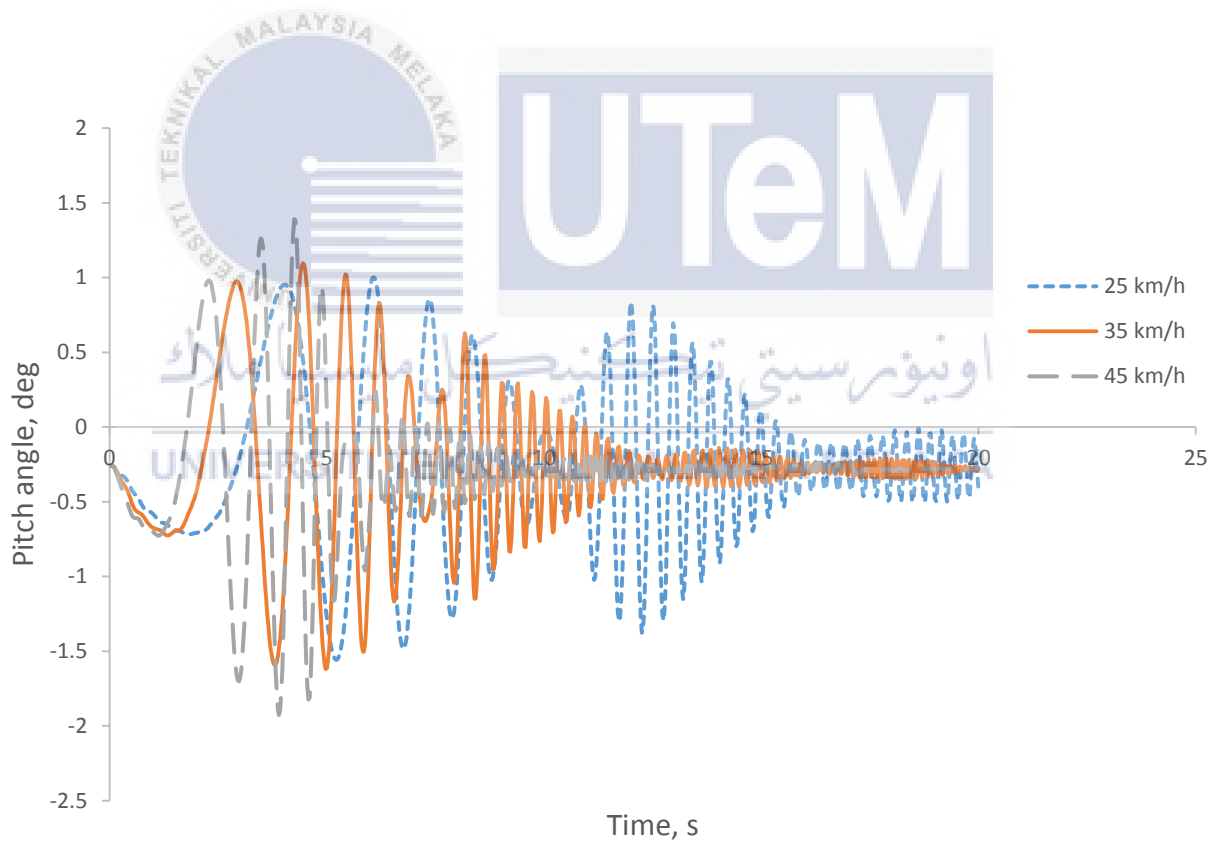


Figure 4.3: Pitch angle of sprung masses with different speed

Table 4.1: Maximum pitch angle comparison for different speeds

Speed, km/h	Maximum pitch angle, degree	Time, s
25	-1.558	5.225
35	-1.619	4.975
45	-1.927	3.900

Figure 4.4 shows the graph of pitch angle of sprung mass when fully laden and unladen vehicle which represent the different value sprung mass of bus during the test. The value of sprung mass for fully laden vehicle is higher than unladen vehicle. Based on **Table 4.2**, the value of maximum pitch angle when the vehicle is fully laden is higher than the unladen vehicle because the momentum for the fully laden vehicle is higher due to its higher weight and resulting in greater motion of the body.

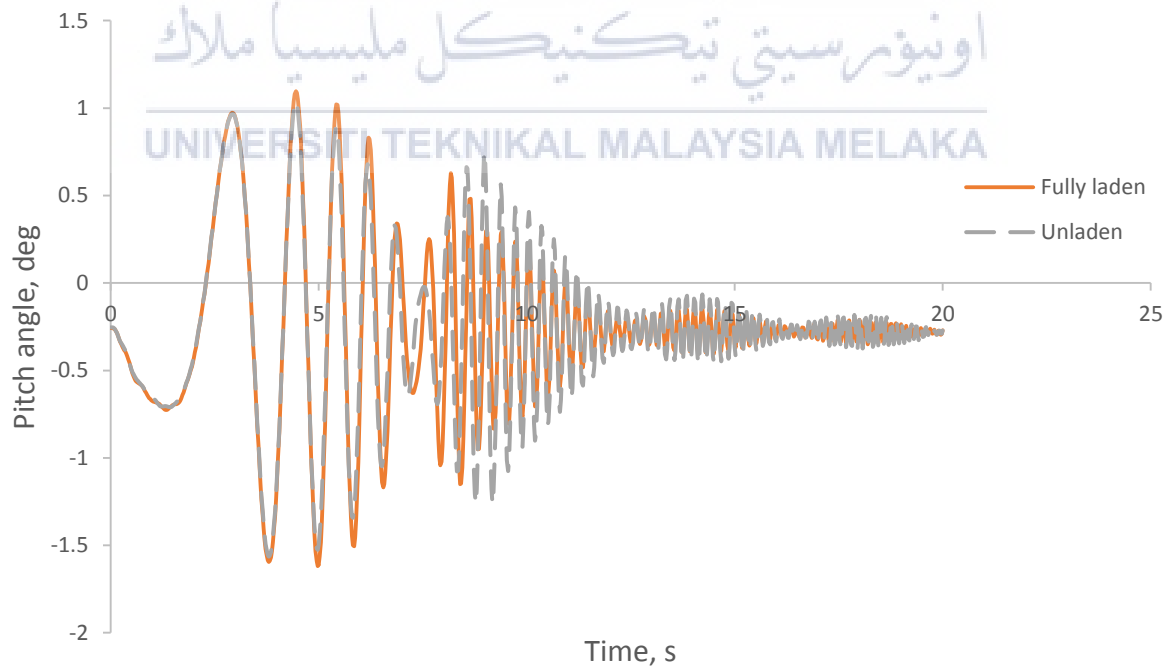


Figure 4.4: Pitch angle of sprung masses with different when fully laden and unladen vehicle

Table 4.2: Maximum pitch angle comparison for different masses

Vehicle condition	Maximum pitch, degree	Time, s
Unladen	-1.564	3.80
Fully laden	-1.619	4.98

4.1.2 Maximum pitch moment calculation

The pitch moment of the vehicle is the moment that acting on Y axis of the vehicle which resulting in upward and downward moment of the front rear part of the vehicle. The diagram of pitch moment, M_y that acting on the bus is based on **Figure 4.5**. The sprung mass of the bus is represented as m_b , longitudinal acceleration is a_x and the height of CG to the ground is h .

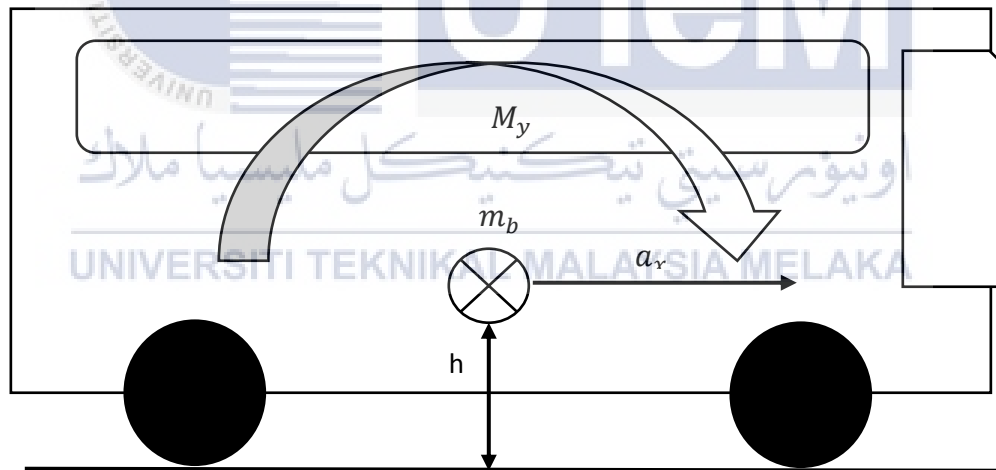


Figure 4.5: Diagram of pitch moment acting on the bus

In order to determine the maximum pitch moment acting on the bus, it can be calculated from the maximum longitudinal acceleration that have been obtained from the simulation run by using Eq. (4.1) which then is derived to Eq. (4.2).

$$F_x h = M_y \quad (4.1)$$

$$m_b a_{xmax} h = M_{ymax} \quad (4.2)$$

where F_x is the longitudinal force and h is the height of CG to the ground. The pitch moment is denoted by M_y and the maximum pitch moment is M_{ymax} which is derived from the multiplication of m_b , a_{xmax} and h .

The maximum longitudinal acceleration from the simulation result is in form of gravitational acceleration, g which must be converted into standard form, ms^{-2} to find the pitch moment as calculated in Eq. (4.3) and Eq. (4.4).

$$1 g = 9.81 ms^{-2} \quad (4.3)$$

$$-0.066 g = -0.65 ms^{-2} \quad (4.4)$$

Then, substitute the value of m_b , a_{xmax} and h into Eq. (4.5) to find the maximum pitch moment.

$$M_{xmax} = (6360)(-0.65)(1.2) \quad (4.5)$$

$$= -4.96 \times 10^3 Nm$$

The value of maximum pitch moment for different vehicle speed can be referred as in **Table 4.3**. When the vehicle travel at speed of 45 km/h, it recorded the highest value of maximum pitch moment compared to the other speed at value of $10.68 \times 10^3 Nm$ in clockwise direction. The higher the speed of vehicle, the higher the value of maximum pitch moment. It is because of higher speed vehicle produce higher longitudinal force during manoeuvring which resulting in high value of pitch moment.

Table 4.3: Maximum pitch moment value at different speeds

Vehicle speed, km/h	Maximum longitudinal acceleration, ms^{-2}	Maximum pitch moment, Nm
25	-0.65	-4.96×10^3
35	-1.01	-7.71×10^3
45	1.40	10.68×10^3

Next, the value of maximum pitch moment when unladen and fully laden condition can be calculated by using Eq. (4.6) and change the value of sprung mass, m_b for every condition as below.

$$\begin{aligned}
 M_{xmax} &= (4500)(-1.22)(1.2) \\
 &= -6.59 \times 10^3 \text{ Nm}
 \end{aligned}
 \tag{4.6}$$

The value of maximum pitch moment when unladen and fully laden vehicle can be referred in **Table 4.4**. Fully laden vehicle has the lower value of maximum pitch moment compared to unladen vehicle at $-5.45 \times 10^3 \text{ Nm}$ while unladen vehicle is $-6.59 \times 10^3 \text{ Nm}$. As for unladen vehicle, the highest value of longitudinal acceleration obtained when the vehicle is braking at the end of the test because the lower mass vehicle experience higher amount of longitudinal force that resulting in greater braking effect.

Table 4.4: Maximum roll moment when unladen and fully laden vehicle

Vehicle condition	Maximum lateral acceleration, ms^{-2}	Maximum roll moment, Nm
Unladen	-1.22	-6.59×10^3
Fully laden	-1.01	-5.45×10^3

4.1.3 Vertical acceleration of sprung masses

Vertical acceleration of sprung mass is the motion of the vehicle at Z-axis. **Figure 4.6** shows the graph for vertical acceleration of sprung mass for the standard speed of 35 km/h. The acceleration at the beginning of the test is high and gradually decrease as going through the bumps because the suspension of the bus dampen the motion of body.

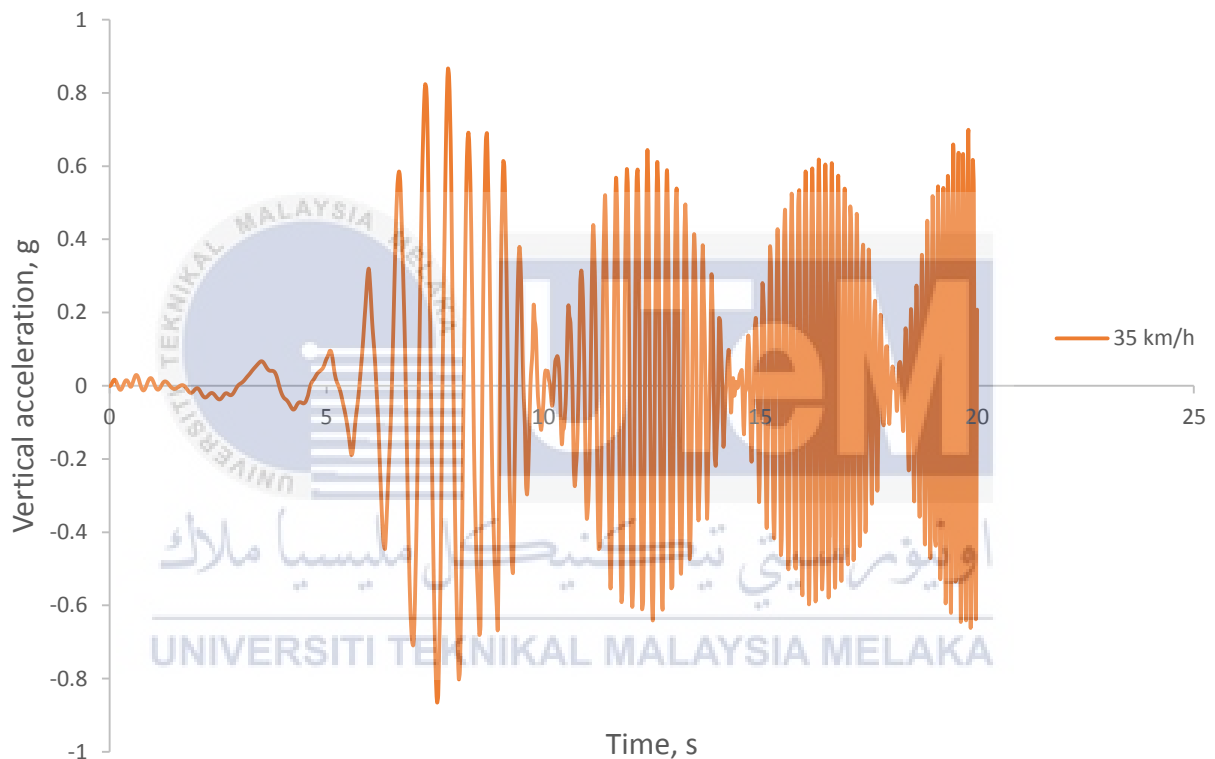


Figure 4.6: Vertical acceleration of sprung masses with standard speed

Based on **Figure 4.7**, the highest maximum vertical acceleration is recorded when the bus is travelling at the speed of 45 km/h which is -1.908 g at 5.48 seconds as shown in **Table 4.5** because the inertia mass of the bus is higher when the bus passing through the bumpy road at higher speed. The lower the speed of the bus, the lower the value of maximum vertical acceleration. The vertical vibration that is transmitted to sprung mass is high at this point.

Negative value of the vertical acceleration represent the movement of the bus when going up the bump and the weight of the sprung mass affect the deceleration of the bus at this situation.

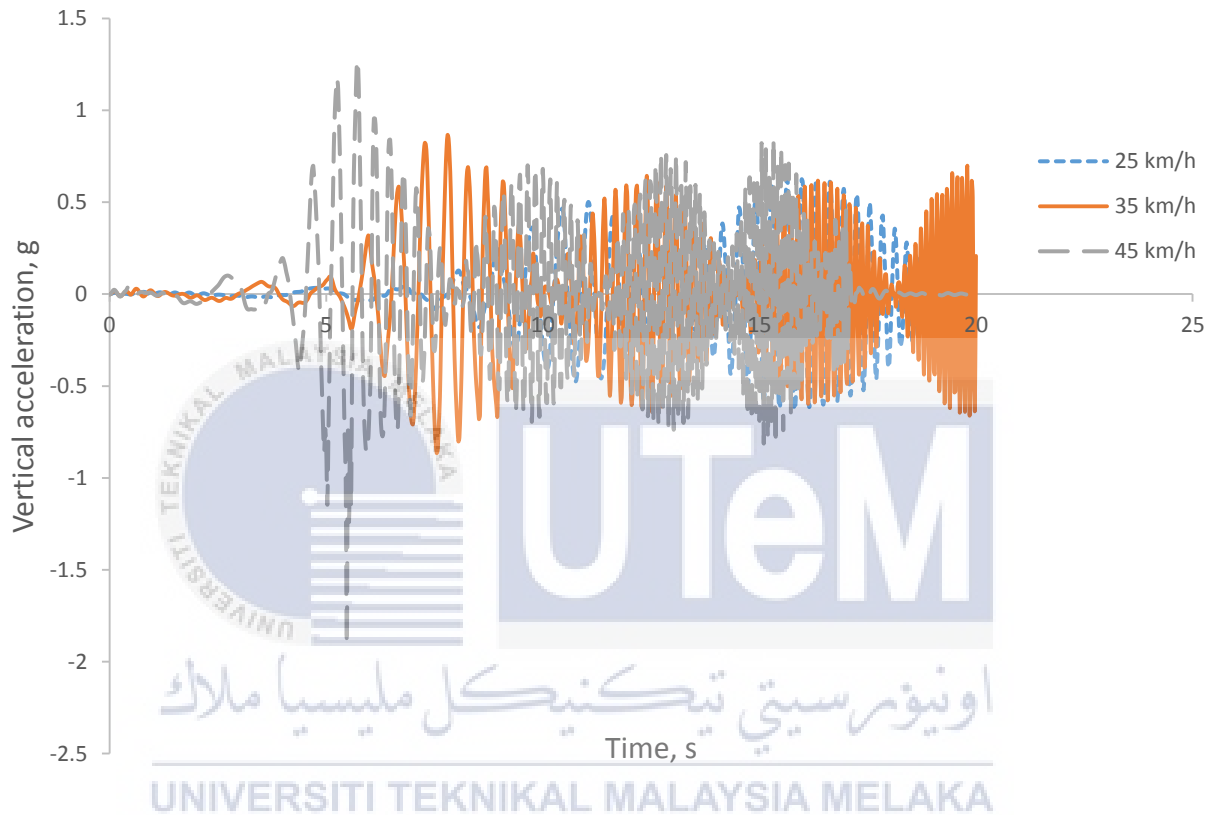


Figure 4.7: Vertical acceleration of sprung masses with different speed

Table 4.5: Comparison of maximum vertical acceleration at different speeds

Speed, km/h	Maximum vertical acceleration, g	Time, s
25	0.628	15.65
35	0.866	7.8
45	-1.908	5.475

Figure 4.8 shows the vertical acceleration of sprung mass when fully laden and unladen vehicle. The maximum vertical acceleration recorded by unladen vehicle is higher than fully laden vehicle at 1.025 g while fully laden vehicle is 0.866 based on **Table 4.6**. Unladen vehicle recorded higher vertical acceleration compared to fully laden vehicle because the lower mass of the vehicle influence the vertical acceleration of the sprung mass and increase the value of vertical acceleration. The lower the mass of the vehicle, the higher the value of vertical acceleration of sprung mass.

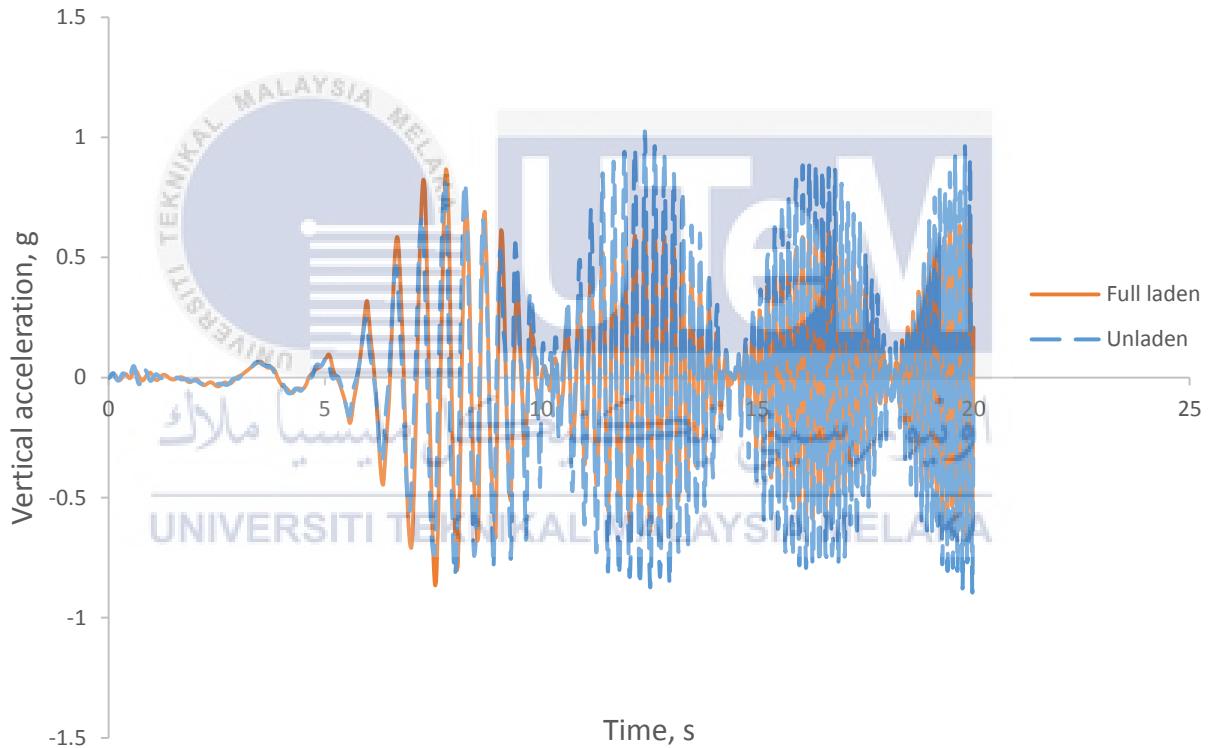


Figure 4.8: Vertical acceleration of sprung masses when fully laden and unladen vehicle

Table 4.6: Comparison of maximum vertical acceleration when fully laden and unladen vehicle

Vehicle condition	Maximum vertical acceleration, g	Time, s
Unladen	1.025	12.4
Fully laden	0.866	7.8

4.1.4 Comparison between tire forces of R1

Tire forces of R1 from three axis are compared in the graph as shown in **Figure 4.9** to determine the significant effect of tire force resulting from the test. Only tire force that show the significant effect will be used for the analysis. From the graph, it can be determined that vertical tire force shown a significant effect resulting from the test.

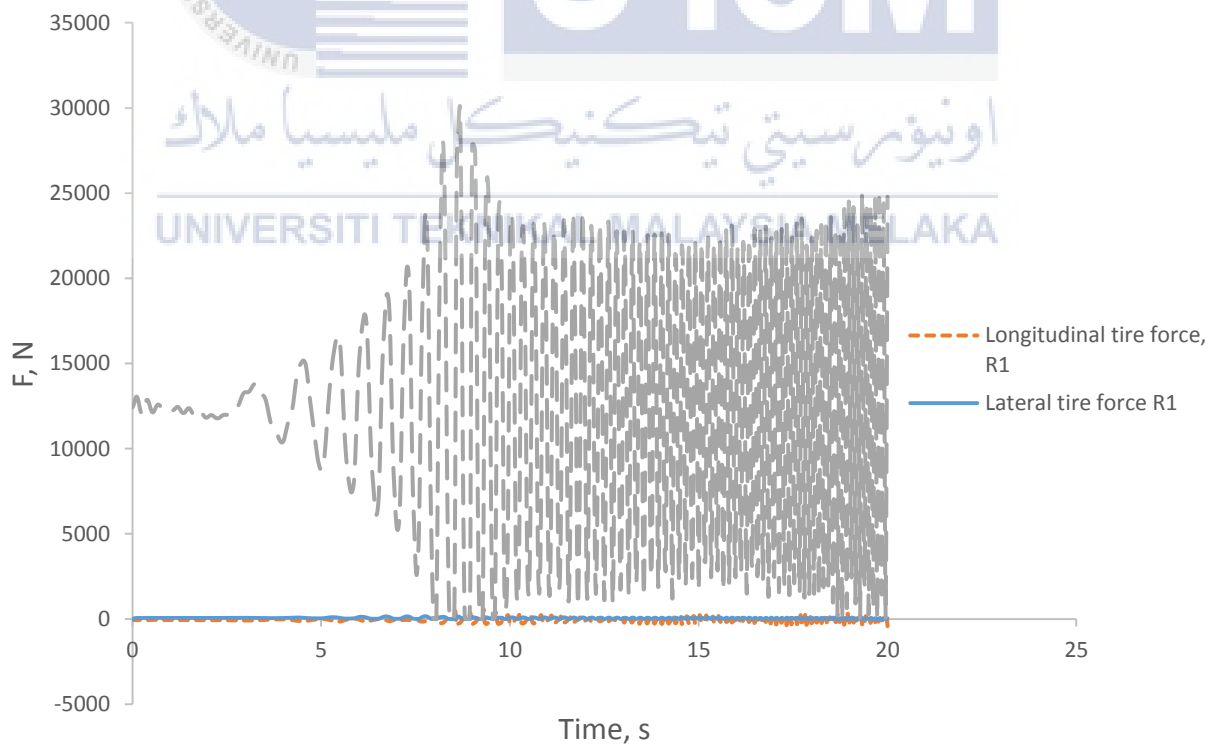


Figure 4.9: Comparison between tire forces of R1

4.1.5 Vertical tire force, R1

Vertical tire force is the force that is analysed at Z-axis and influenced by upward and downward movement of the vehicle. The vertical load sourcing from the sprung mass is transmitted to the tire form the vertical force of the tire. From **Figure 4.10**, the value of vertical tire force is increasing until region A and slightly reduced and remain uniform at region B.

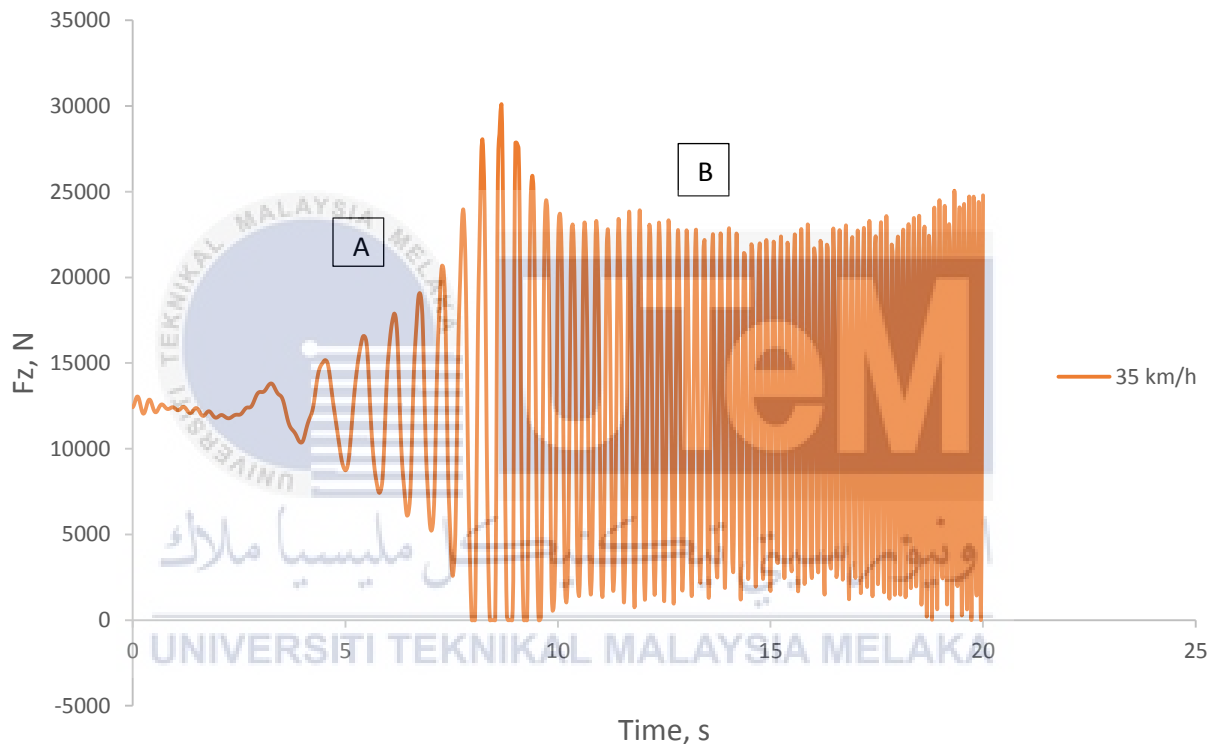


Figure 4.10: Vertical tire force of R1 at standard speed

Figure 4.11 shows that when the vehicle travels at speed of 45 km/h, the value of vertical tire force recorded is highest compared to other speeds. The highest vertical tire force is recorded at 32611.7N at time of 6.075s when the vehicle is travelling at the speed of 45 km/h as in **Table 4.7**. When the vehicle is travelling at higher speed, the vertical tire force is higher because the force is directly proportional to the acceleration and the vehicle with higher speed is having a greater acceleration compared to the lower speed.

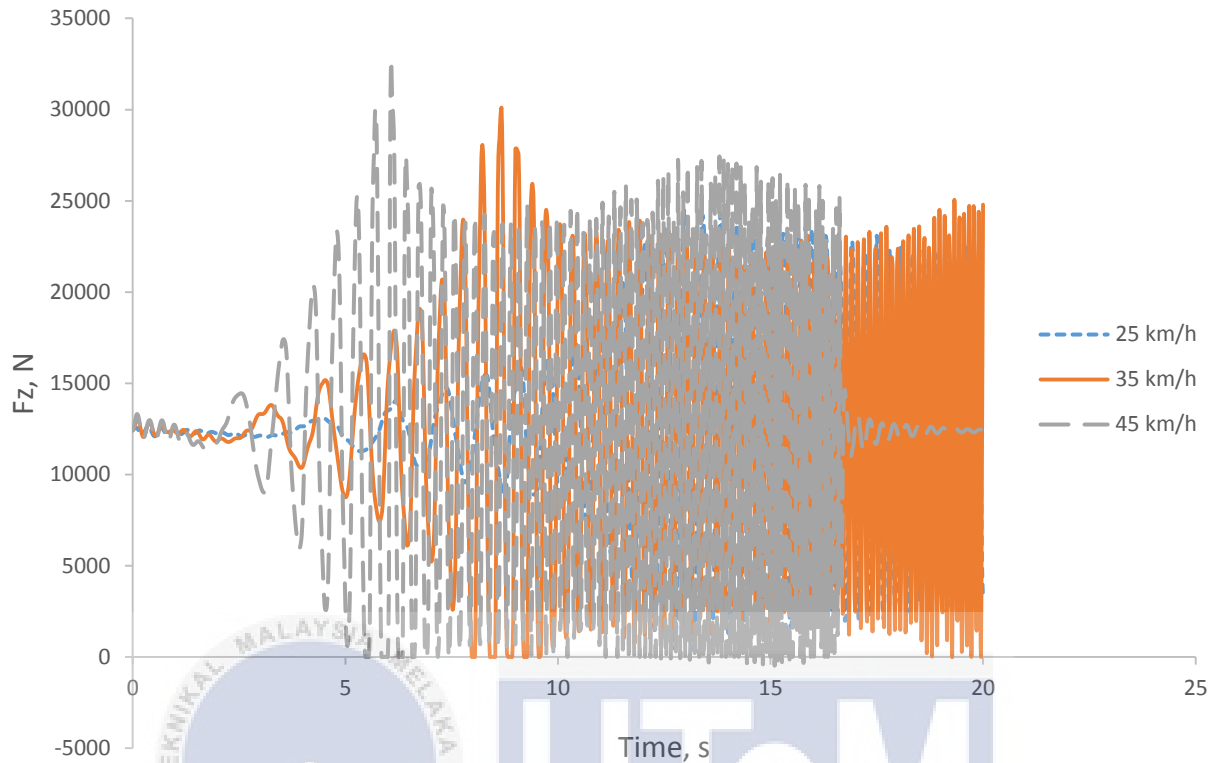


Figure 4.11: Vertical tire force of R1 at different speeds

Table 4.7: Comparison of vertical tire force at different speeds

Speed, km/h	Vertical Tire Force, N	Time, s
25	24542.5	12.975
35	30059.3	8.675
45	32611.7	6.075

Figure 4.12 shows the vertical tire force when fully laden vehicle and unladen vehicle. Both vehicle condition is travelling at the same speed with different sprung mass. The vertical tire force of fully laden vehicle is higher than unladen vehicle at 30059.3N at the time of 8.675s while unladen vehicle recorded 29840N at the time of 9.35s as in **Table 4.8**. The higher the value of sprung mass, the higher the value of vertical tire force because it resulting in greater load to the tire.

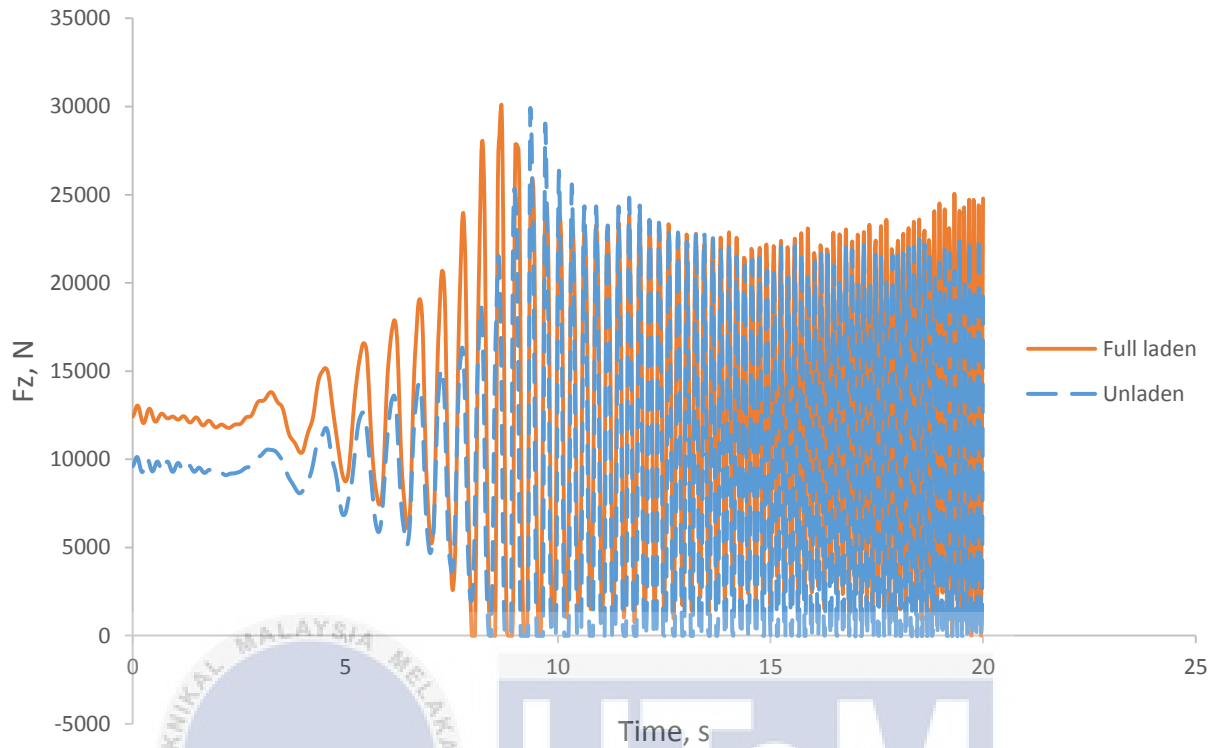


Figure 4.12: Vertical tire force of R1 when fully laden and unladen vehicle

Table 4.8: Comparison of vertical tire force when fully laden and unladen vehicle

Vehicle condition	Vertical Force, N	Time, s
Unladen	29840.0	9.350
Fully Laden	30059.3	8.675

4.2 Double lane change (Handling)

4.2.1 Trajectory Y vs X

Trajectory of the vehicle is based on X-axis and Y-axis and represent the movement of the car respected to the steering input. **Figure 4.13** shows the trajectory of vehicle at the standard speed of 90 km/h. At region A, the vehicle is the phase of vehicle changing into another lane and the trajectory is increasing until region B where the vehicle is at the left-end of the lane

which can be considered as the highest displacement of the car from the original lane. Region C is where the vehicle is in the phase of changing into the original lane and this is the region where the vehicle understeer is present which resulting in deviation of the vehicle trajectory to the targeted trajectory. After that, the vehicle need to counter-steer to remain in the lane. The analysis for the trajectory will be focused on region C where the difference between the vehicle speed and condition is really significant.

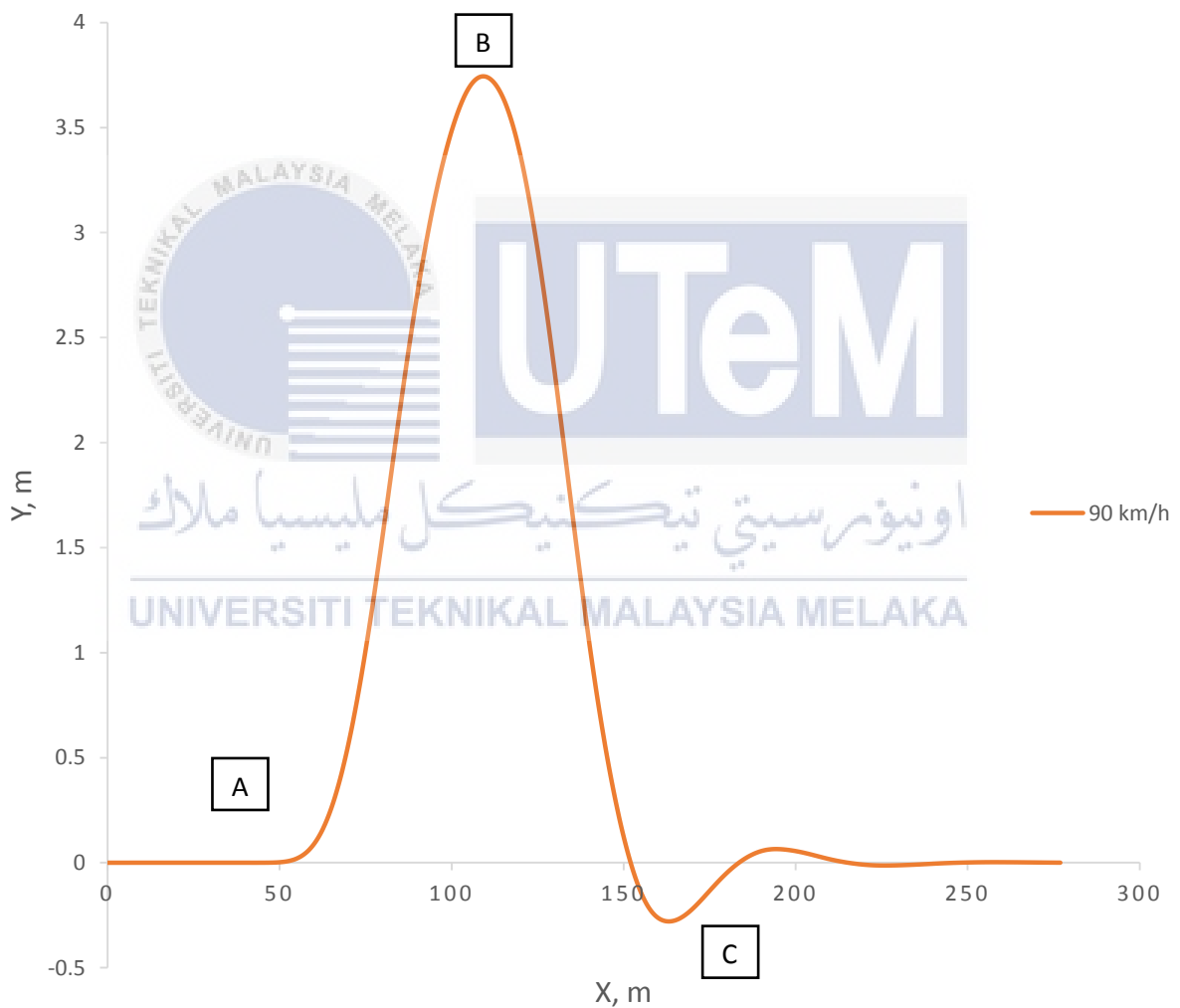


Figure 4.13: Vehicle trajectory for standard speed

Based on **Figure 4.14**, the vehicle speed at 110 km/h deviates from the targeted trajectory at region C higher than the other speeds. **Table 4.9** shows that the highest maximum Y axis displacement is recorded at -0.471 m when the vehicle is travelling at the speed of 110 km/h. The maximum displacement is recorded when the bus is at the phase of changing back into the original lane. The higher the speed of the vehicle, the higher the difference of displacement of the bus compared to the target path due to understeer of the vehicle. Understeer problem occur when the vehicle less responding to the steering input by the driver during higher speed cornering because the inertia value of the vehicle is increased.

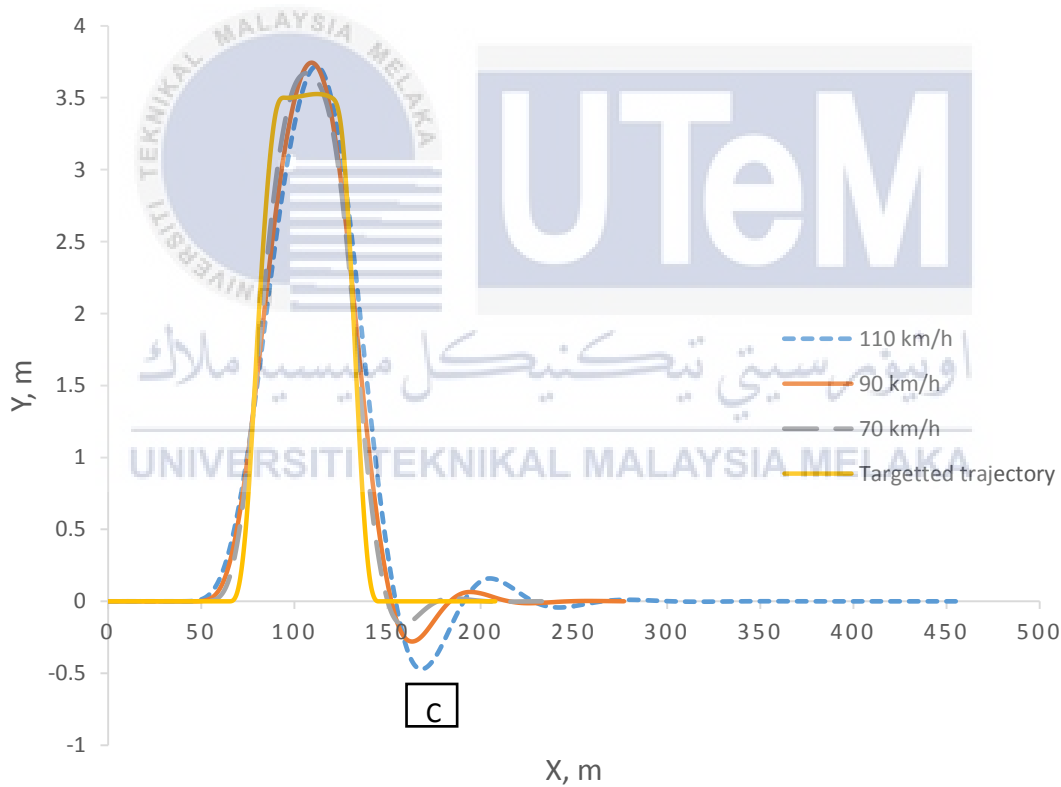


Figure 4.14: Vehicle trajectory at different speeds

Table 4.9: Comparison of maximum Y displacement at region C at different speeds

Speed, km/h	Maximum Y displacement at region C, m
70	-0.160
90	-0.280
110	-0.471

Figure 4.15 show the vehicle trajectory when the vehicle is tested with fully laden condition and unladen condition. The maximum Y displacement at region C for fully laden vehicle is higher than unladen vehicle which is -0.280 m while unladen vehicle is -0.262 m as in **Table 4.10**. This different in displacement is resulting from different value of sprung mass during the test. The higher the value of sprung mass, the higher the maximum Y displacement at region C because of the inertia value of vehicle with higher mass is greater than vehicle with lower mass.

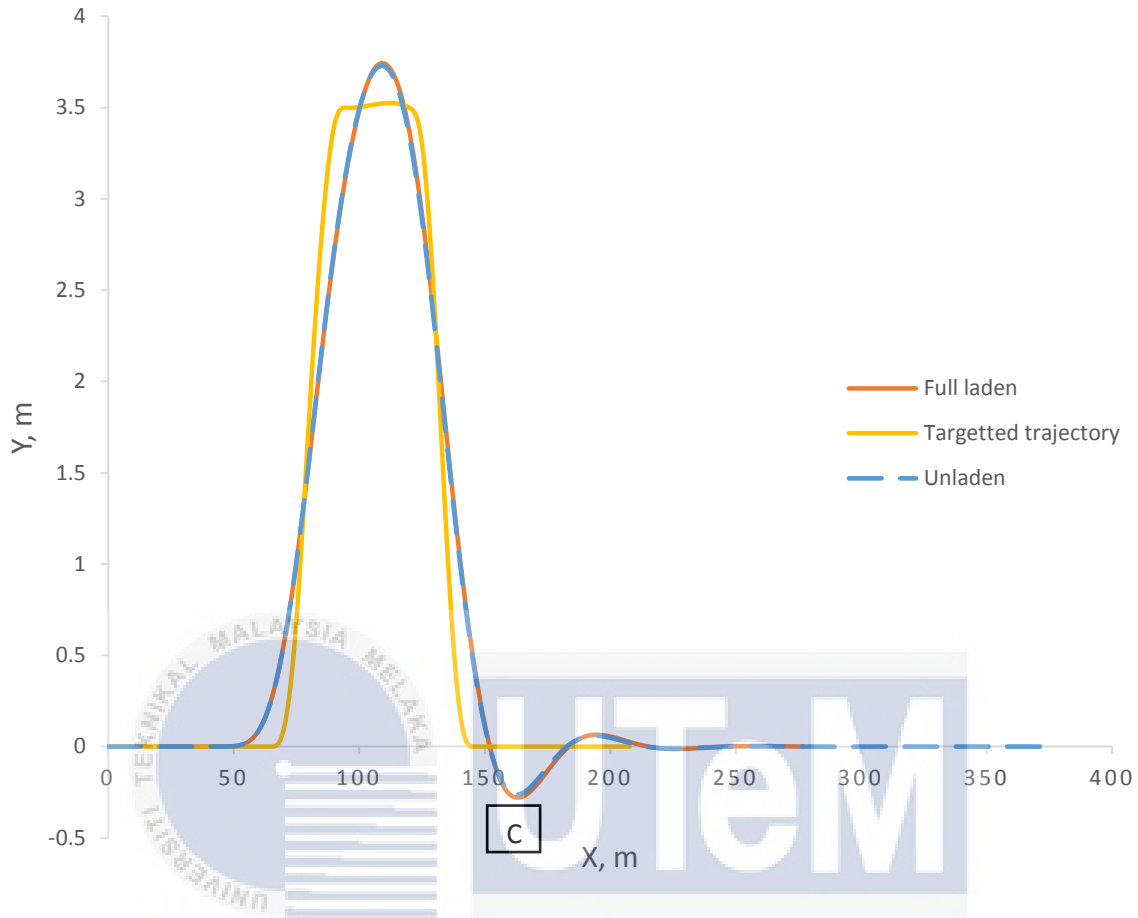


Figure 4.15: Vehicle trajectory when fully laden and unladen vehicle

Table 4.10: Comparison of maximum Y displacement at region C when fully laden and unladen vehicle

Vehicle condition	Maximum Y displacement at region C, m
Unladen	-0.262
Fully laden	-0.280

4.2.2 Lateral acceleration of CG

Lateral acceleration of vehicle's centre of gravity for standard speed of 90 km/h is represented in **Figure 4.16**. The vehicle start to change lane in the region A where the first steering input is applied and the positive value of lateral acceleration represent the movement

of the vehicle laterally to the left. After changing into another lane, the vehicle overcomes the lateral acceleration and moving to the right in response to its lateral damping in region B where the vehicle is about to enter the original lane. When the vehicle is entering the original lane, the vehicle laterally moving to the left and right as in region C to straighten up the vehicle in response of the lateral weight transfer.

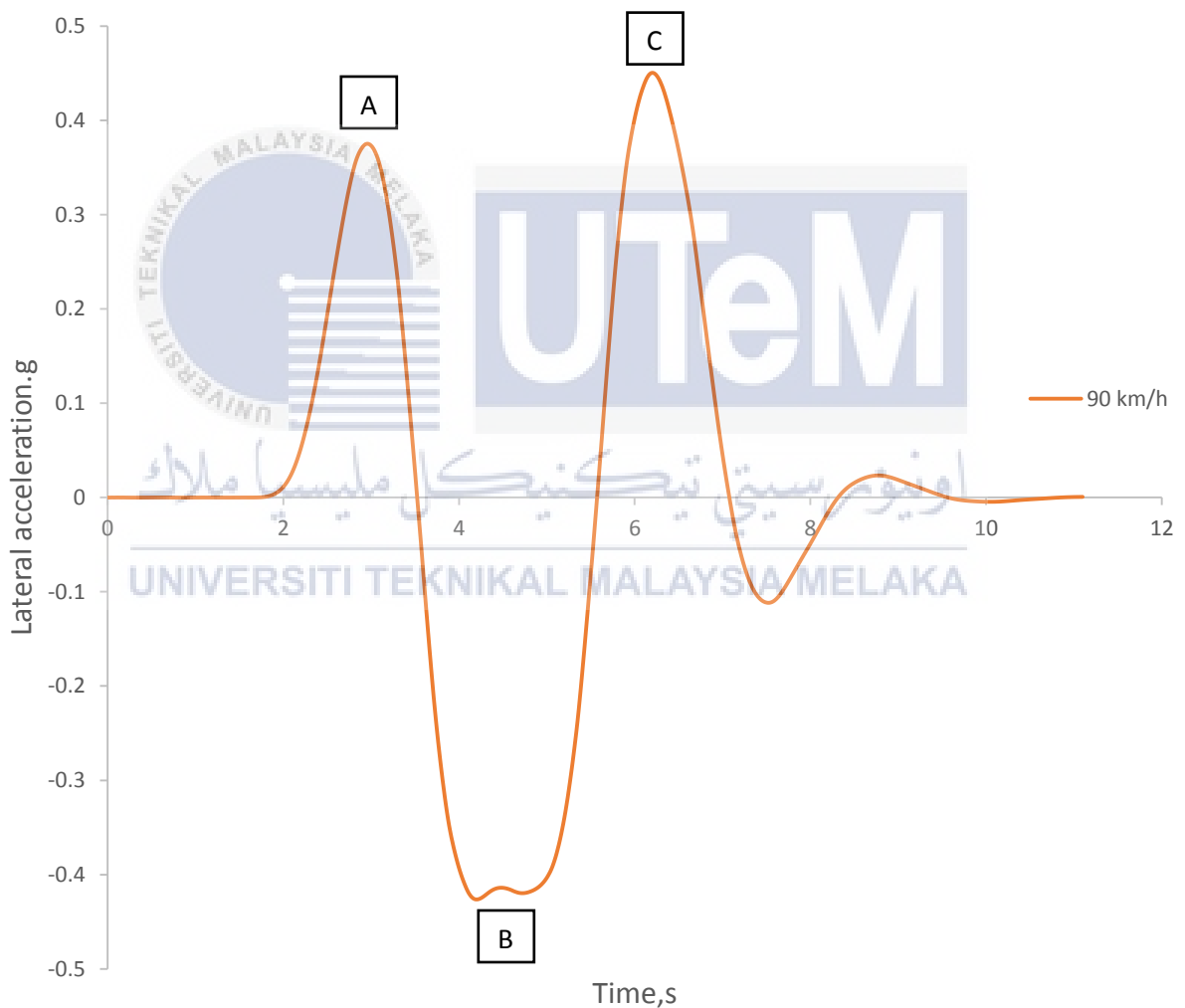


Figure 4.16: Lateral acceleration of vehicle's center of gravity at standard speed

Figure 4.17 shows the graph of lateral acceleration of vehicle's center of gravity at different speeds. The highest maximum lateral acceleration of the center of gravity of the bus is $-0.652g$ when the bus is travelling at the speed of 110 km/h which is recorded at 3.93 s as shown in **Table 4.11**. The maximum value of lateral acceleration is recorded when the bus is in the end of changing lane phase and about to enter the original lane. The value of maximum lateral acceleration is higher when the speed of the vehicle is higher.

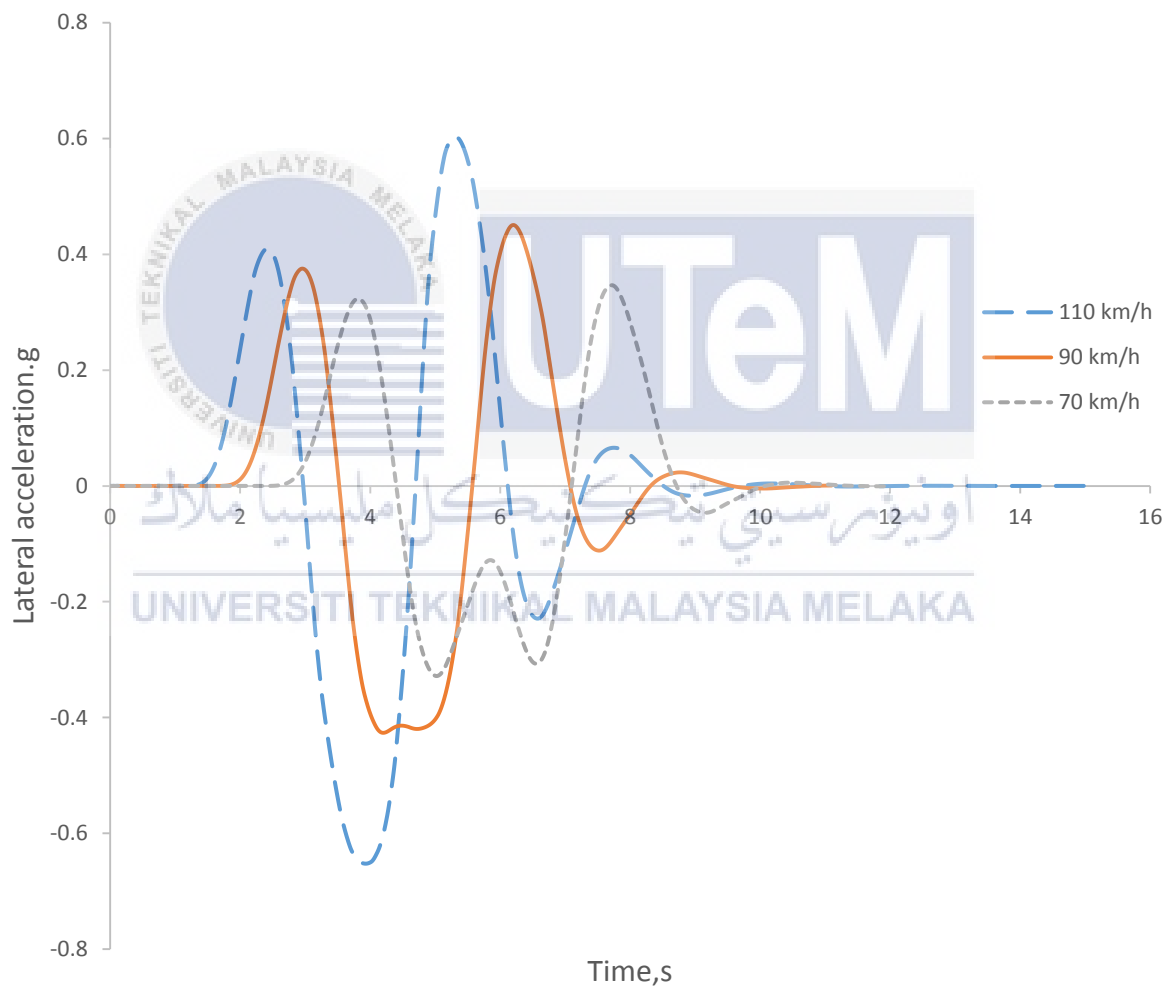
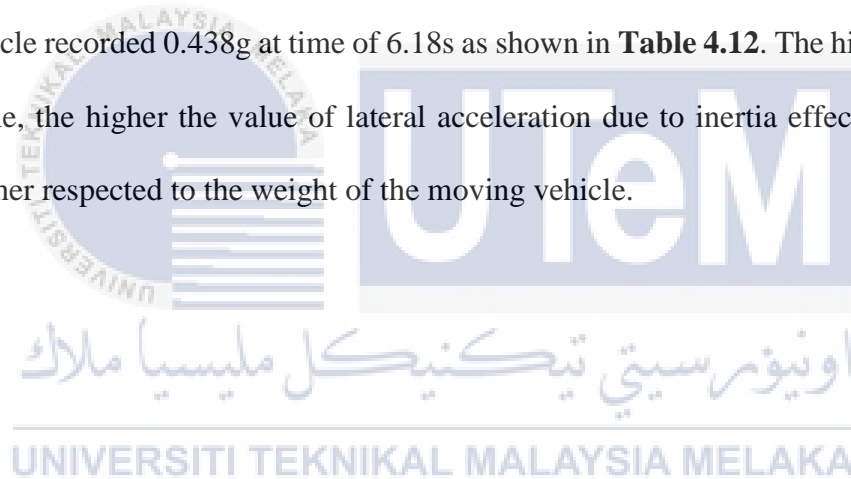


Figure 4.17: Lateral acceleration of CG at different speeds

Table 4.11: Comparison of maximum lateral acceleration at different speeds

Speed, km/h	Maximum lateral acceleration, g	Time, s
70	0.346	7.73
90	0.451	6.20
110	-0.652	3.93

Based on **Figure 4.18**, the maximum lateral acceleration of vehicle's center of gravity for fully laden vehicle is higher than unladen vehicle which is 0.451g at time of 6.20s while unladen vehicle recorded 0.438g at time of 6.18s as shown in **Table 4.12**. The higher the weight of the vehicle, the higher the value of lateral acceleration due to inertia effect of the vehicle which is higher respected to the weight of the moving vehicle.



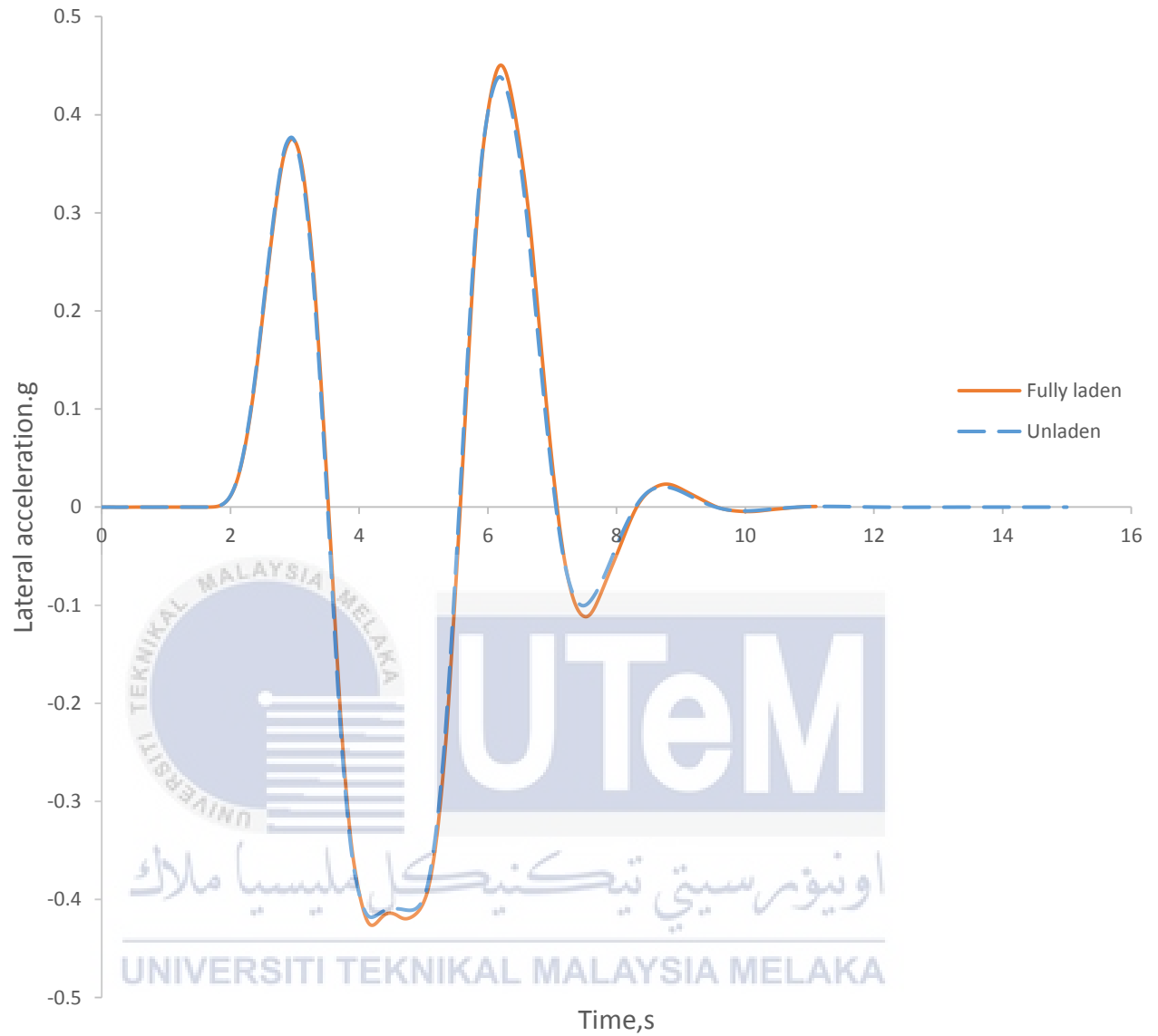


Figure 4.18: Lateral acceleration of CG when fully laden and unladen vehicle

Table 4.12: Comparison of maximum lateral acceleration when fully laden and unladen vehicle

Vehicle condition	Maximum lateral acceleration, g	Time, s
Unladen	0.438	6.18
Fully laden	0.451	6.20

4.2.3 Yaw angle of sprung masses

Yaw angle is the difference between X-axis vehicle projected direction and the heading angle. **Figure 4.19** shows the graph for yaw angle of sprung mass at standard speed in double lane change test. The vehicle start to have positive yaw angle when the vehicle is about to change lane as represented by phase A in the graph. The positive yaw angle means that the vehicle is moving to the left direction. Then the vehicle complete the lane changing and come back to the original lane as in phase B where the value of yaw angle is positive that represent the movement of the vehicle to the right. Phase C is when the vehicle is already in the original lane and the yaw angle present here is due to the vehicle response to the lateral load transfer for straightening the vehicle in the lane.

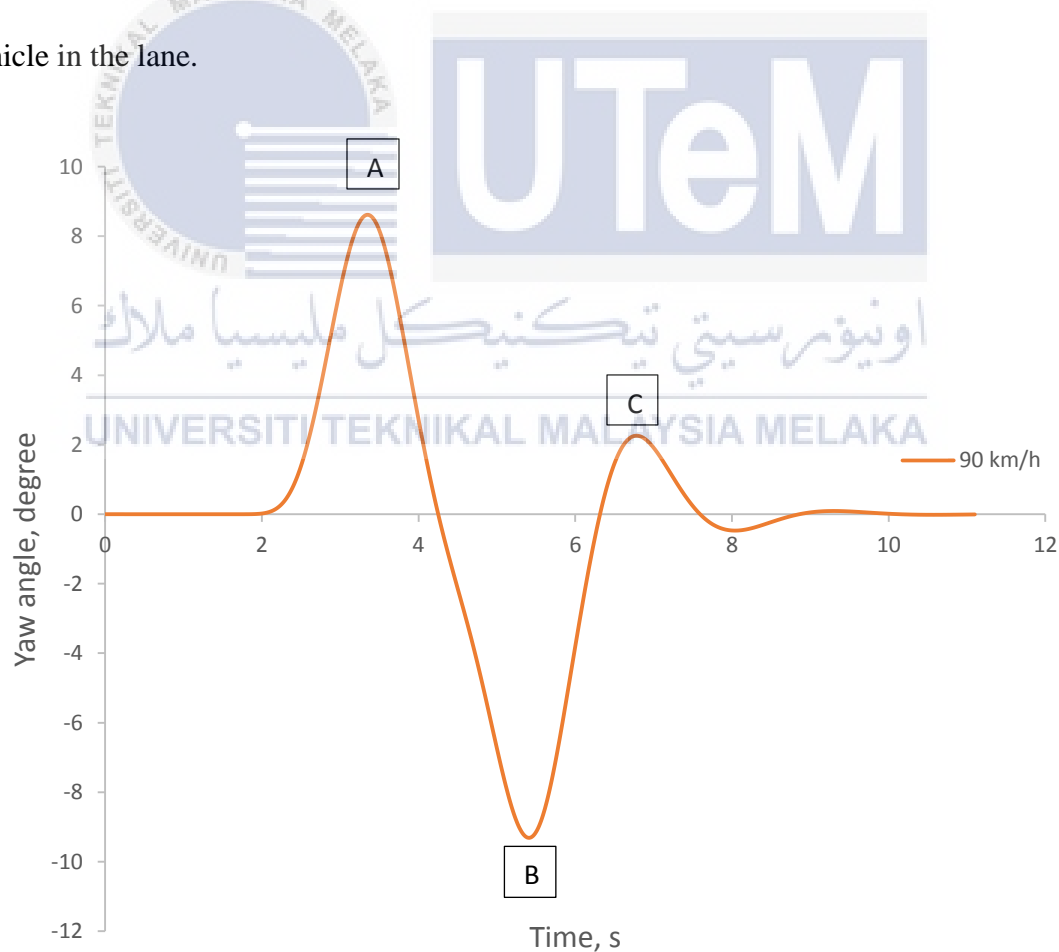


Figure 4.19: Yaw angle of sprung masses at standard speed

Figure 4.20 shows that when the vehicle travel at the speed of 110 km/h, the maximum yaw angle of sprung mass obtained is -10.691 degree which is the highest yaw angle compared to the other speed as shown in **Table 4.13**. The maximum yaw angle is recorded at 4.45 s when the vehicle is changing to the original lane as in phase B. It shows that the higher speed of the vehicle resulting in higher yaw angle obtained during double lane change manoeuvre.

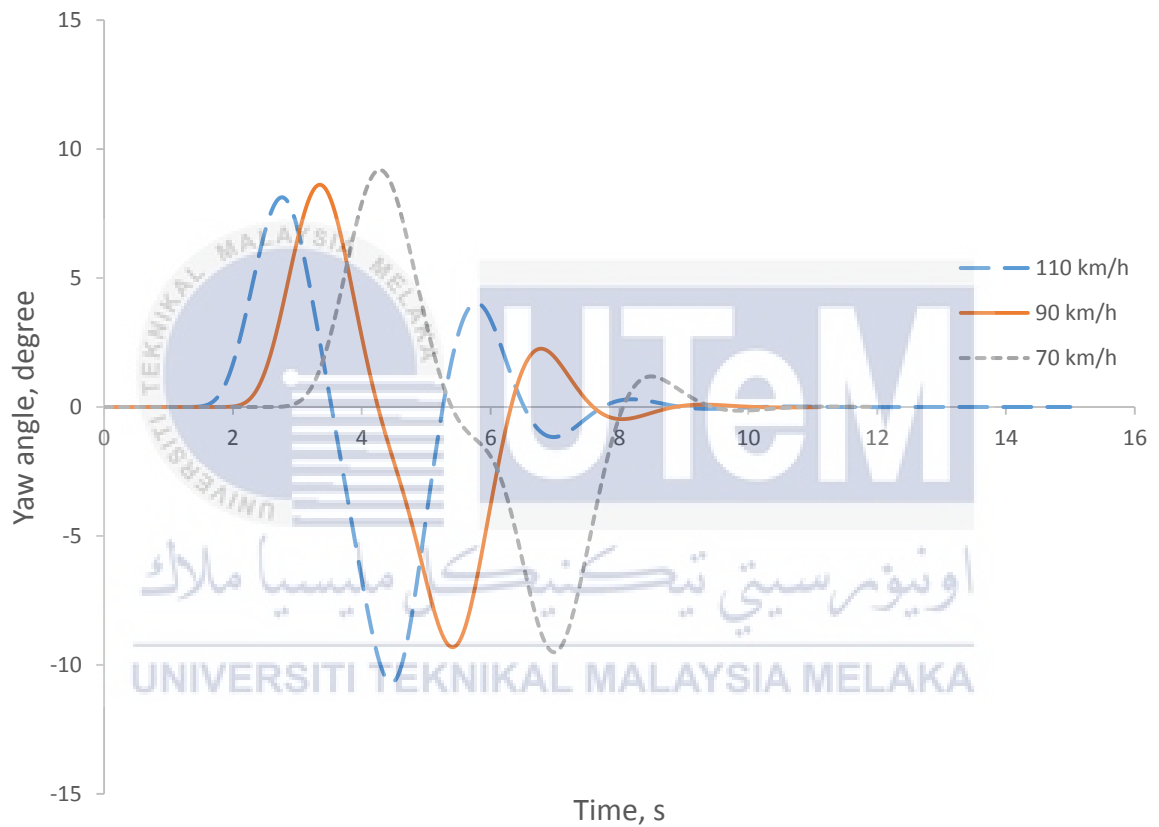


Figure 4.20: Yaw angle of sprung masses at different speeds

Table 4.13: Comparison of maximum yaw angle at different speeds

Speed, km/h	Yaw angle, degree	Time, s
70	-9.504	7.00
90	-9.310	5.40
110	-10.691	4.45

Figure 4.21 shows the graph for yaw angle of sprung mass when the vehicle is travelling with fully laden and unladen. The maximum yaw angle obtained by this two condition of vehicle is at the phase B where the vehicle is changing into the original lane. Based on **Table 4.14**, the maximum yaw angle for fully laden vehicle is higher than the unladen vehicle which is -9.310 degree while unladen vehicle is -9.126 degree because of the inertia value for fully laden vehicle is higher than unladen vehicle during the maneuver so, the inertia of the vehicle will affect the behavior of the vehicle.

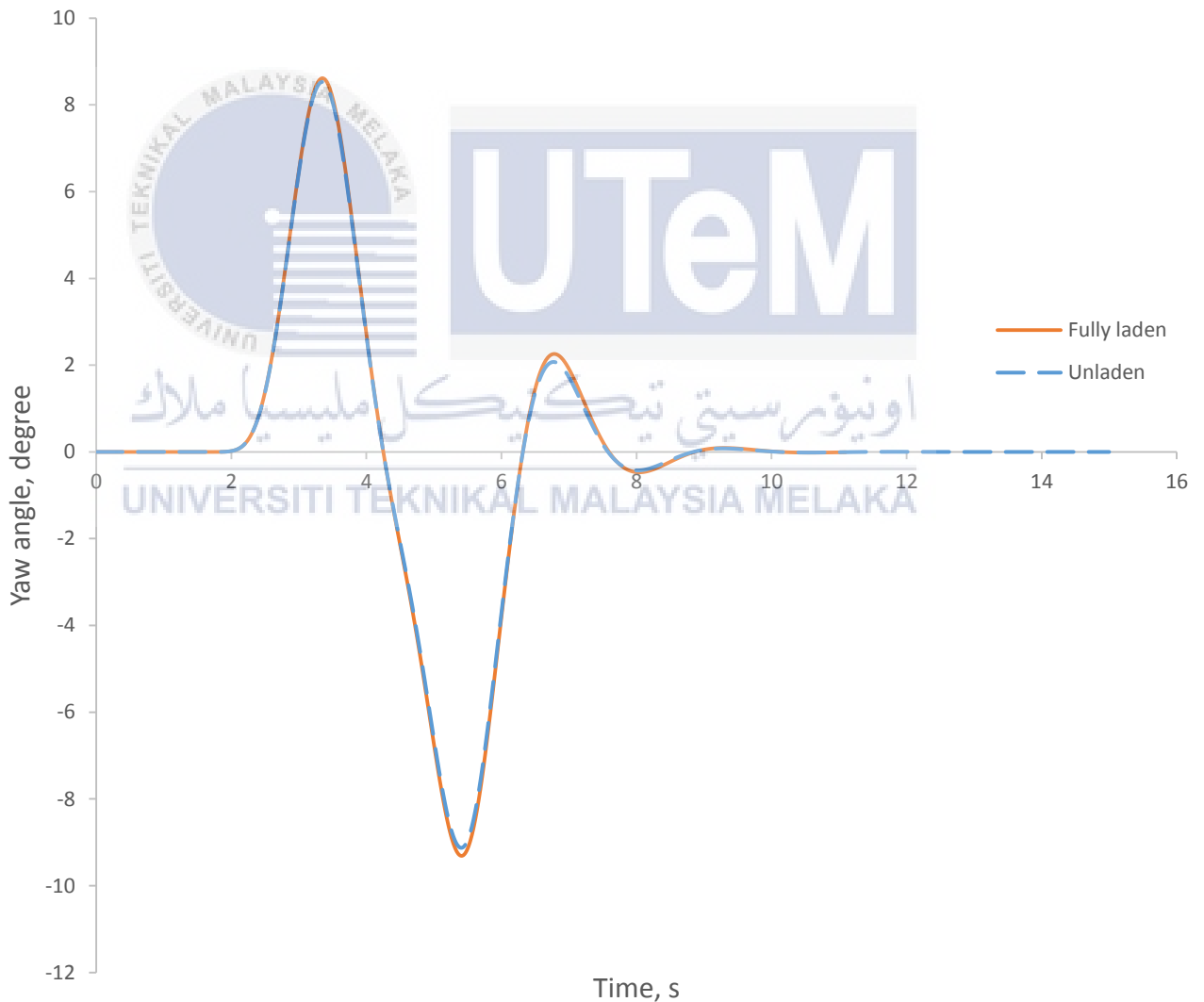


Figure 4.21: Yaw angle of sprung masses when fully laden and unladen vehicle

Table 4.14: Comparison of maximum yaw angle when fully laden and unladen vehicle

Vehicle condition	Yaw angle, degree	Time, s
Unladen	-9.126	5.40
Fully laden	-9.310	5.40

4.2.4 Comparison between tire forces for tire R1

Tire forces of R1 from three axis are compared in the graph as shown in **Figure 4.22** to determine the significant effect of tire force resulting from the test. Only tire force that show the significant effect will be used for the analysis. From the graph, it can be determined that vertical and lateral tire forces shown a significant effect resulting from the test.

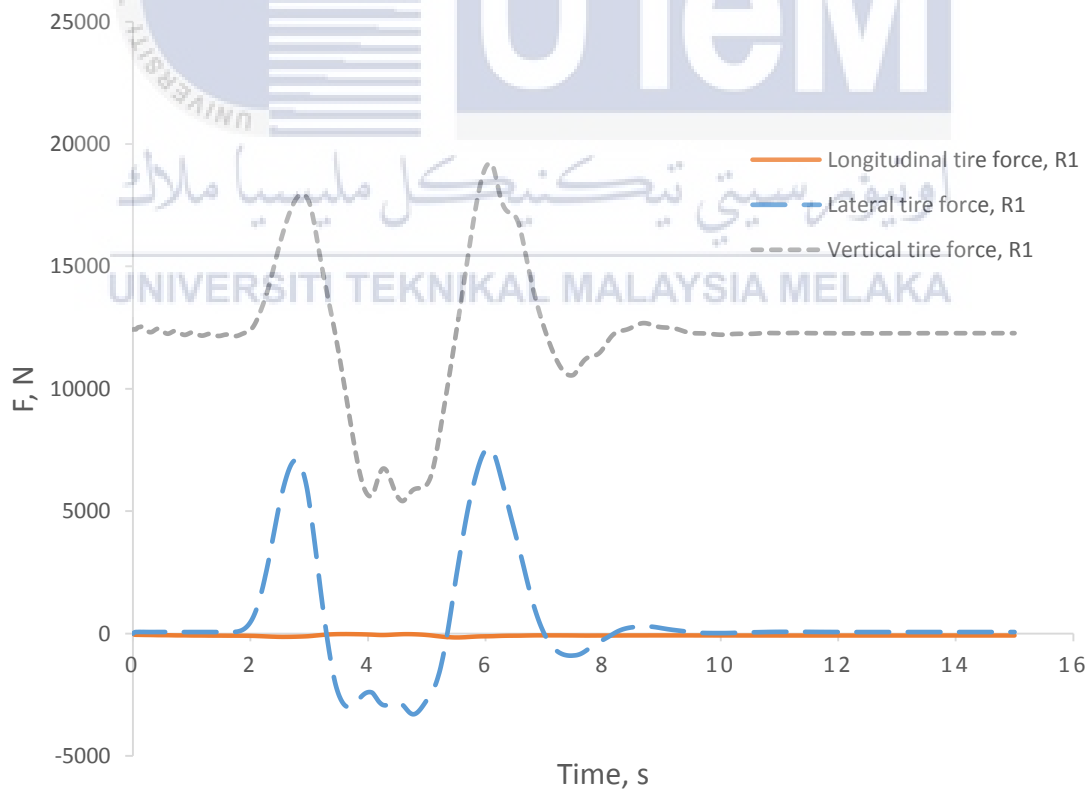


Figure 4.22: Comparison between three tire forces

4.2.5 Lateral tire force

Lateral tire force for tire R1 when travelling at standard speed of 90 km/h is represented in graphical form as in **Figure 4.23**. The positive value of lateral tire force obtained when the vehicle move to the left direction and the negative value obtained when the vehicle move to the right direction. The vehicle start to have positive lateral tire force when the vehicle is about to change lane as represented by phase A in the graph. Then the vehicle complete the lane changing and come back to the original lane as in phase B where the value of lateral tire force is positive that represent the movement of the vehicle to the right. Phase C is when the vehicle is already in the original lane and the lateral tire force present here is due to the vehicle response to the lateral load transfer for straightening the vehicle in the lane. The maximum value of lateral force is obtained in phase C when the vehicle is entering the original lane because it need to have a large amount of grip to maintain the vehicle in the lane after changing lane.

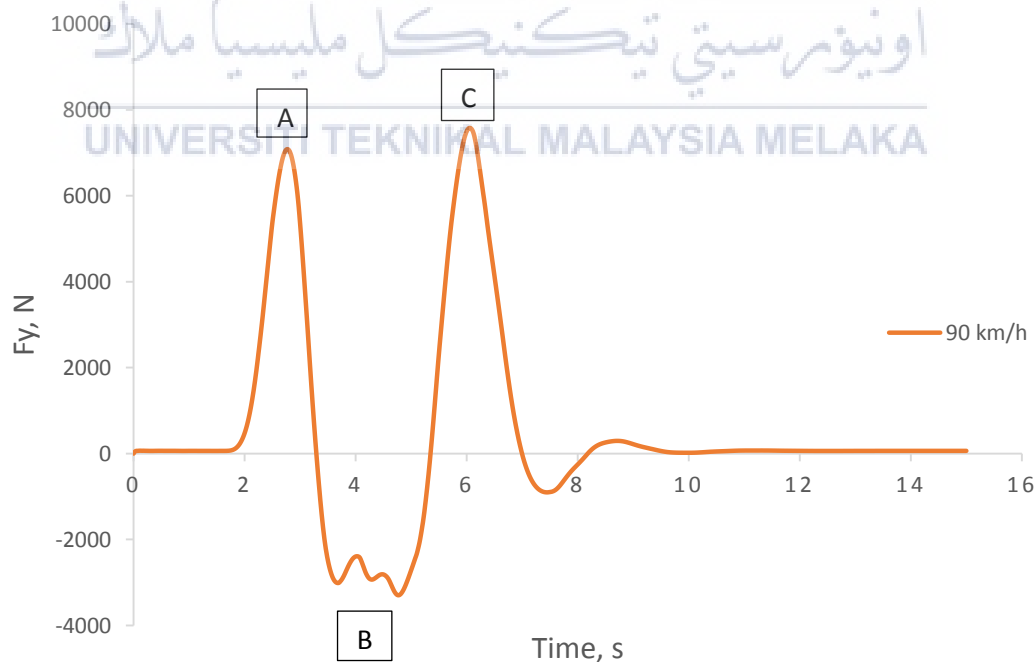


Figure 4.23: Lateral tire forces of R1 at standard speed

Figure 4.24 shows the graph for lateral tire force of R1 when the vehicle travel at different speeds. The vehicle with speed of 70 km/h recorded maximum lateral tire force when in region A while the other two vehicle speed recorded maximum lateral tire force at region C. Based on **Table 4.15**, the highest maximum lateral tire force recorded by vehicle with speed 110 km/h at 10514 N at the time of 5.18 s because the vehicle with higher speed need more lateral grip to maintain in the lane after changing lane.

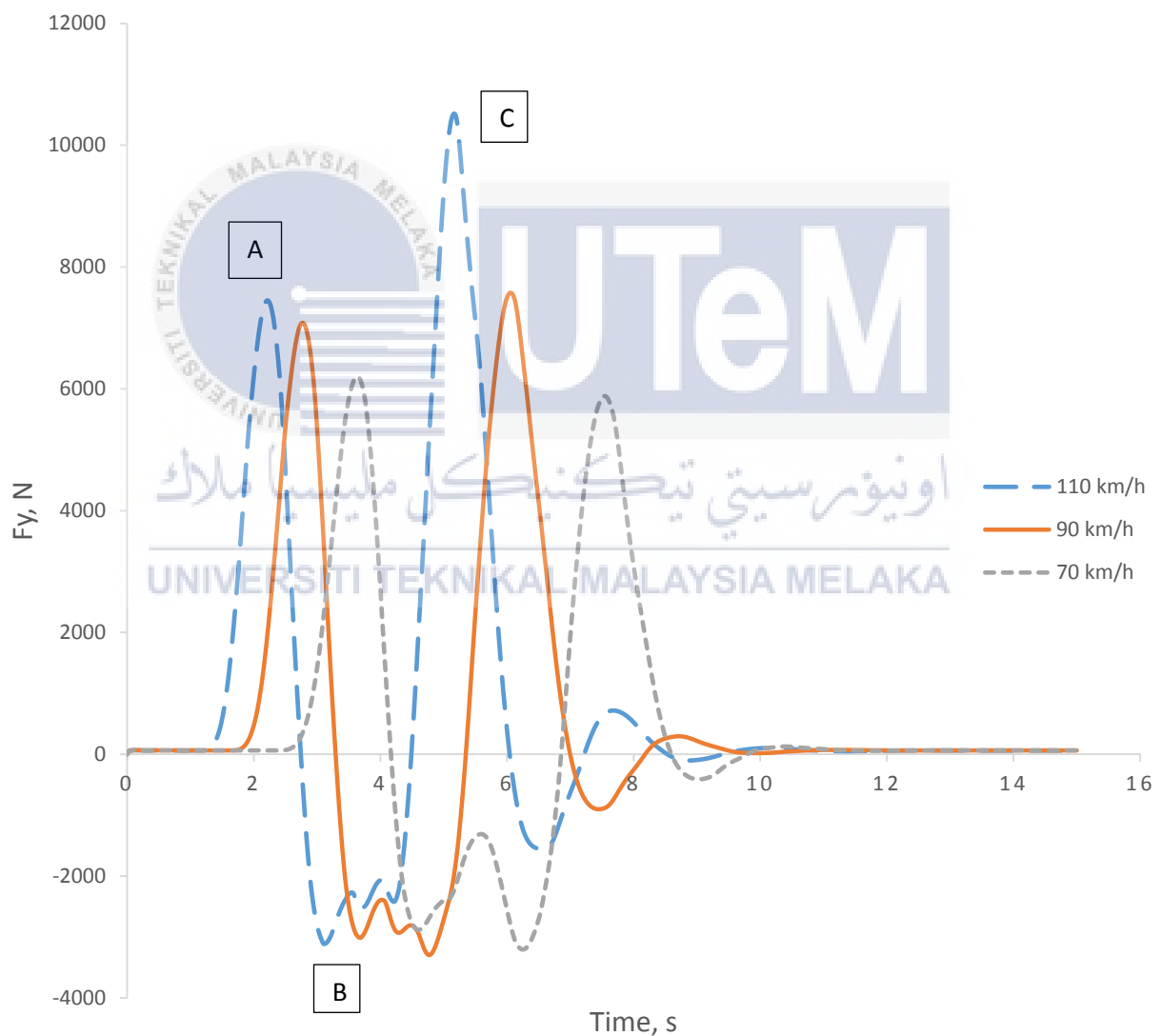


Figure 4.24: Lateral tire force of R1 at different speeds

Table 4.15: Comparison of lateral tire forces at different speeds

Speed, km/h	Lateral force, N	Time, s
70	6201	3.63
90	7577	6.05
110	10514	5.18

Figure 4.25 shows the graph of lateral tire force when the vehicle is in fully laden and unladen condition. Based on **Table 4.16**, vehicle with fully laden recorded higher amount of maximum lateral tire force which is 7577 N at time of 6.05 s while unladen vehicle recorded 5497 N at time of 6.03 s. Both vehicle recorded the maximum lateral tire force at region C. The higher the mass of the vehicle, the higher the maximum value of lateral tire force because the higher load is transferred to the tire during lane changing.

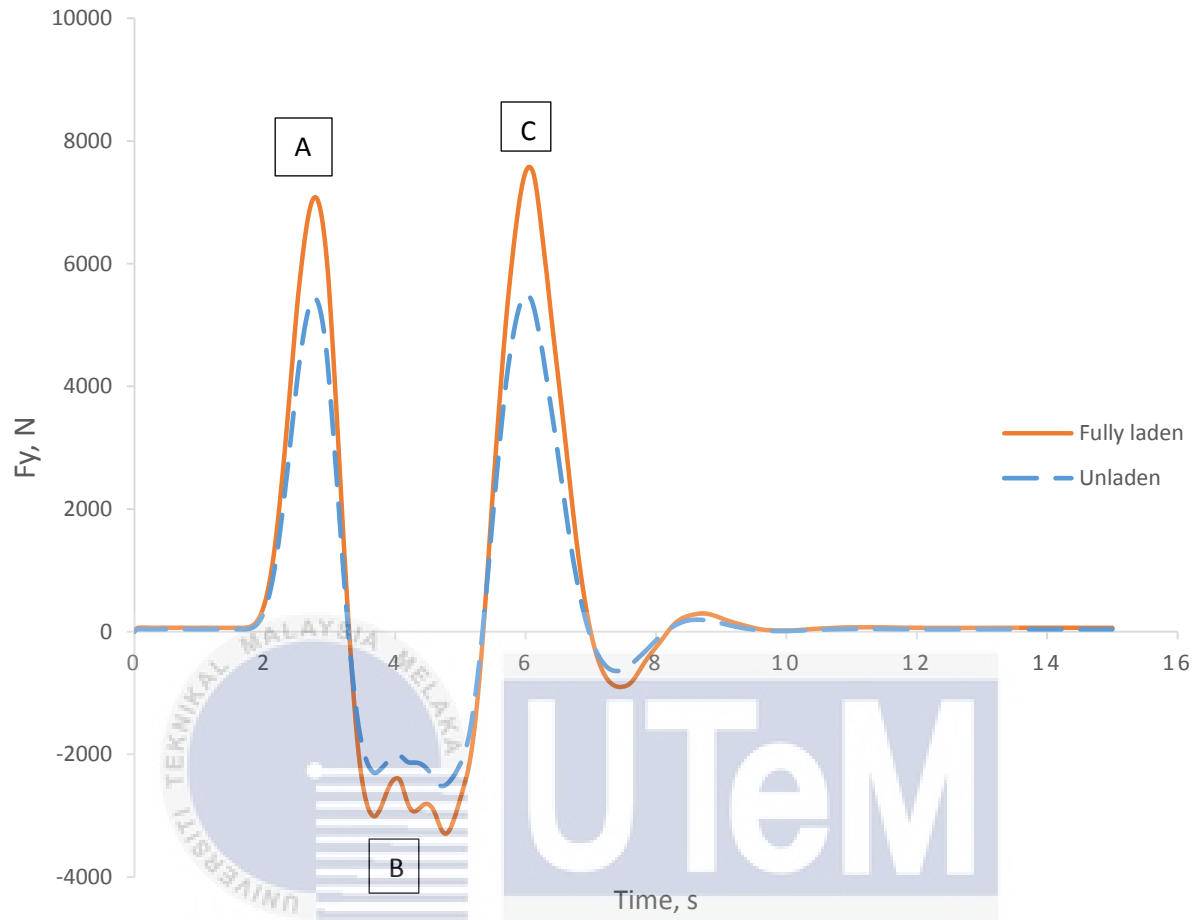


Figure 4.25: Lateral tire force of R1 when fully laden and unladen vehicle

Table 4.16: Comparison of lateral tire forces when fully laden and unladen vehicle

Vehicle condition	Lateral force, N	Time, s
Unladen	5497	6.03
Fully laden	7577	6.05

4.2.6 Vertical tire force, R1

Vertical tire force is the force that is transmitted at Z-axis as in **Figure 4.26** when the vehicle travel at the standard speed of 90 km/h. The vertical tire force that is being analysed is

for front right tire, R1. In region A, the vehicle is turning to the left and the vehicle body is experiencing roll moment in counter clockwise direction and increase the vertical tire force. Then, after the vehicle is already on another lane, the vehicle is turning to the right to enter the original lane and roll moment in clockwise direction is present and decrease the vertical tire force as in region B. In region C, the vehicle is already changing into the original lane and the vertical tire force present here is because of the vehicle is in response to straighten up the vehicle in the lane.

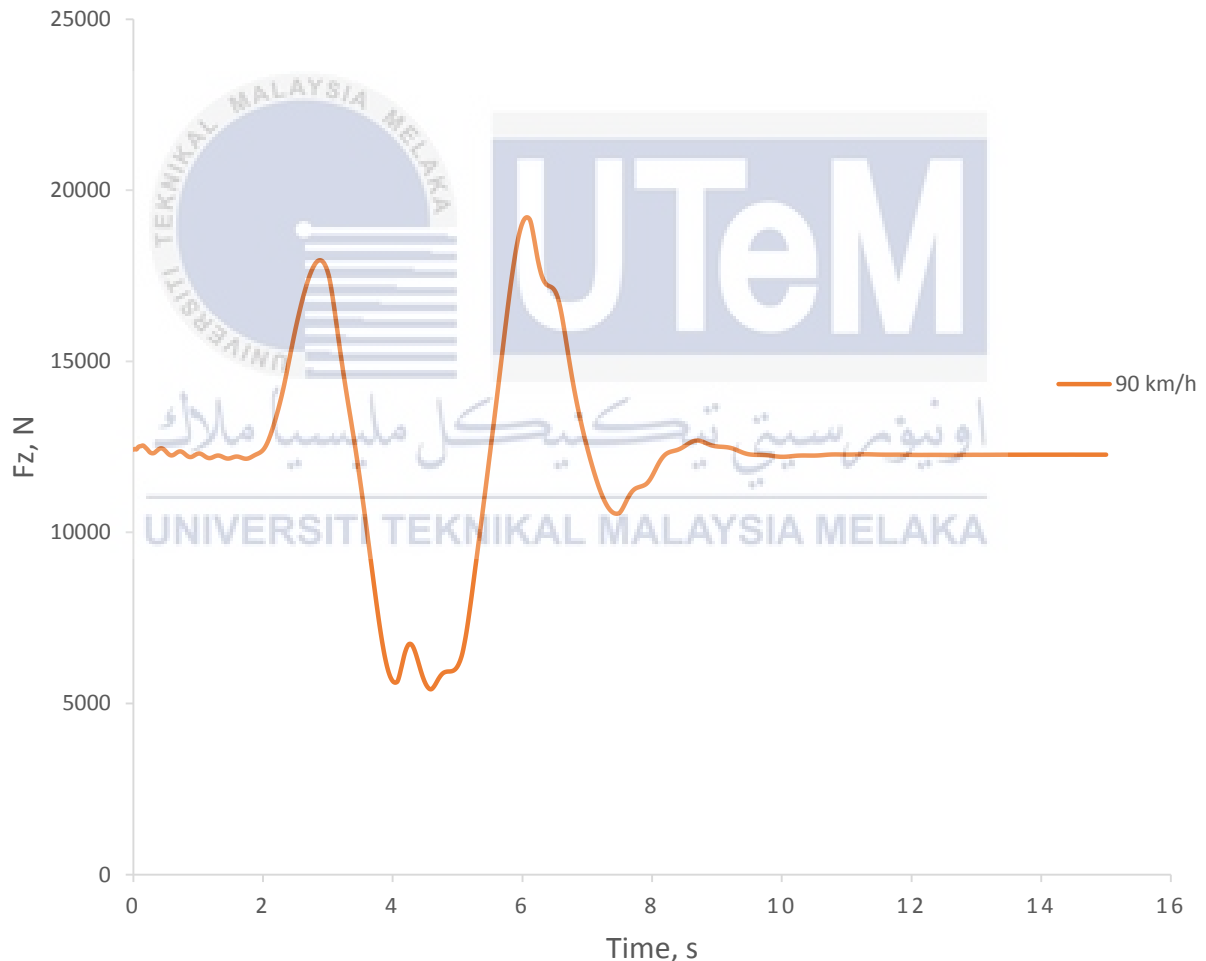


Figure 4.26: Vertical tire force of R1 at standard speed

Figure 4.27 shows the graph for vertical tire force of R1 at different speeds. Based on **Table 4.17**, vehicle with speed of 110 km/h recorded the highest value of vertical tire force which is 21352 N at time of 5.15 s where the vehicle is about to enter the original lane. The higher the speed of vehicle, the higher the value of vertical tire force of R1.

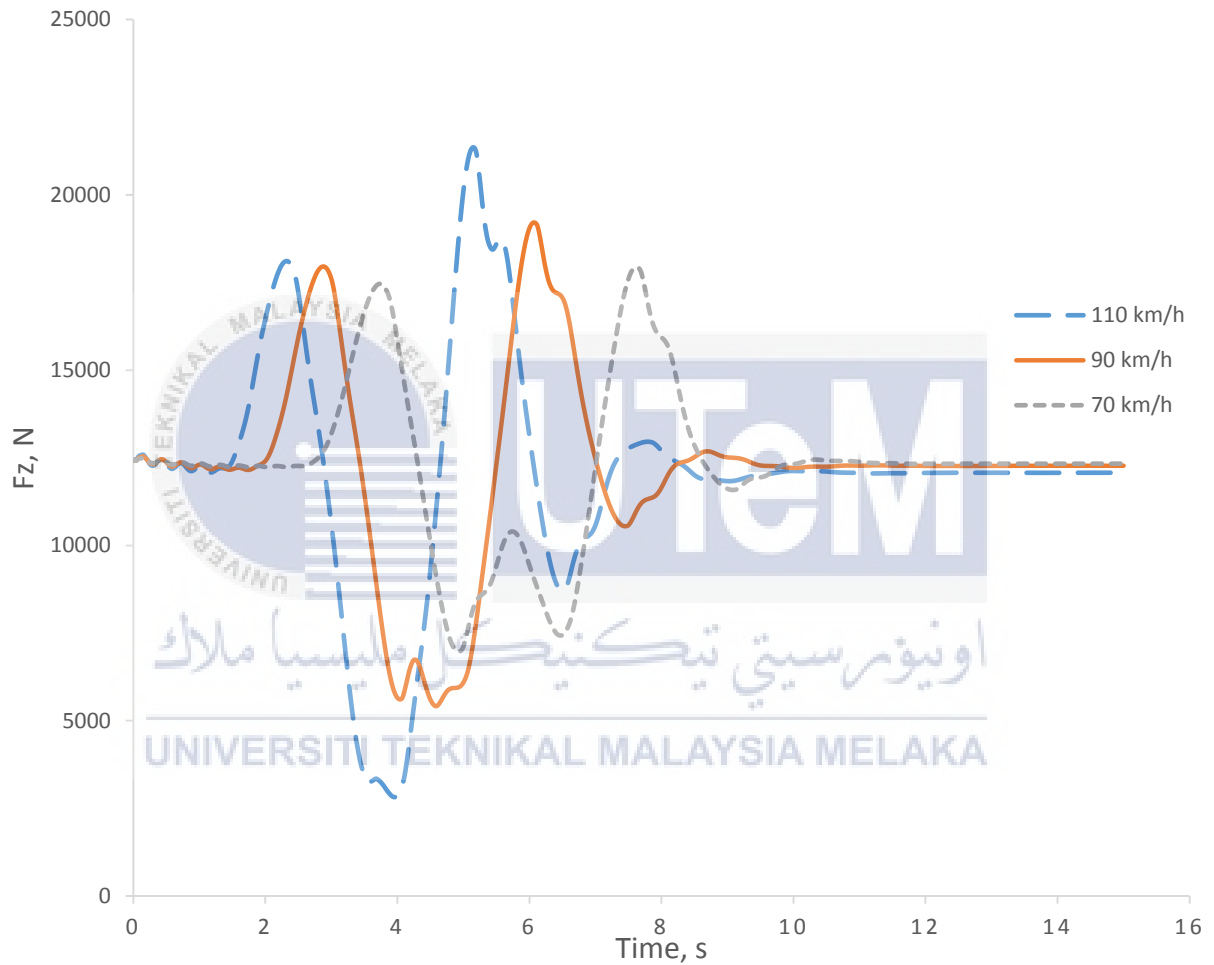


Figure 4.27: Vertical tire force of R1 at different speeds

Table 4.17: Comparison of vertical tire force at different speeds

Speed, km/h	Vertical tire force, N	Time, s
70	17941	7.63
90	19209	6.08
110	21352	5.15

Figure 4.28 shows the graph of vertical tire force of R1 when the vehicle is fully laden and unladen condition. From **Table 4.18**, the vehicle with fully laden recorded higher vertical tire force than unladen vehicle at 19209 N while unladen vehicle is 14042 N. Both vehicle condition recorded maximum vertical tire force at the same region. The higher the mass of vehicle when travelling, the higher the value of maximum vertical tire force recorded.

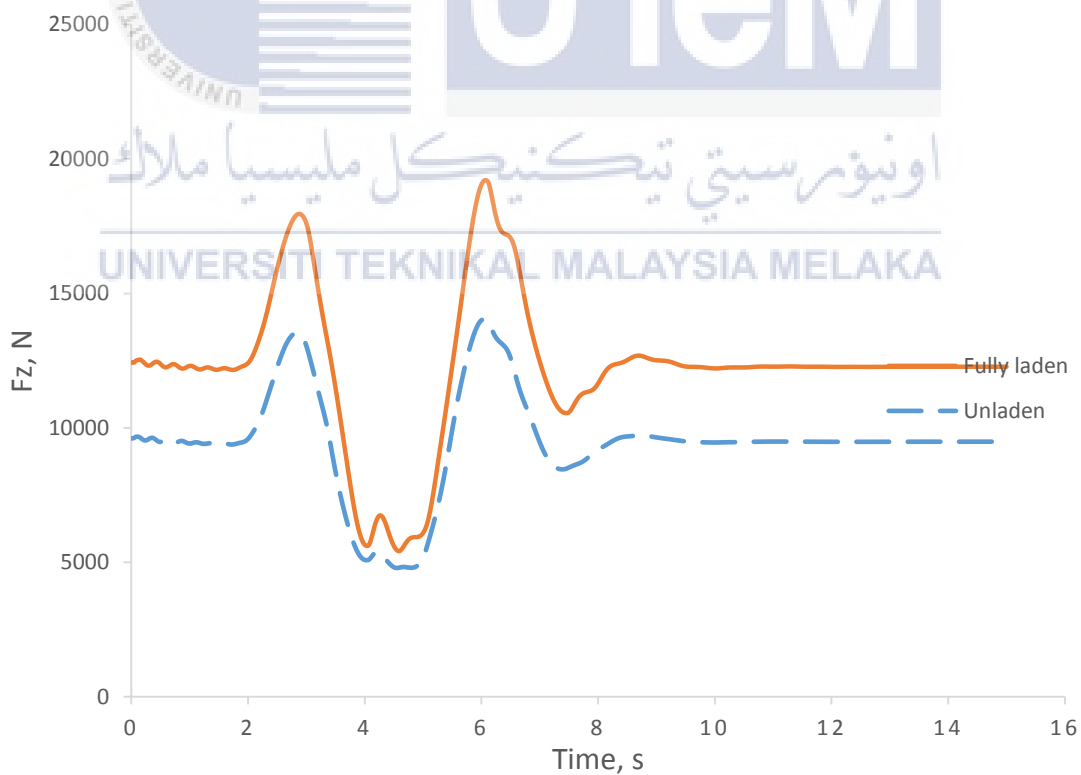


Figure 4.28: Vertical tire force of R1 when fully laden and unladen vehicle

Table 4.18: Comparison of vertical tire force when fully laden and unladen vehicle

Vehicle condition	Vertical tire force, N	Time, s
Unladen	14042	6.05
Fully laden	19209	6.08

4.3 J-turn-type test (Stability)

4.3.1 Trajectory Y vs X

Trajectory is the movement of the vehicle on the road that is represented by coordinate on X-Y plane as in **Figure 4.29**. Positive Y coordinate indicates that the vehicle is moving to the left while negative Y coordinate indicates that the vehicle is moving to the right. The Y coordinate starting to increase when the vehicle receive steering input to the left until the maximum Y coordinate and the counter steering input the right is applied which resulting in decreasing value of Y coordinate. The steering input applied are based on the J-turn type test. The vehicle trajectory difference is significant when at region A where the left steering input is applied right before the vehicle changing steering input to the right.

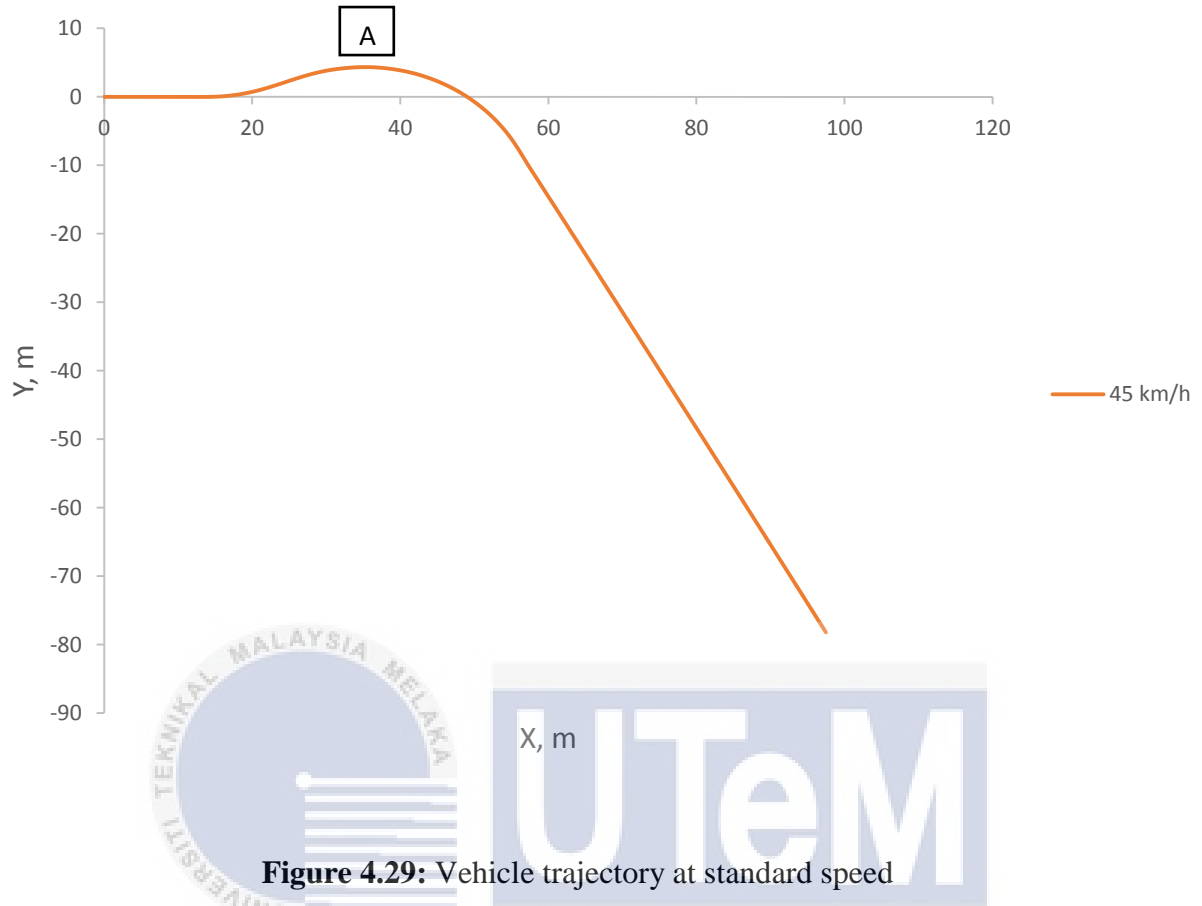


Figure 4.29: Vehicle trajectory at standard speed

Based on **Figure 4.30**, the trajectory of the vehicle at region A when travelling at the speed of 55 km/h is highest compared to the other speed during J turn-type test. Based on **Table 4.19**, the vehicle recorded 5.78 in Y coordinate when left steering input is applied which is highest compared to the other speed. The higher the speed of the vehicle, the higher the value of the vehicle trajectory due to understeer effect.

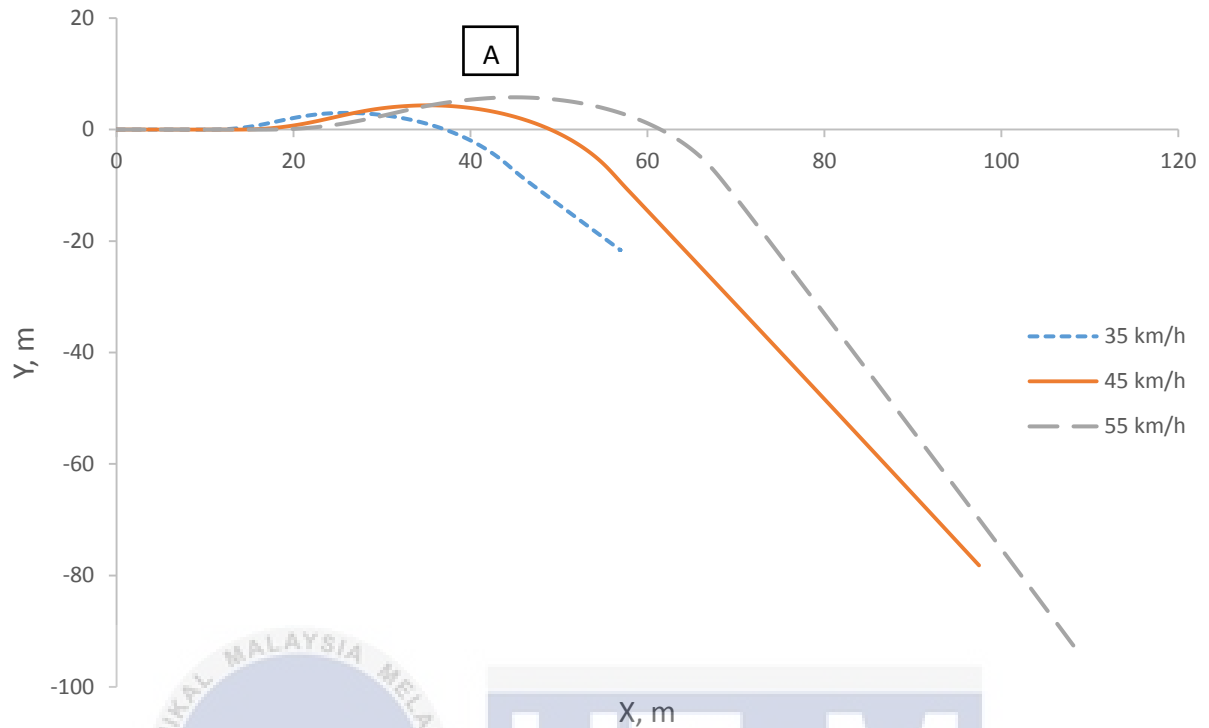


Figure 4.30: Vehicle trajectory at different speeds

Table 4.19: Vehicle trajectory comparison at different speeds

Speed, km/h	Maximum Y coordinate at region A
35	2.89
45	4.30
55	5.78

Figure 4.31 shows the graph for vehicle trajectory when the vehicle is fully laden and unladen. Both vehicle travel at the same speed of 45 km/h. From Table 4.20, vehicle with fully laden recorded higher maximum Y trajectory than unladen vehicle which is 4.30 m while unladen vehicle recorded 3.01 m at region A. The higher the mass of the vehicle during the test,

the higher the maximum Y coordinate of the vehicle recorded due to inertia value of the vehicle is higher compared to lower mass vehicle.

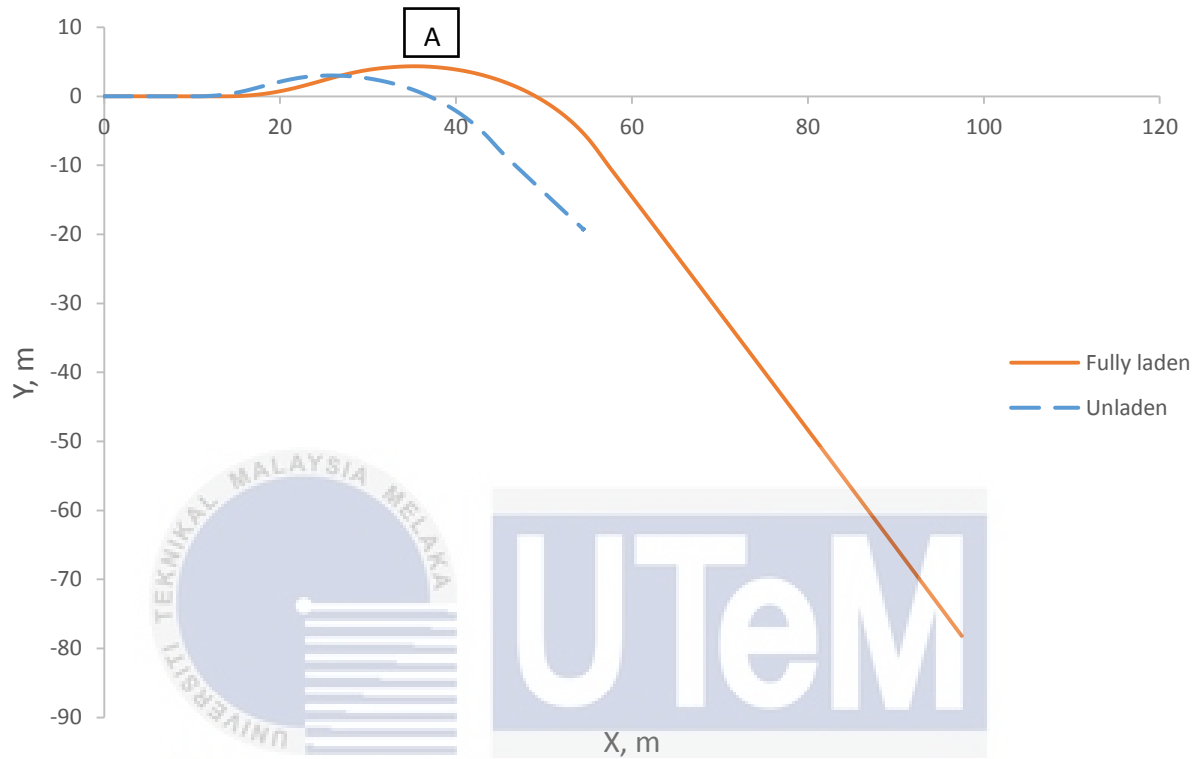


Figure 4.31: Vehicle trajectory for fully laden and unladen vehicle

Table 4.20: Comparison of vehicle trajectory when fully laden and unladen vehicle

Vehicle condition	Maximum Y coordinate at region A
Unladen	3.01
Fully laden	4.30

4.3.2 Lateral Acceleration of CG

The acceleration of the vehicle is based on the vehicle's center of gravity movement in lateral direction. From **Figure 4.32**, the positive lateral acceleration indicates that the vehicle is

moving to the left while negative value indicates that the vehicle is moving to the right. The positive lateral acceleration of the vehicle start to increase when the vehicle is turning to the left and the value of lateral acceleration decrease to the negative value when the vehicle changing direction to the right to complete the J-turn Type test.

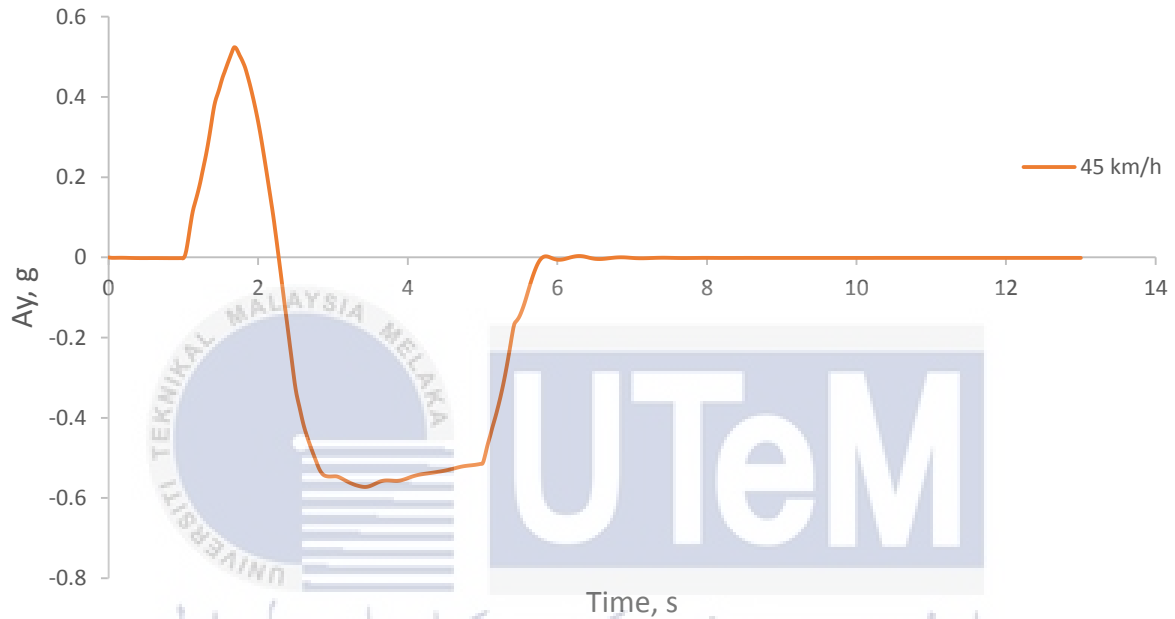


Figure 4.32: Lateral acceleration at standard speed

Figure 4.33 shows that the lateral acceleration of center of gravity of the vehicle during cornering. Based on **Table 4.21**, the highest value of maximum lateral acceleration obtained is -0.741g when the vehicle travel at the speed of 55 km/h. The value is recorded at 3.55 s when the second steering input in counter clockwise direction is applied to the vehicle. The higher the speed of the vehicle, the higher the value of lateral acceleration because the inertia value of the vehicle is higher.

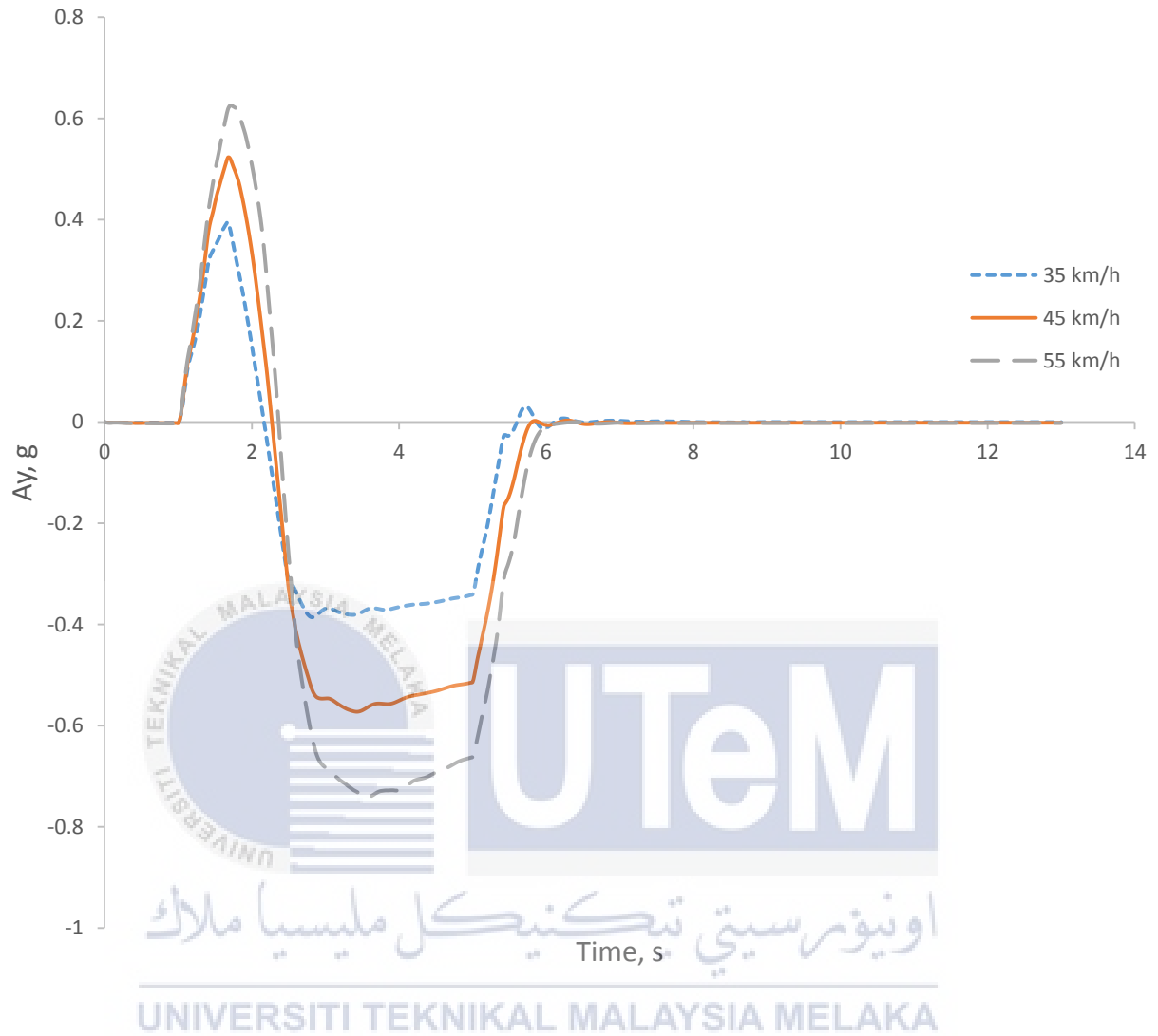


Figure 4.33: Lateral acceleration at different speeds

Table 4.21: Comparison of maximum lateral acceleration at different speeds

Speed, km/h	Maximum lateral acceleration, g	Time, s
35	-0.386	2.83
45	-0.572	3.43
55	-0.741	3.55

Figure 4.34 shows the lateral acceleration when vehicle is in fully laden and unladen condition. From **Table 4.22**, vehicle with fully laden condition recorded higher maximum value of lateral acceleration which is -0.572 g while unladen vehicle recorded -0.384 g. Both vehicle recorded the maximum value at the same region which is when the second steering input in counter clockwise direction is applied to the vehicle. The higher the mass of the vehicle, the higher the maximum value of lateral acceleration.

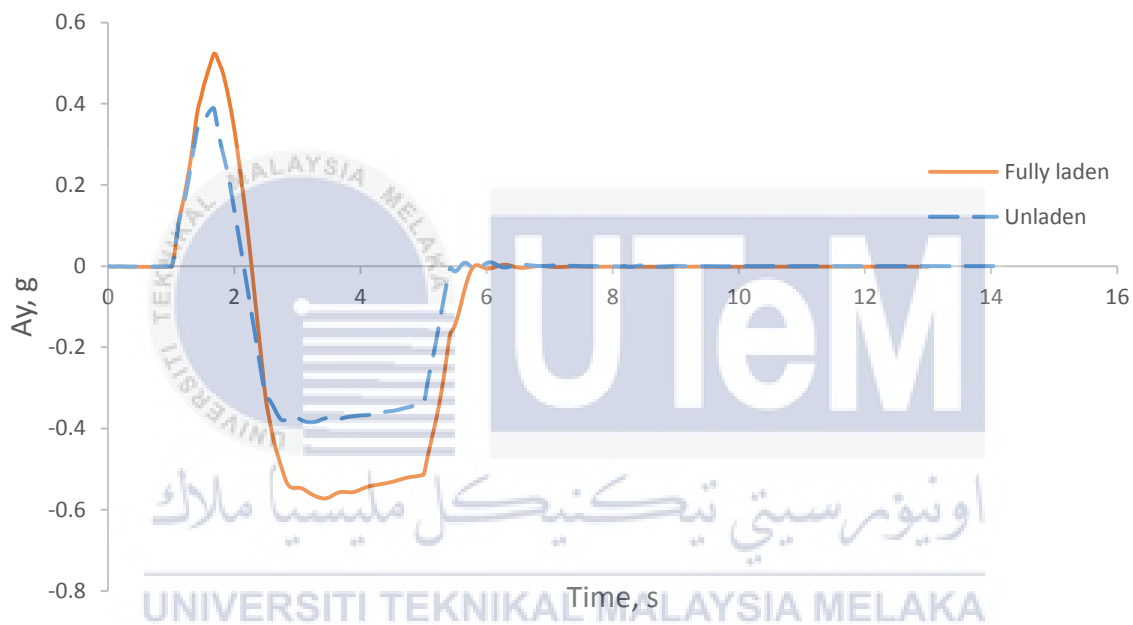


Figure 4.34: Lateral acceleration when fully laden and unladen vehicle

Table 4.22: Comparison of maximum lateral acceleration when fully laden and unladen vehicle

Speed, km/h	Maximum lateral acceleration, g	Time, s
Unladen	-0.384	3.23
Fully laden	-0.572	3.43

4.3.3 Roll moment calculation

The roll moment of the vehicle is the moment that acting on X axis of the vehicle which resulting in motion of the vehicle in clockwise and counter clockwise about X axis. The diagram of pitch moment, M_x that acting on the bus is based on **Figure 4.35**. The sprung mass of the bus is represented as m_b , longitudinal acceleration is a_x and the height of CG to the ground is h .

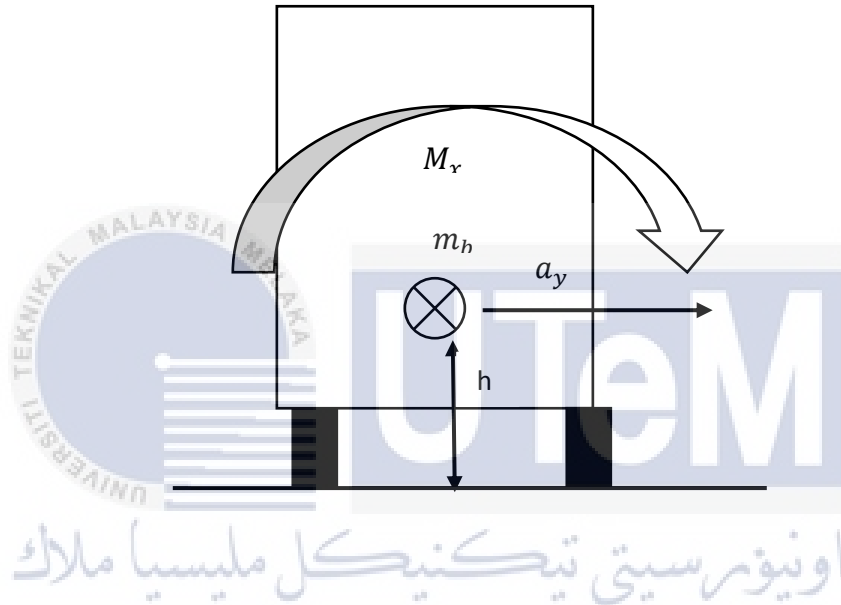


Figure 4.35: Diagram of roll moment acting on the bus

In order to determine the maximum roll moment acting on the bus, it can be calculated from the maximum lateral acceleration that have been obtained from the simulation run by using Eq. (4.7) which then is derived to Eq. (4.8).

$$F_y h = M_x \quad (4.7)$$

$$m_b a_{ymax} h = M_{xmax} \quad (4.8)$$

where F_y is the lateral force and h is the height of CG to the ground. The roll moment is denoted by M_x and the maximum roll moment is M_{xmax} which is derived from the multiplication of m_b , a_{ymax} and h .

The maximum lateral acceleration from the simulation result is in form of gravitational acceleration, g which must be converted into standard form, ms^{-2} to find the roll moment as calculated in Eq. (4.9) and Eq. (4.10).

$$1\ g = 9.81\ ms^{-2} \quad (4.9)$$

$$0.386\ g = 3.79\ ms^{-2} \quad (4.10)$$

Then, substitute the value of m_b , a_{ymax} and h into Eq. (4.11) to find the maximum roll moment.

$$M_{xmax} = (6360)(3.79)(1.2) \quad (4.11)$$

$$= 2.89 \times 10^4\ Nm$$

The value of maximum roll moment for different vehicle speeds can be referred as in **Table 4.23**. When the vehicle travel at speed of 55 km/h, it recorded the highest value of maximum roll moment compared to the other speed at value of $5.55 \times 10^4\ Nm$. The higher the speed of vehicle, the higher the value of maximum roll moment. It is because of higher speed vehicle produce higher lateral force during manoeuvring which resulting in high value of roll moment.

Table 4.23: Maximum roll moment value at different speeds

Vehicle speed, km/h	Maximum lateral acceleration, ms^{-2}	Maximum roll moment, Nm
35	3.798	2.89×10^4
45	5.611	4.28×10^4
55	7.269	5.55×10^4

Next, the value of maximum roll moment when unladen and fully laden condition can be calculated by using Eq. (4.12) and change the value of sprung mass, m_b for every condition as below.

$$M_{xmax} = (4500)(5.611)(1.2) \quad (4.12)$$

$$= 3.03 \times 10^4 Nm$$

The value of maximum roll moment when unladen and fully laden vehicle can be referred in **Table 4.24**. Unladen vehicle has the lower value of maximum roll moment compared to fully laden vehicle at $2.03 \times 10^4 Nm$ while fully laden vehicle is $4.28 \times 10^4 Nm$. The lower the value of sprung mass, the lower the value of maximum roll moment because the lateral force produced is low.

Table 4.24: Maximum roll moment when unladen and fully laden vehicle

Vehicle condition	Maximum lateral acceleration, ms^{-2}	Maximum roll moment, Nm
Unladen	5.611	2.03×10^4
Fully laden	5.611	4.28×10^4

4.3.3 Yaw angle of sprung mass

Yaw angle is the angle between the vehicle is heading and the X-axis of the vehicle. Yaw also the moment of the vehicle at Z-axis. **Figure 4.36** shows the yaw angle of sprung mass of the vehicle when travel at standard speed of 45 km/h which represent the movement of the

body of vehicle about Z-axis. The vehicle starts to experience yaw when first left direction steering input is applied and the value is in positive value that indicates the movement the vehicle to the left. Then, right direction of steering is applied to the vehicle and the value of angle is in negative that indicates the movement of vehicle to the right. The significant different of yaw angle when parameters are changed present at the region where the vehicle is turning to the left.

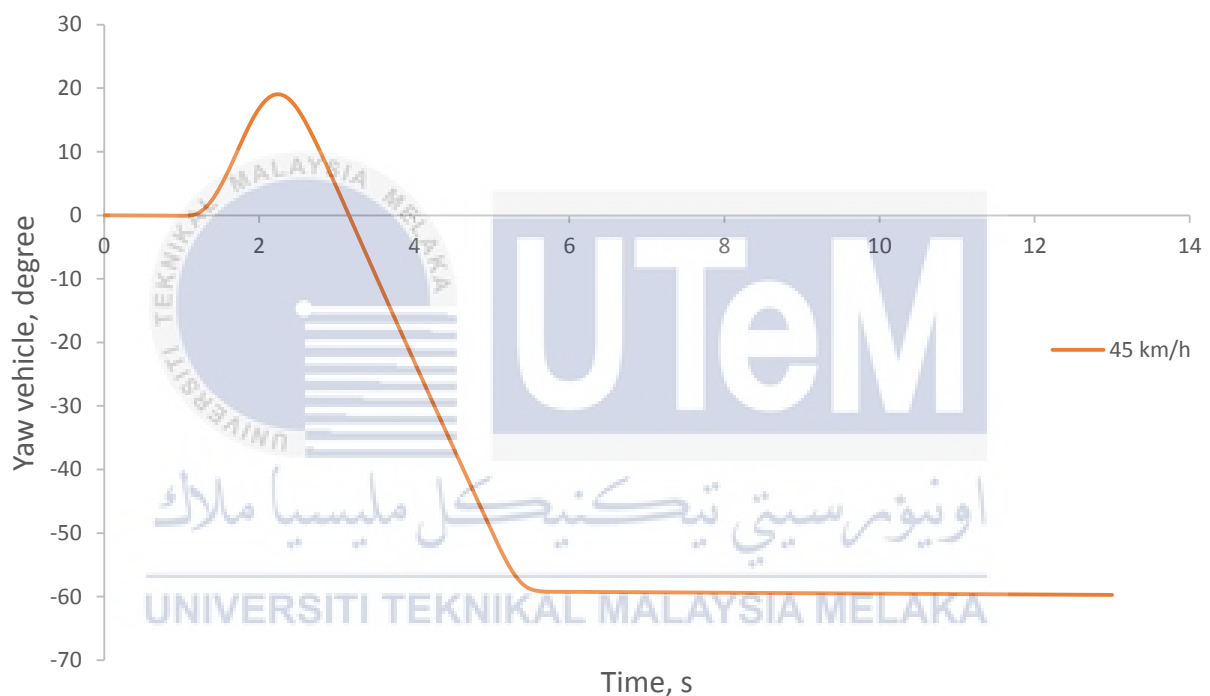


Figure 4.36: Yaw angle of sprung mass at standard speed

Based on **Figure 4.37**, the vehicle experience the highest yaw angle at 21.71 degree when the vehicle travel at the speed of 55 km/h. Based on **Table 4.25**, the value is recorded at 2.28 s when the vehicle is about to change direction from left to the right. The higher the speed

of the vehicle, the higher the value of yaw angle recorded due to the effect of vehicle momentum when cornering and drag away the vehicle from the targeted path.

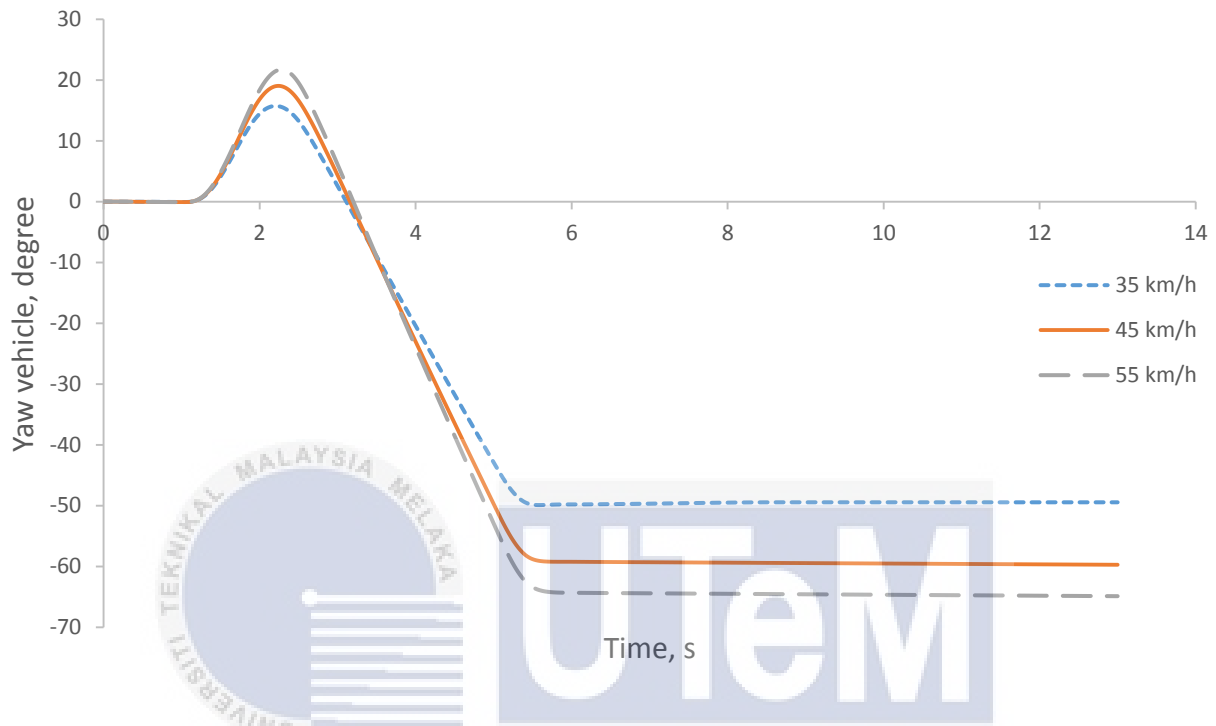


Figure 4.37: Yaw angle of sprung mass at different speeds

Table 4.25: Comparison of maximum yaw angle at different speeds

Speed, km/h	Maximum yaw angle, degree	Time, s
35	15.47	2.30
45	19.04	2.25
55	21.71	2.28

Figure 4.38 shows the graph for yaw angle of sprung mass when vehicle is fully laden and unladen condition. From **Table 4.26**, vehicle with fully laden condition experienced higher yaw angle compared to the unladen vehicle at 19.04 degree while unladen vehicle is 15.79 degree. Both vehicle experienced the highest yaw angle at the same region. The higher the mass

of the vehicle, the higher the yaw angle of sprung mass because vehicle with higher mass has greater inertia compared to lower mass vehicle.

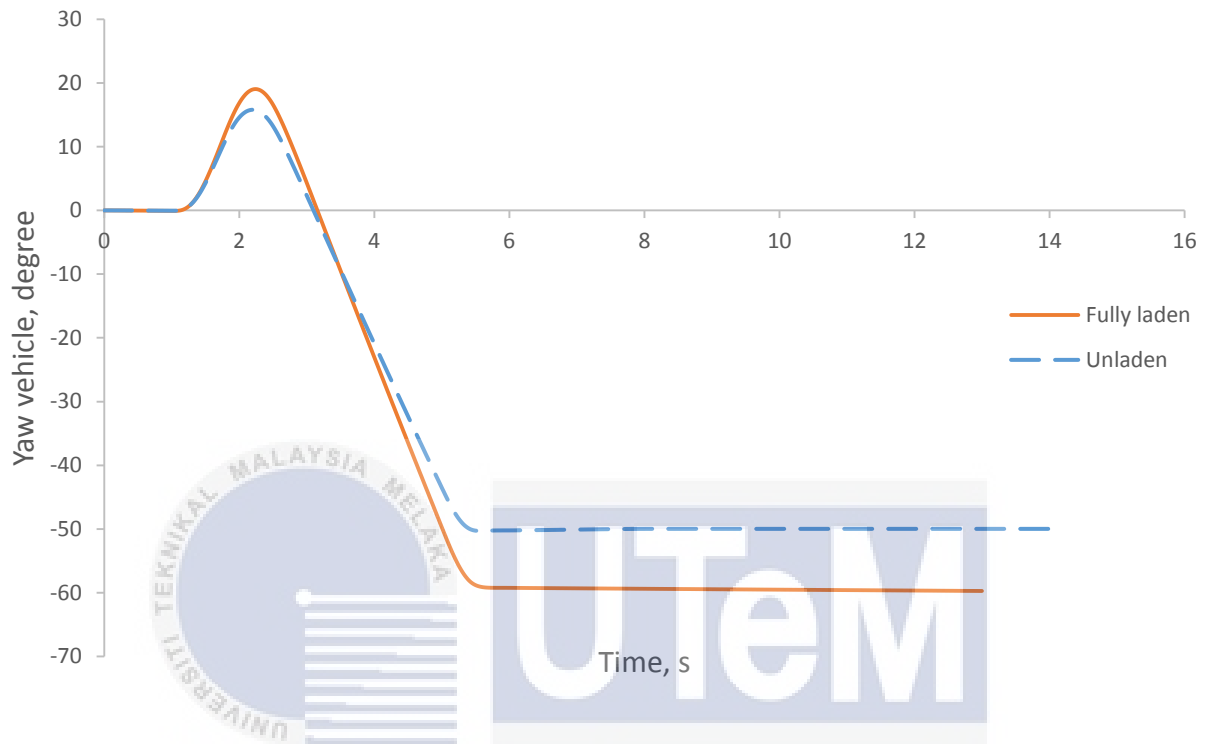


Figure 4.38: Yaw angle of sprung mass when fully laden and unladen vehicle

Table 4.26: Comparison of maximum yaw angle when fully laden and unladen vehicle

Vehicle condition	Maximum yaw angle, degree	Time, s
Unladen	15.79	2.20
Fully laden	19.04	2.25

4.3.4 Roll angle of sprung mass

Roll angle of sprung mass is the movement of the vehicle body about X-axis in clockwise and counter clockwise direction. **Figure 4.39** shows the example roll moment of the vehicle about X-axis. The roll angle for sprung mass is based on **Figure 4.40** where the positive value

of angle represent the movement of vehicle in clockwise direction about X-axis while negative value of angle represent the movement of vehicle in counter clockwise direction about X-axis. The vehicle experience roll when the vehicle is moving to the right which is in positive value and then experience negative roll angle when the vehicle is moving to the right.

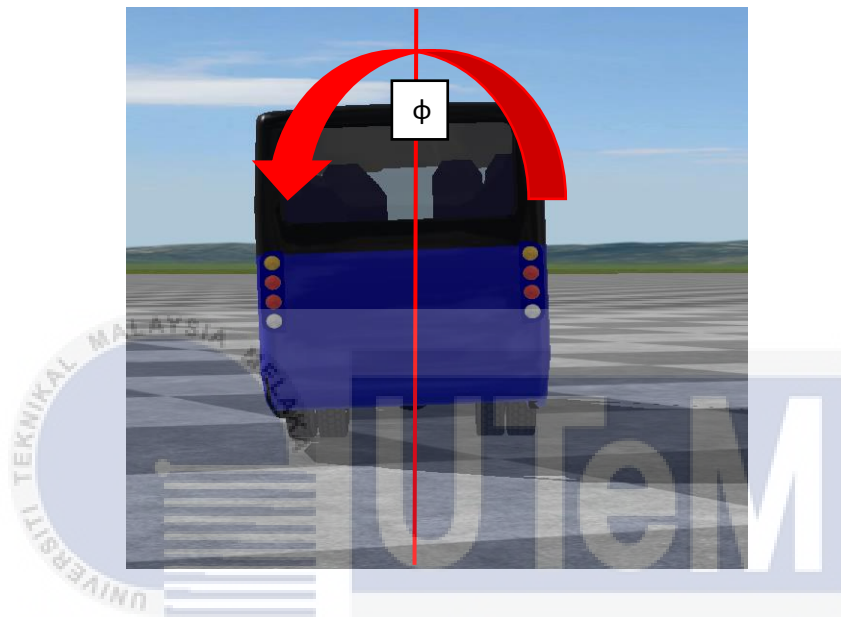


Figure 4.39: Representation of roll moment of vehicle

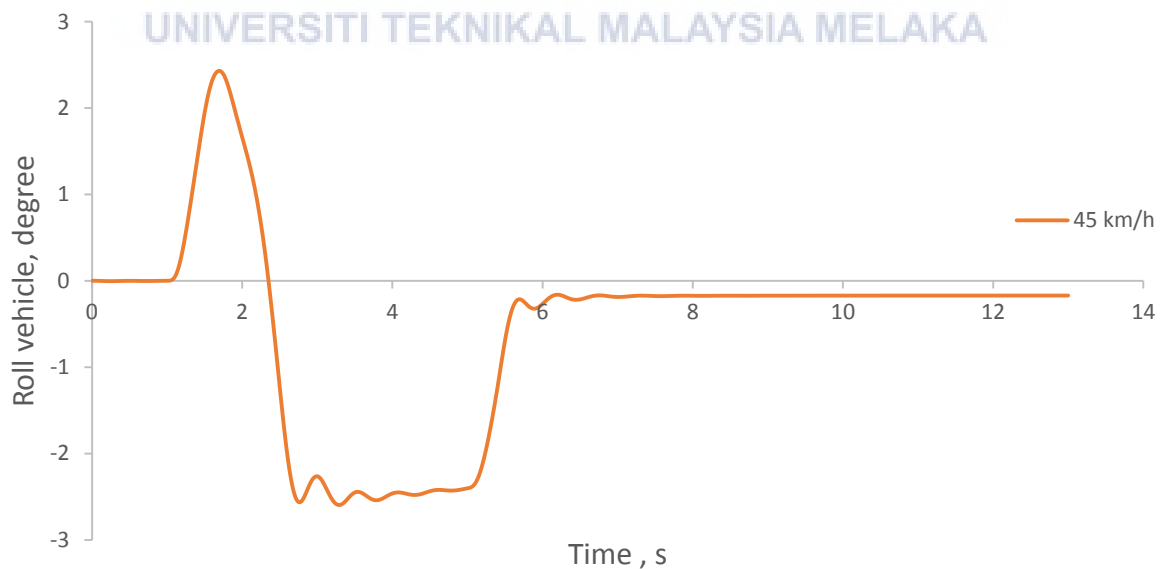


Figure 4.40: Roll angle of sprung mass at standard speed

Based on **Figure 4.41**, the maximum roll angle of sprung mass obtained is -3.32 degree when the vehicle move at the speed of 55 km/h at the time of 3.35 s when the vehicle is turning to the right direction as in **Table 4.27**. The higher the speed of vehicle, the higher the value of roll angle experienced by the vehicle during turning.

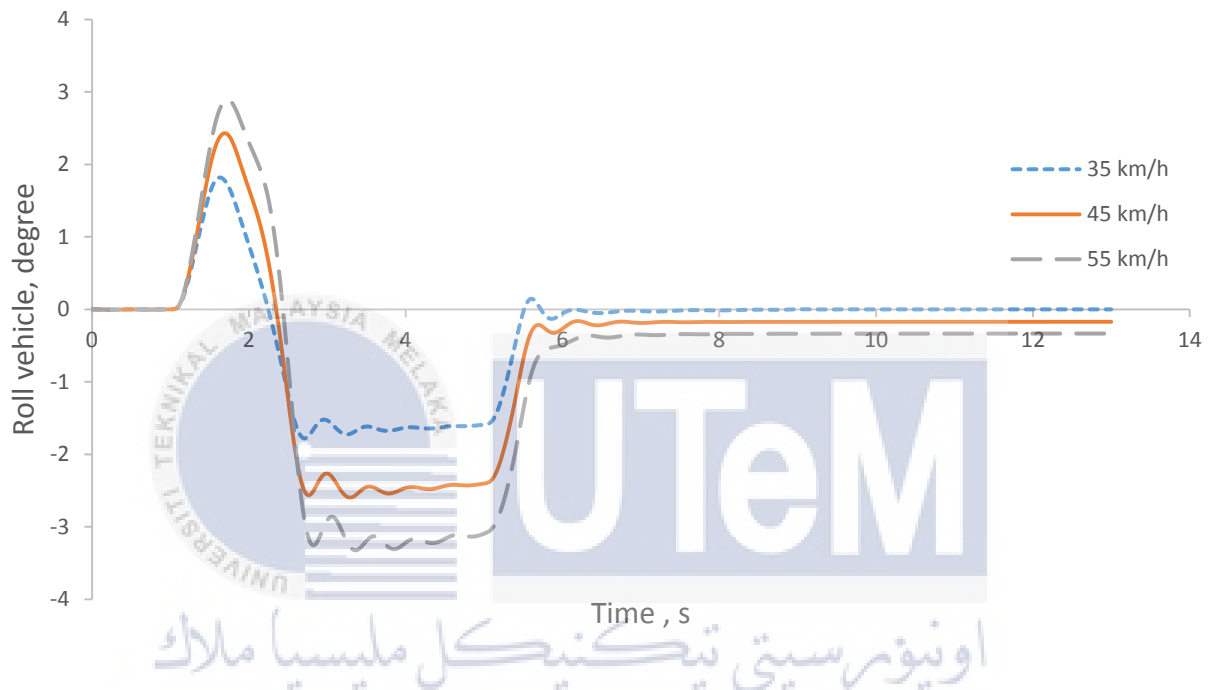


Figure 4.41: Roll angle of sprung mass at different speeds

Table 4.27: Comparison of roll angle at different speeds

Speed, km/h	Roll angle, degree	Time, s
35	-1.78	2.73
45	-2.60	3.30
55	-3.32	3.35

Figure 4.42 shows the roll angle of sprung mass when the vehicle is in fully laden condition and unladen condition. Based on **Table 4.28**, the roll angle for fully laden vehicle is -

2.60 degree which is higher than unladen vehicle, -1.10 degree. The higher the mass of vehicle, the higher the value of roll angle.

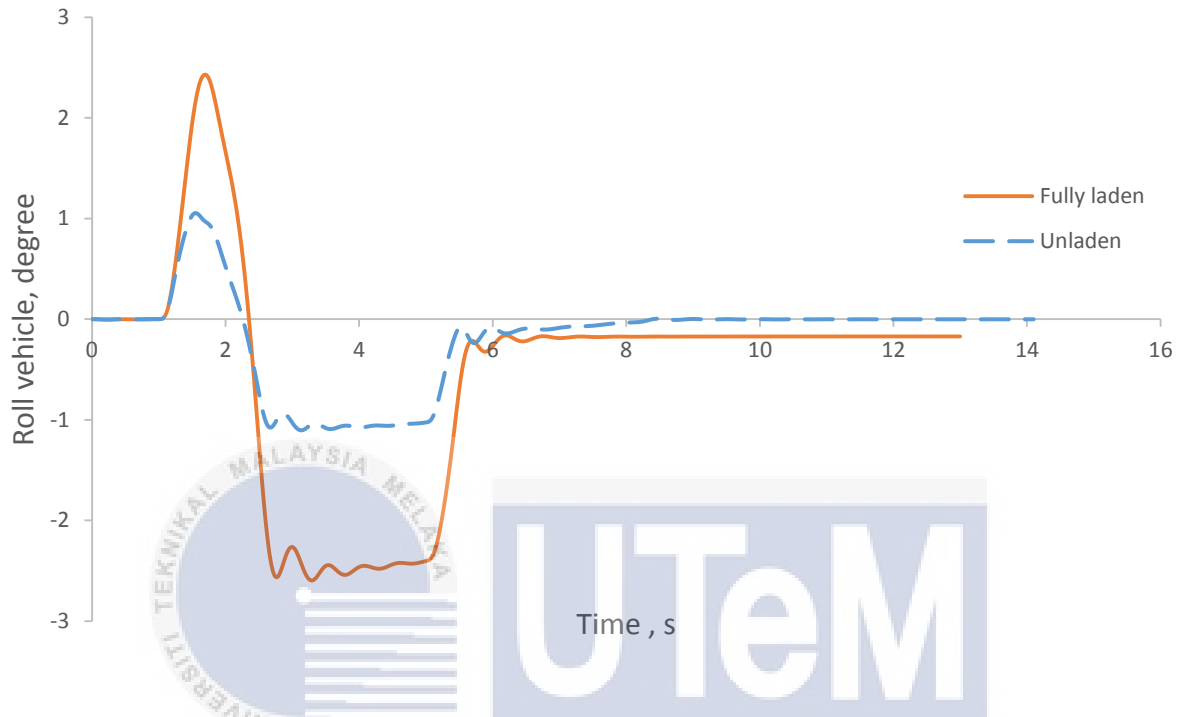


Figure 4.42: Roll angle of sprung mass when fully laden and unladen vehicle

Table 4.28: Comparison of roll angle when fully laden and unladen vehicle

Vehicle condition	Roll angle, degree	Time, s
Unladen	-1.10	3.13
Fully laden	-2.60	3.30

4.3.5 Comparison between tire forces R1

Tire forces of R1 from three axis are compared in the graph as shown in **Figure 4.43** to determine the significant effect of tire force resulting from the test. Only tire force that show the significant effect will be used for the analysis. From the graph, it can be determined that vertical and lateral tire forces shown a significant effect resulting from the test. The value of longitudinal

tire force from braking force at the end of the test can be neglected as this test do not cover the braking force of the vehicle. The tire forces will only analyze the movement of vehicle during J-turn type test.

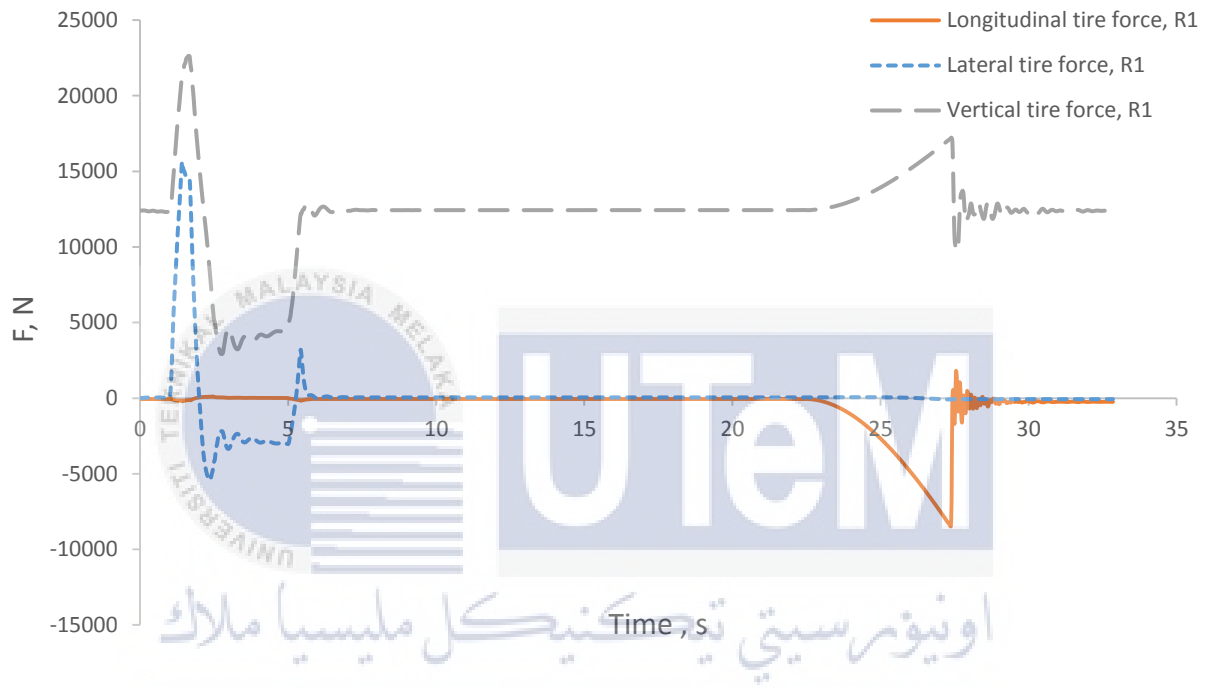


Figure 4.43: Comparison of tire force of R1

4.3.6 Lateral tire force, R1

Lateral tire force tire R1 is represented in **Figure 4.44** when the vehicle travel at standard speed of 45 km/h. The lateral tire force increasing up to 15646.34 N in region A which is the highest value of lateral tire force when the vehicle is turning to the left and it put a lot amount of stress to the right tire. Then, the force decreasing in region B due to the vehicle is turning to the right and the amount of stress to the right tire is reduced. Next, the lateral tire force that is present in region C is when the tire is about to compensate force from straightening movement of the vehicle.

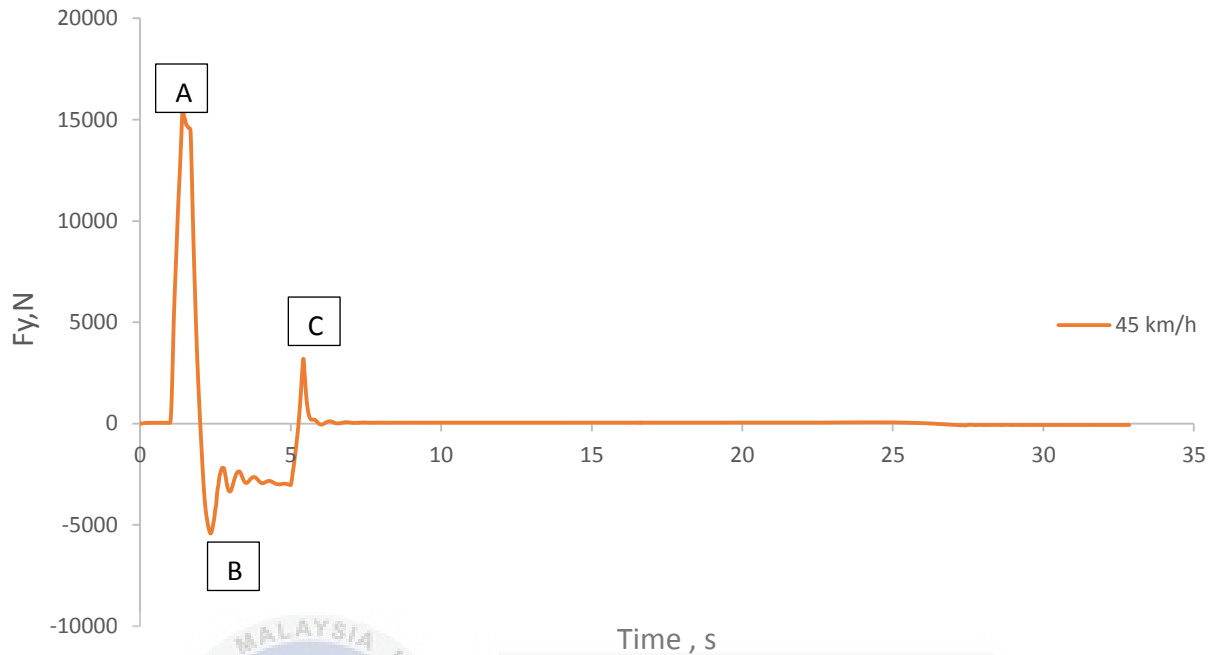


Figure 4.44: Lateral tire force of R1 at standard speed

Figure 4.45 shows the lateral tire force of R1 when the vehicle is moving at different speeds. The significant different of lateral tire force present at region A. Based on **Table 4.29**, the highest maximum value of lateral tire force is when the vehicle travel at speed of 55 km/h which is 18454.56 N. The higher the speed of vehicle, the higher the value of lateral tire force recorded on tire R1.

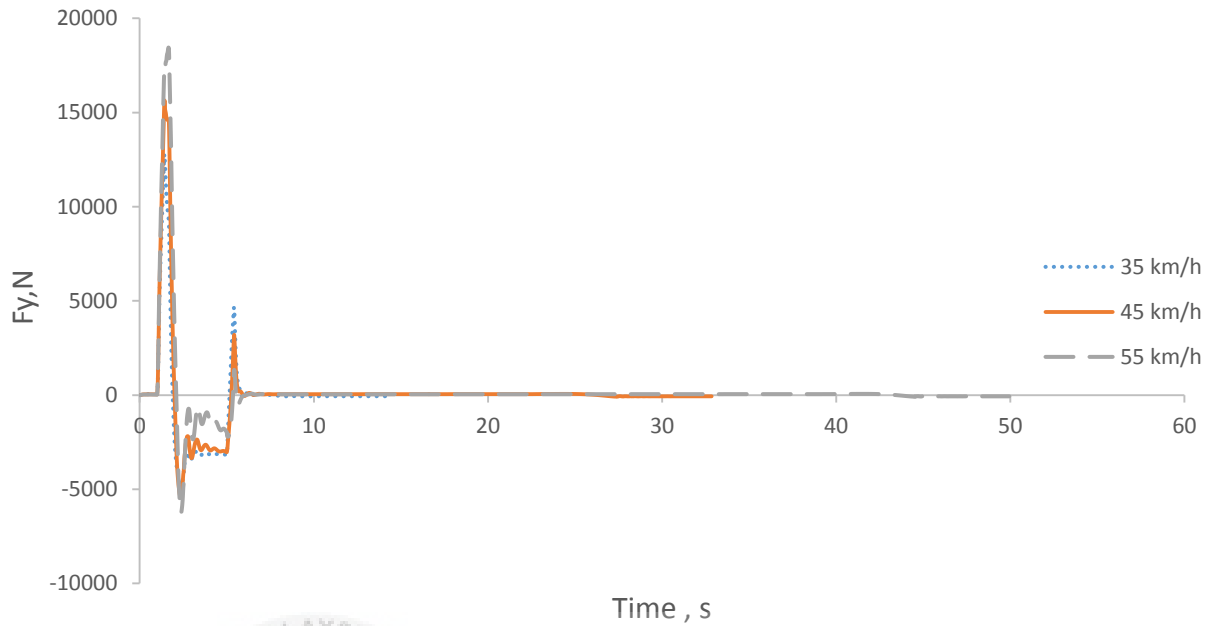


Figure 4.45: Lateral tire forces of R1 at different speeds

Table 4.29: Comparison of lateral tire forces at different speeds

Speed, km/h	Maximum lateral tire force, N	Time, s
35	12800.11	1.43
45	15646.34	1.43
55	18454.56	1.65

Figure 4.46 shows the lateral tire force of R1 when the vehicle is fully laden and unladen condition. From **Table 4.30**, vehicle with fully laden recorded higher maximum value of lateral tire force than unladen vehicle which is 15646.34 N compared to 10227.02 N. Both vehicle recorded the maximum value of lateral tire force at the same region.

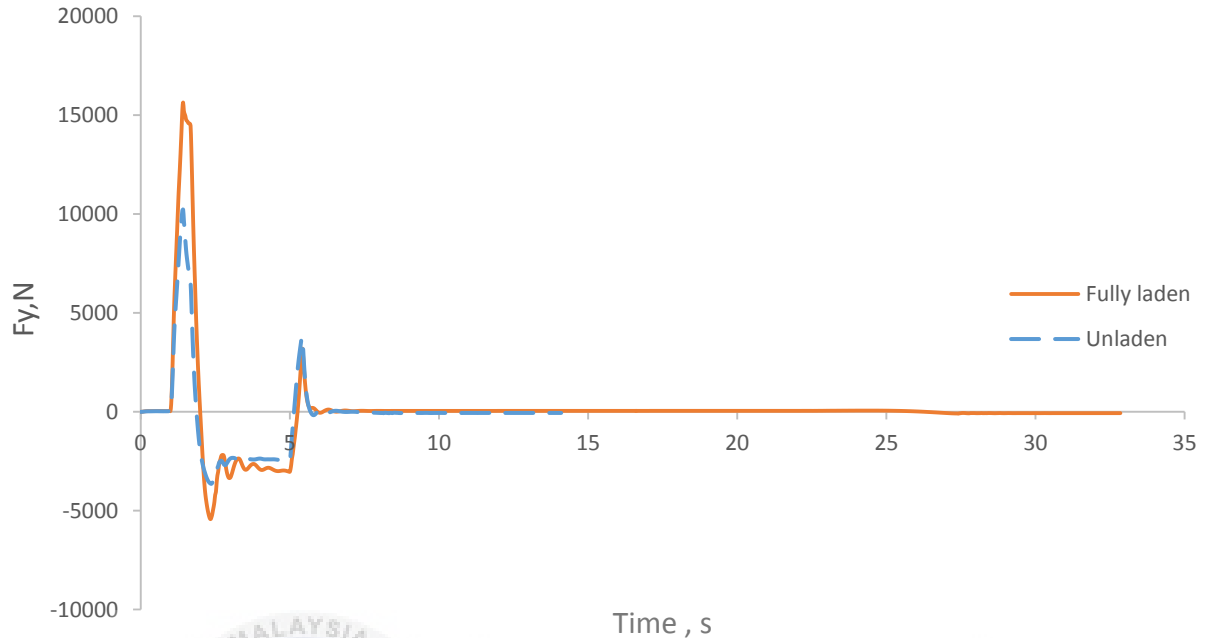


Figure 4.46: Lateral tire force of R1 when fully laden and unladen vehicle

Table 4.30: Comparison of lateral tire forces of R1 when fully laden and unladen vehicle

Vehicle condition	Maximum lateral tire force, N	Time, s
Unladen	10227.02	1.43
Fully laden	15646.34	1.43

4.3.7 Vertical tire force, R1

Vertical tire force is the force that is transmitted at Z-axis as in **Figure 4.47** when the vehicle travel at the standard speed of 45 km/h. The vertical tire force that is being analyzed is for front right tire, R1. In region A, the vehicle is turning to the left and the vehicle body is experiencing roll moment in clockwise direction and increase the vertical tire force. Then, the vehicle is turning to the right roll moment in counter clockwise direction is present and decrease

the vertical tire force as in region B. In region C, the vertical tire force present here is because of the vehicle is in response to straighten up the vehicle.

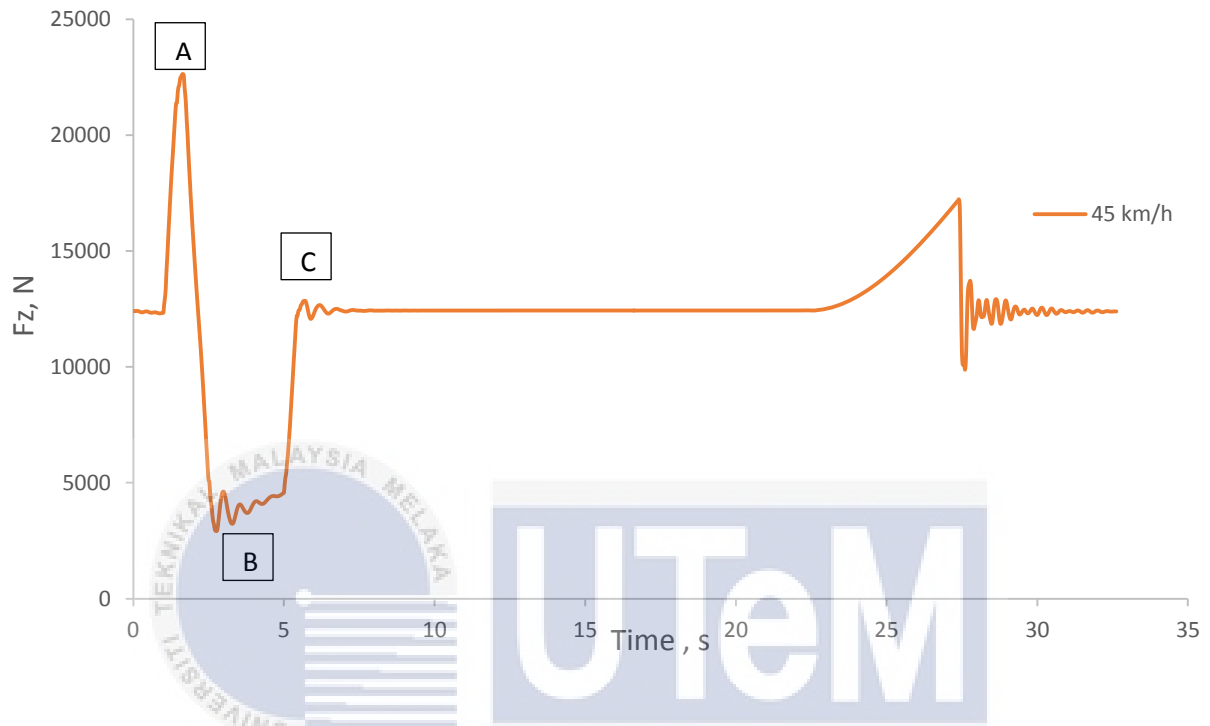


Figure 4.47: Vertical tire force of R1 at standard speed

Figure 4.48 shows the graph for vertical tire force of R1 when vehicle travel at different speeds. Based on **Table 4.31**, vehicle with speed of 55 km/h recorded highest value of vertical tire force which is 24283.60 N when the vehicle is at region A. At region A, the vehicle body experiencing roll moment in clockwise direction and increase the vertical load to the right tire. The higher the speed of vehicle, the higher the vertical tire force recorded.

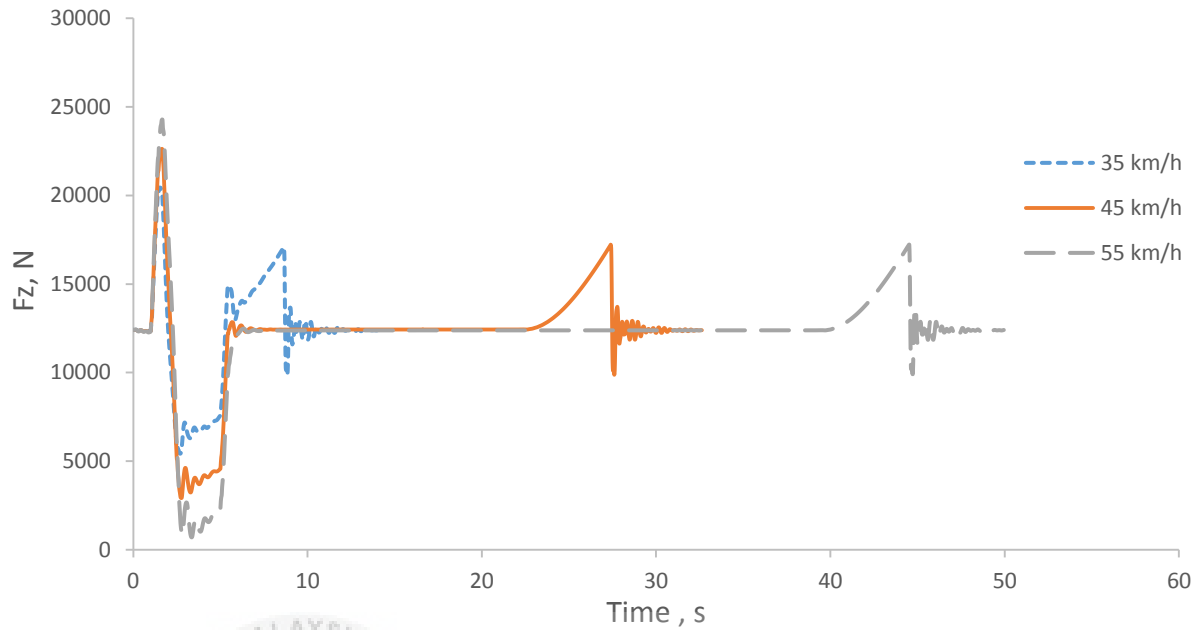


Figure 4.48: Vertical tire force of R1 at standard speed

Table 4.31: Comparison of vertical tire force of R1 at different speeds

Speed, km/h	Maximum vertical tire force, N	Time, s
35	20450.21	1.50
45	22634.80	1.65
55	24283.60	1.68

Figure 4.49 shows the vertical tire force of R1 when vehicle is fully laden and unladen condition. The significant different in vertical tire force is present at region A. From **Table 4.32**, vehicle with fully laden condition recorded 22634.80 N which is higher than unladen condition. The higher the mass of vehicle, the higher the value of vertical tire force on tire R1.

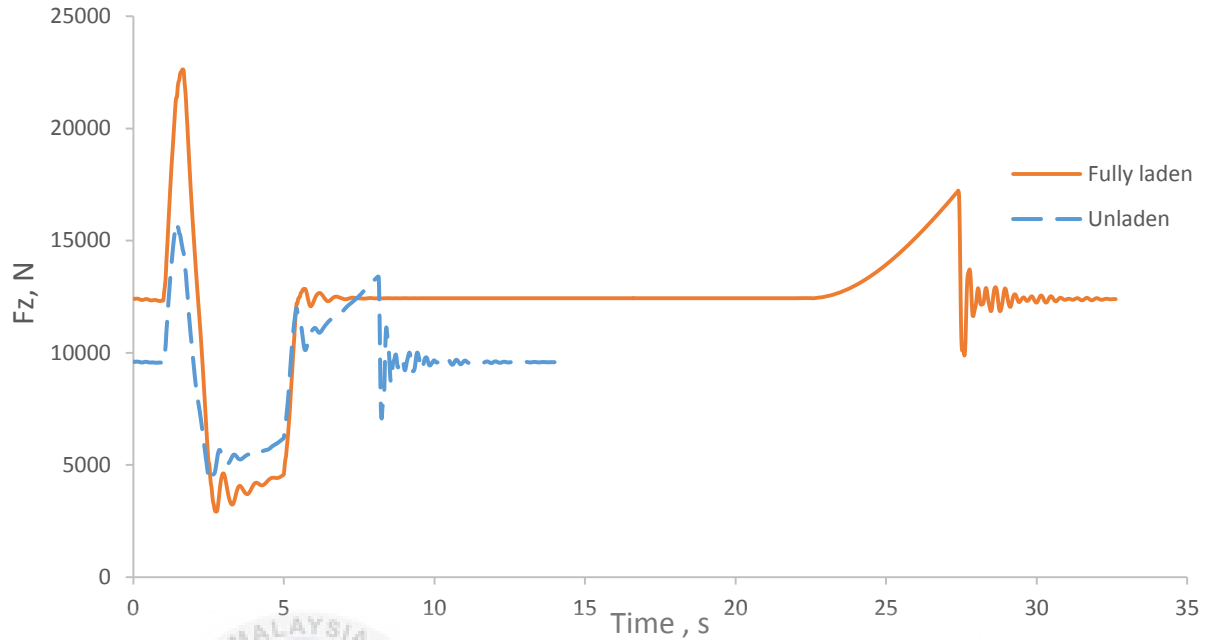


Figure 4.49: Vertical tire force of R1 when fully laden and unladen vehicle

Table 4.32: Comparison of vertical tire force when fully laden and unladen vehicle

Vehicle condition	Maximum vertical tire force, N	Time, s
Unladen	15684.12	1.43
Fully laden	22634.80	1.65

4.3.8 Rollover index

In order to evaluate the tendency for vehicle to rollover during manoeuvre, rollover index is used as the reference. This rollover index use real-time difference in vertical tire load between left and right side of vehicle. Since the vehicle has two axle, the force for two axles are combined for each side as in Eq. (4.13) and Eq. (4.14). The calculation for rollover index is based on Eq. (4.15).

$$F_{zr} = F_{zr1} + F_{zr2} \quad (4.13)$$

$$F_{zl} = F_{zl1} + F_{zl2} \quad (4.14)$$

$$R = \frac{F_{zr} - F_{zl}}{F_{zr} + F_{zl}} \quad (4.15)$$

where F_{zr} is the vertical tire force for right side of the vehicle and F_{zl} is the vertical tire force for left side of the vehicle. Both of the tire forces are substituted into Eq. (4.15) to find rollover index, R .

The tire of vehicle will lift off when $R = 1$ and $R = -1$ while the value of rollover index will be zero when the vehicle is travelling in straight line. As for this test, the maximum value of rollover index will be analysed with respect to different test parameters.

When the vehicle is tested with different speeds, the highest value of maximum rollover index is obtained when the vehicle is travelling at the speed of 55 km/h as shown in **Figure 4.50**. The rollover index obtained as in **Table 4.33** is $R = -0.898$ which is the closest value to $R = -1$ which means the right tire of the vehicle is about to lift off as shown in **Figure 4.51**. This value is obtained at time of 3.35 s when the vehicle is counter steer to the right after turning to the left to complete J turn manoeuvre.

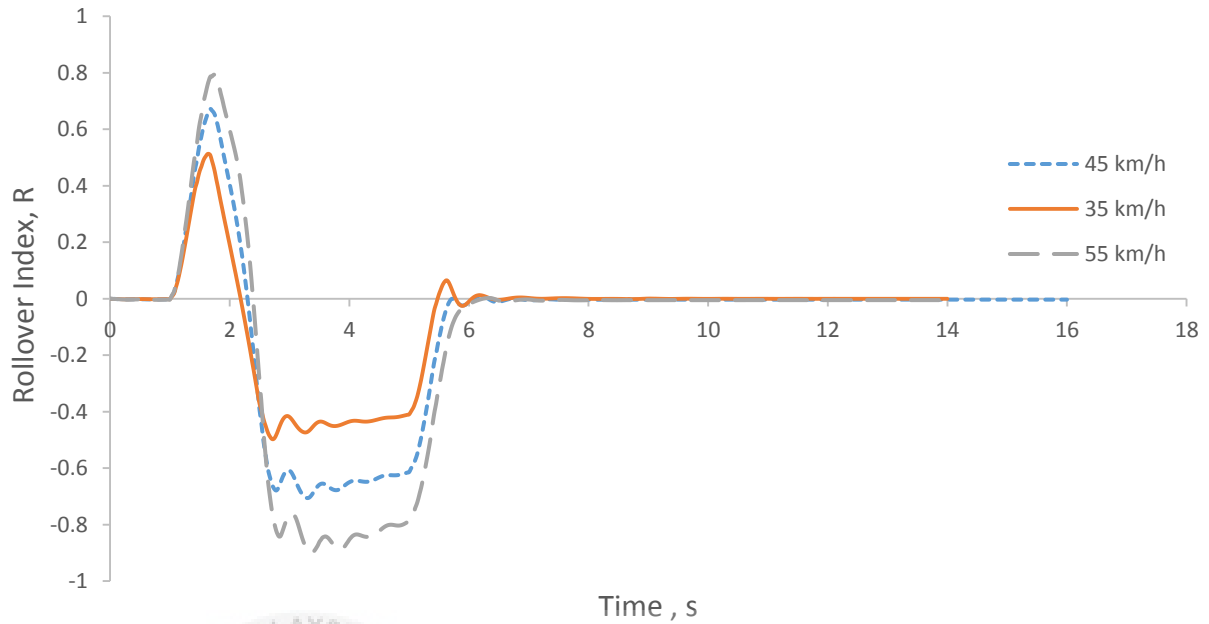


Figure 4.50: Rollover index when vehicle travel at different speeds

Table 4.33: Maximum rollover index for different speeds

Speed, km/h	Maximum Rollover Index	Time, s
35	0.513	1.65
45	-0.704	3.33
55	-0.898	3.35

As for the next test parameter, the vehicle mass is changed for fully laden and unladen condition. Based on **Figure 4.52**, vehicle with fully laden condition obtained the higher value of maximum rollover index compared to the unladen vehicle. The value of maximum rollover index when the vehicle is fully laden is $R = -0.704$ while unladen vehicle is $R = -0.462$ as shown in **Table 4.34**. Maximum value is obtained at time of 3.33 s when the vehicle is counter steer to the right after making a left turn. The negative sign of the rollover index indicates that the right tire of the vehicle is about to lift off as shown in Figure 4..

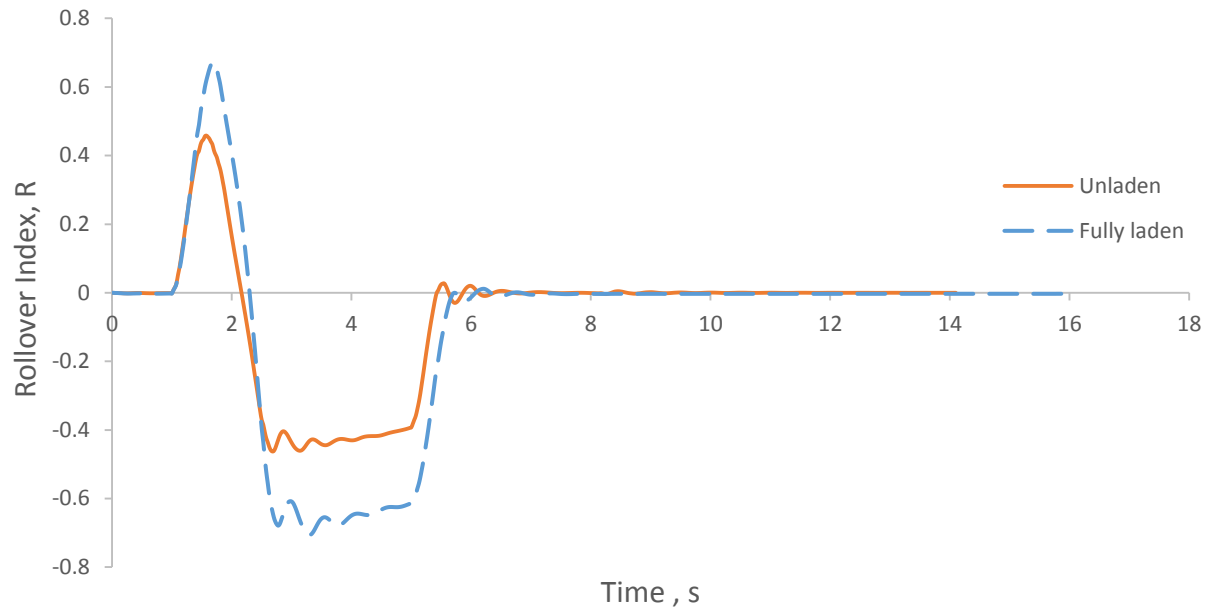


Figure 4.51: Rollover index when fully laden and unladen vehicle



Figure 4.52: The condition of the bus when the right tire is about to lift off.

Table 4.34: Maximum rollover index when fully laden and unladen vehicle

Vehicle condition	Maximum Rollover Index	Time, s
Unladen	-0.462	2.68
Fully laden	-0.704	3.33



CHAPTER 5

CONCLUSION AND RECOMMENDATIONS

5.1 Conclusion

As a conclusion, all of the objectives for this project were successfully achieved after simulate the dynamic behaviour of long commercial vehicle with different test parameters. The simulation for three different criteria were completed which include ride, handling and stability of the vehicle. As for the ride criteria, the higher speed and heavier vehicle will resulting in high value of output results which cause the low comfort for the passengers on board. Handling criteria is related to the steering input from the driver which when tested with higher speed and higher mass, will resulting in higher value of output results in lateral direction. It will make the driver more difficult to control the vehicle so, it is better for the vehicle to manoeuvre in lower speed and lower mass. The stability criteria determine the tendency for the vehicle to rollover after abrupt steering input was given to the vehicle. When the vehicle was travelling with higher speed and higher mass, the vehicle will resulting in high output results which increase the tendency for the vehicle to rollover during manoeuvring. It can be concluded that the vehicle must travel at lower speed and lower mass for more comfortable and higher level of safety driving.

5.2 Recommendation

Based on this research, there are some recommendations for further research in order to produce more variety and accurate results which are the vehicle should be tested with different type of suspension setup which include the spring stiffness and damper coefficient. This parameter will give different behaviour for the vehicle during manoeuvre, the wheelbase for the vehicle also can be changed to different length as it will affect the vehicle during turning and the different set of tire size for the vehicle should be tested to determine the different in vehicle behaviour.



REFERENCES

- [1] Tiago N. (n.d.). Experimental evaluation of comfort and safety in light-duty vehicles. 1-4.
- [2] Meywerk, M. (2015). *Vehicle Dynamics*. Somerset: Wiley.
- [3] Yi, F., Qiu, X., & Fan, W. (2011). Study on Vehicle Ride Comfort Simulation Based on Simulink Environment. *2011 3rd International Workshop on Intelligent Systems and Applications*.
- [4] Solah, M. S., Ariffin, A. H., Md Isa, M. H., & Wong, S. V. (2013). In-depth crash investigation on bus accidents in Malaysia. 5.
- [5] Trigell, A. S., Rothhämel, M., Pauwelussen, J., & Kural, K. (2017). Advanced vehicle dynamics of heavy trucks with the perspective of road safety. *Vehicle System Dynamics*, 55(10), 1572-1617.
- [6] Abdullah, M. A., Jamil, J. F., Mohan, A. E., Mat Yamin, A. K., & Tamaldin, N. (2016). *Vehicle Dynamics Analysis & Experiment* (Vol. Module 13). Melaka: Penerbit Universiti Teknikal Malaysia Melaka.
- [7] Evers, W. J. E. (2010). Improving driver comfort in commercial vehicles: modeling and control of a low-power active cabin suspension system Eindhoven: Technische Universiteit Eindhoven.
- [8] Albinson, A., & Routledge, C. (2013). The damper levels influence on vehicle roll, pitch, bounce and cornering behavior of passenger vehicles. Retrieved November 19, 2018.

- [9] What is an air suspension? How does it work? (2017, November 25). *Engineering Insider*. Retrieved November 28, 2018, from <https://engineeringinsider.org/air-suspension-system-working/>
- [10] Kost F. (2014) Basic principles of vehicle dynamics. In: Reif K. (eds) *Fundamentals of Automotive and Engine Technology*. Bosch Professional Automotive Information. Springer Vieweg, Wiesbaden
- [11] Gillespie, T. D. (1994). *Fundamentals of vehicle dynamics*. Society of Automotive Engineers.
- [12] Mohan, A. E., Abdullah, M. A., Azmi, M. A., Arsaat, A., Abdullah, W. M., Harun, M. H., & Ahmad, F. (2017). Comfort Parameters Tuning Analysis for Vehicle Suspension Pitch Performance. *International Journal of Engineering and Technology*, 9(6), 4471-4480.
- [13] Stone, M. R., & Demetriou, M. A. (2000). Modeling and simulation of vehicle ride and handling performance. *Proceedings of the 2000 IEEE International Symposium on Intelligent Control. Held Jointly with the 8th IEEE Mediterranean Conference on Control and Automation (Cat. No.00CH37147)*.
- [14] Heerwan, P., Asyraf, S., Efistein, A., Seah, C., Zikri, J., & Syawahieda, J. (2017). Experimental study of the vehicle dynamics behavior during lane changing in different speeds. *IOP Conference Series: Materials Science and Engineering*, 257, 012078.
- [15] Allen, R. W., Szostak, H. T., Rosenthal, T. J., & Klyde, D. H. (1990). Field Testing and Computer Simulation Analysis of Ground Vehicle Dynamic Stability. *SAE Technical Paper Series*.
- [16] Jacobson, B. (2016). *Vehicle Dynamics Compendium for course MMF062*. Chalmers.
- [17] Nong Zhang , Guang-Ming Dong & Hai-Ping Du (2008) Investigation into

untripped rollover of light vehicles in the modified fishhook and the sine maneuvers. Part I: Vehicle modelling, roll and yaw instability, *Vehicle System Dynamics: International Journal of Vehicle Mechanics and Mobility*, 46:4, 271-293.

[18] Double lane-change measurements according to ISO 3888-1. (n.d.). Retrieved November 15, 2018, from <https://www.dewetron.com/>

[19] Lundahl, K., Berntorp, K., Olofsson, B., Aslund, J., & Nielsen, L. (n.d.). Studying the influence of roll and pitch dynamics in optimal road-vehicle maneuvers. 2-10.

[20] Xiong, F., Lan, F., Chen, J., & Zhou, Y. (2015). The Study For Anti-Rollover Performance Based On Fishhook and J Turn Simulation. *Proceedings of the 3rd International Conference on Material, Mechanical and Manufacturing Engineering*.

[21] Tomaraee, P. (2016). Active Suspension Analysis of Full Vehicle Model Traversing over Bounce Sine Sweep Road. *Journal of Advances in Vehicle Engineering* 1(1) (2016) 49-56.

[22] Weigand, B. (2011). Mass Properties and Automotive Lateral Acceleration. *70th Annual International Conference of the Society of Allied Weight Engineers, Inc.,.*

[23] Wong, J. Y. (2008). *Theory of ground vehicles*. Hoboken, NJ: John Wiley.

[24] J –turn Maneuver Tests – Logic Tree Diagram (n.d). *NHTSA*. Retrieved May 5, 2019 from https://www.nhtsa.gov/sites/nhtsa.dot.gov/files/tp-136-00_app_c.pdf

[25] Understanding Vehicle Stability Control (2017, October 24). *Auto Service Professional*. Retrieved April 15, 2019 from <https://www.autoserviceprofessional.com/article/100319/understanding-vehicle-stability-control>.

APPENDICES



PROJECT ACTIVITIES	Week 1	Week 2	Week 3	Week 4	Week 5	Week 6	Week 7	Week 8	Week 9	Week 10	Week 11	Week 12	Week 13	Week 14	Week 15	Week 16
Project title selection										M I D S E M E S T E R B R E A K						
Discussion with supervisor																
Research on project title																
Introduction																
Literature review																
Methodology																
Simulation analysis																
Presentation																
Submission of final report																

APPENDIX A: Gantt chart for PSM 1

PROJECT ACTIVITIES	Week 1	Week 2	Week 3	Week 4	Week 5	Week 6	Week 7	Week 8	Week 9	Week 10	Week 11	Week 12	Week 13	Week 14	Week 15	Week 16
Research on test																
Discussion with supervisor																
Test simulation																
Results analysis																
Discussion																
Conclusion																
Final report preparation																
Presentation																
Submission of final report																

APPENDIX B: Gantt chart for PSM 2